The meson-nucleus interaction and the search for meson-nucleus bound states

Volker Metag, Mariana Nanova
II. Physikalisches Institut
JUSTUS-LIEBIG-UNIVERSITÄT GIESSEN

I. Introduction: theoretical predictions
II. mass shifts and broadening from meson line shape analysis
III. meson-nucleus potential from excitation functions, momentum distributions and transparency ratios
IV. meson-nucleus interaction from meson-nucleus bound states
V. summary and outlook

Experimental Physics II

Reimei workshop
“Hadrons in dense matter at J-PARC”
Feb. 21-23. 2022

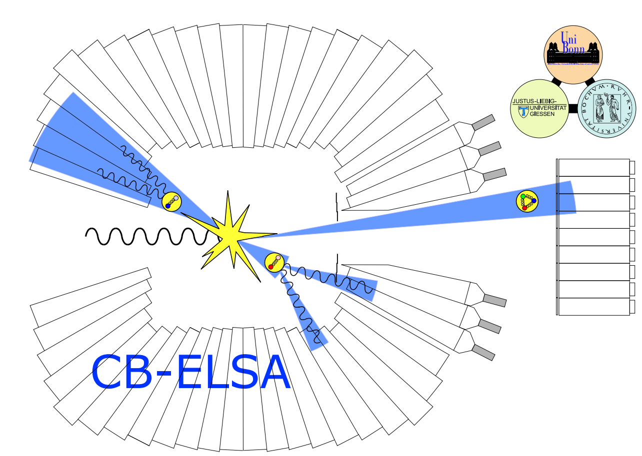

I.
Introduction
(theoretical predictions)

Symmetry breaking in the hadronic sector

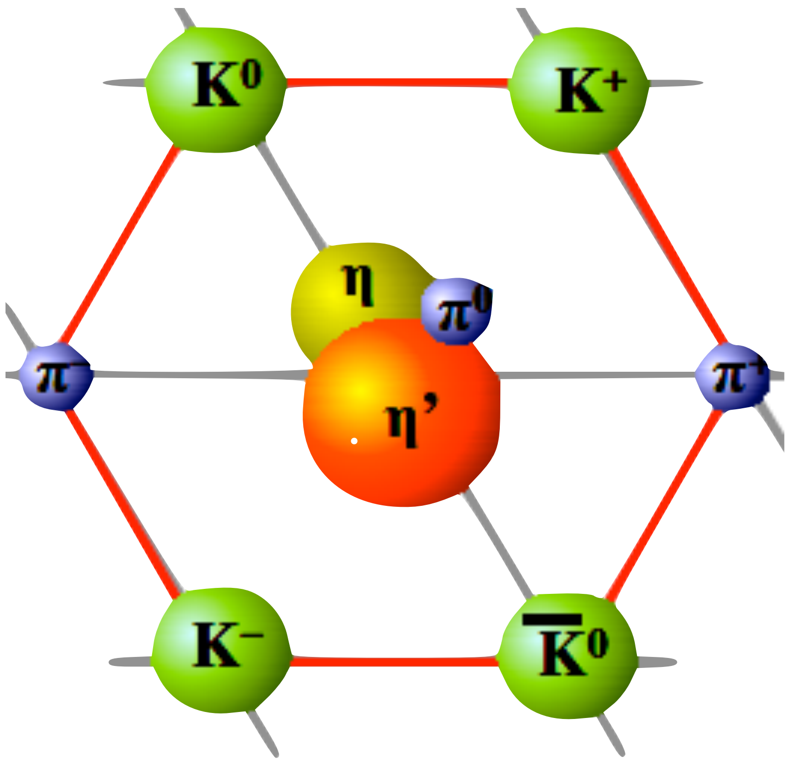

<u>nonet of pseudoscalar mesons</u>

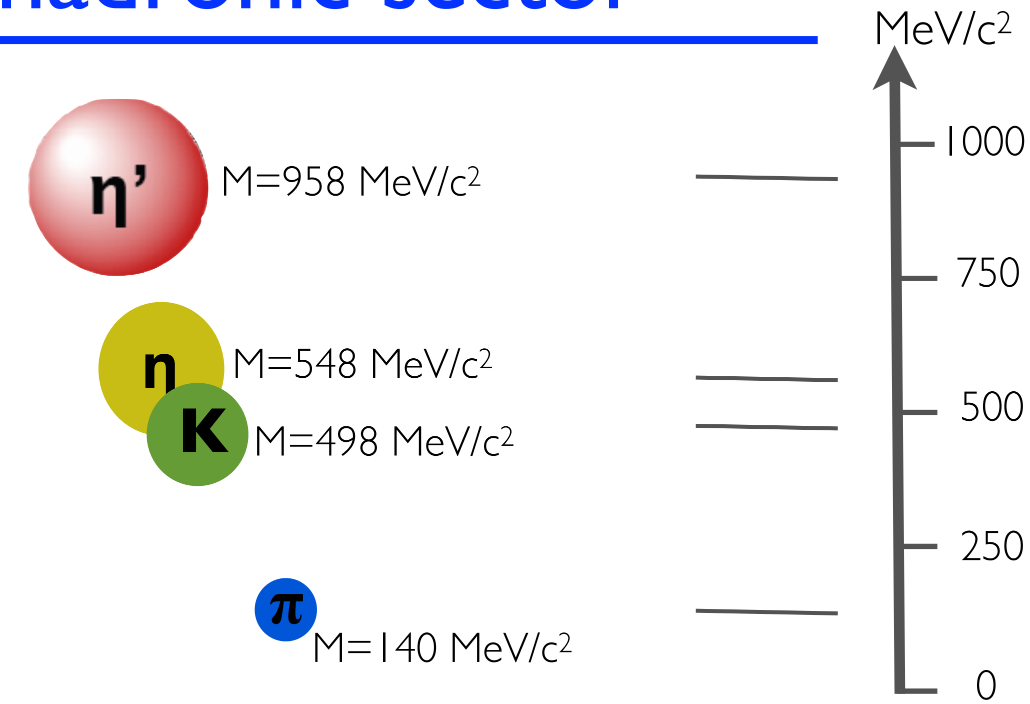

Symmetry breaking in the hadronic sector

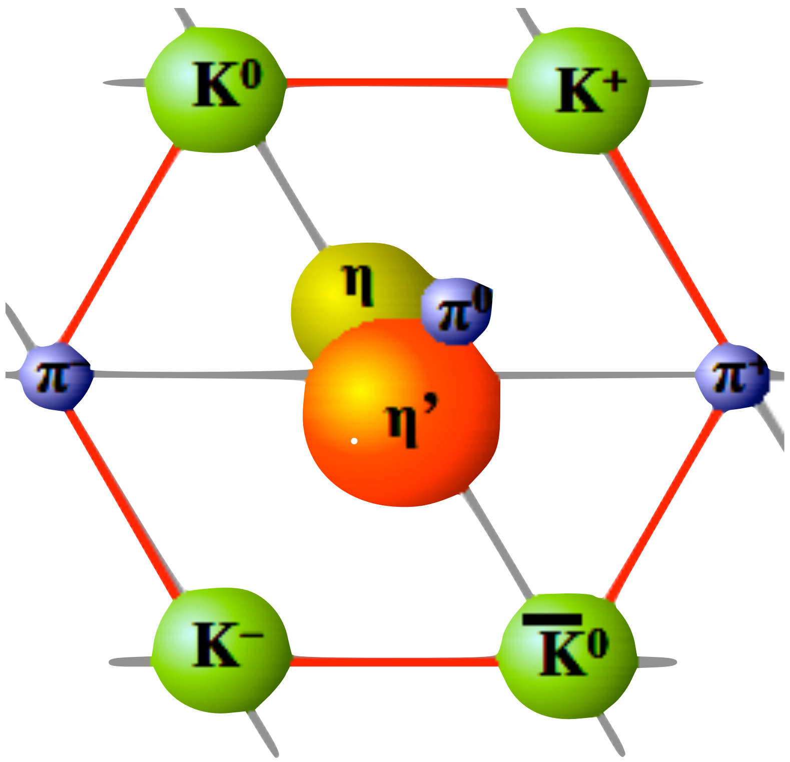

nonet of pseudoscalar mesons

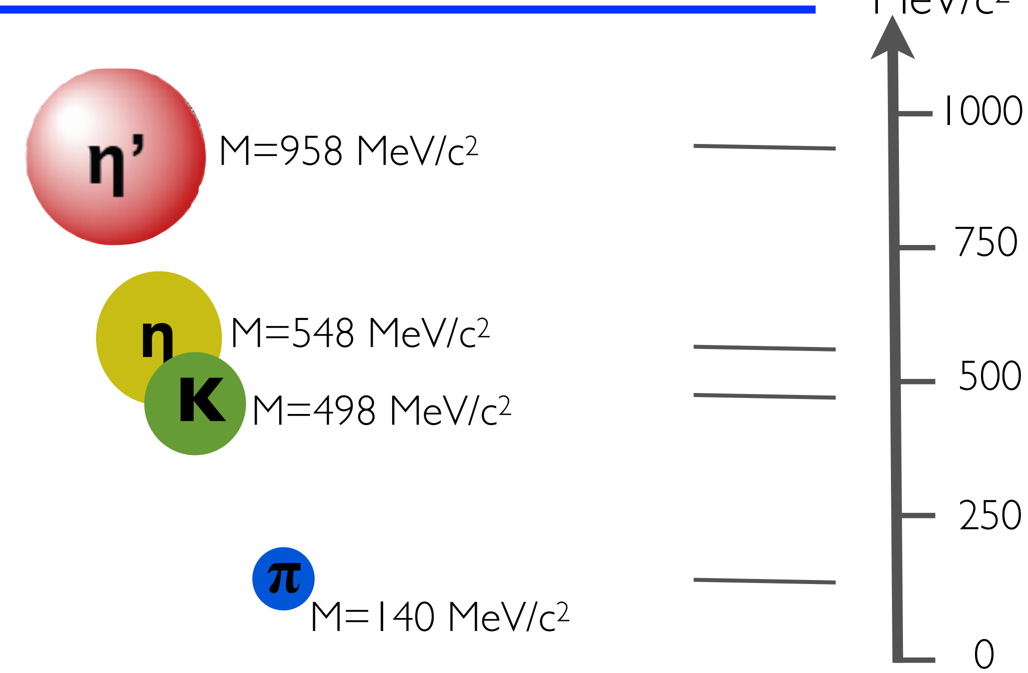

V. Bernard, R.L. Jaffe, U.-G. Meissner, NPB 308 (1988) 753

S. Klimt, M. Lutz, U.Vogel, W.Weise, NPA 516 (1990) 429

H. Nagahiro, D. Jido, H. Fujioka, K. Itahashi, S. Hirenzaki, PRC87 (2013) 045201

mass as a result of symmetry breaking

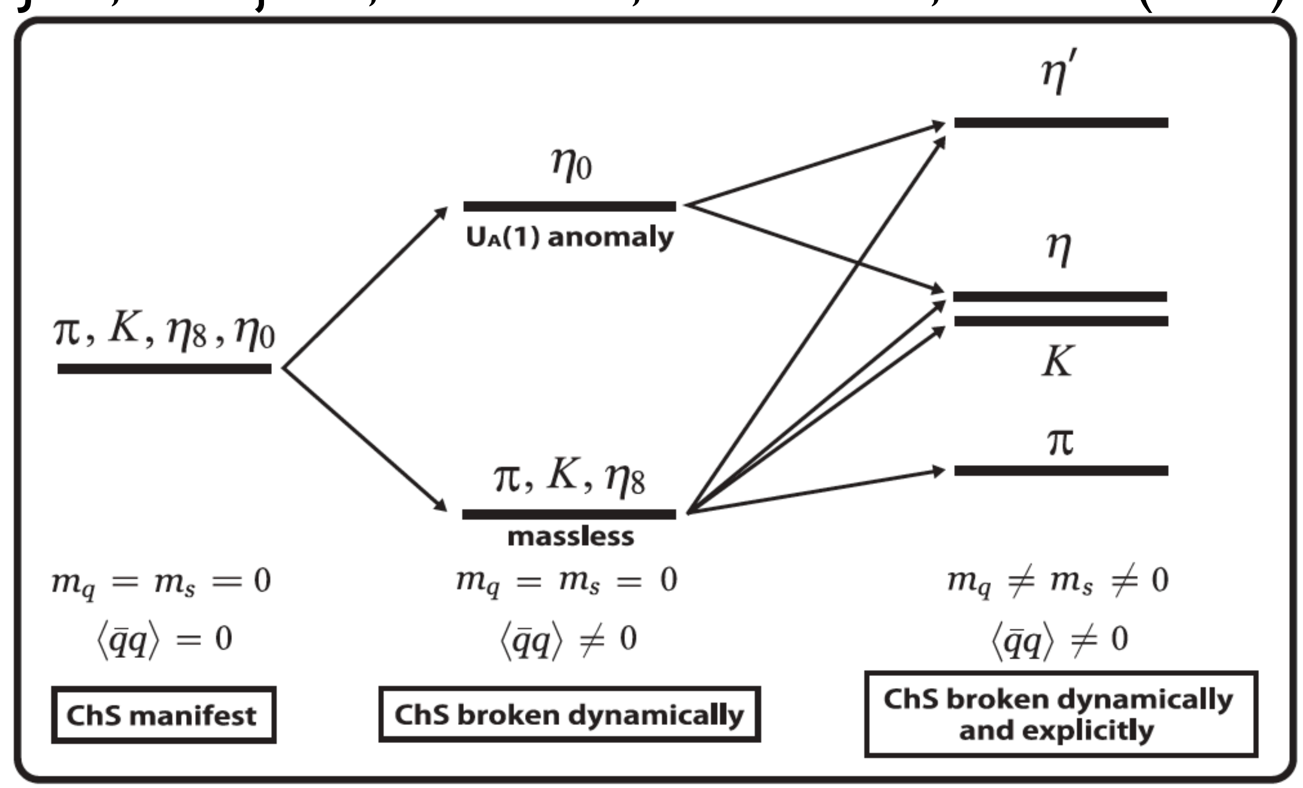

symmetry breaking

Symmetry breaking in the hadronic sector

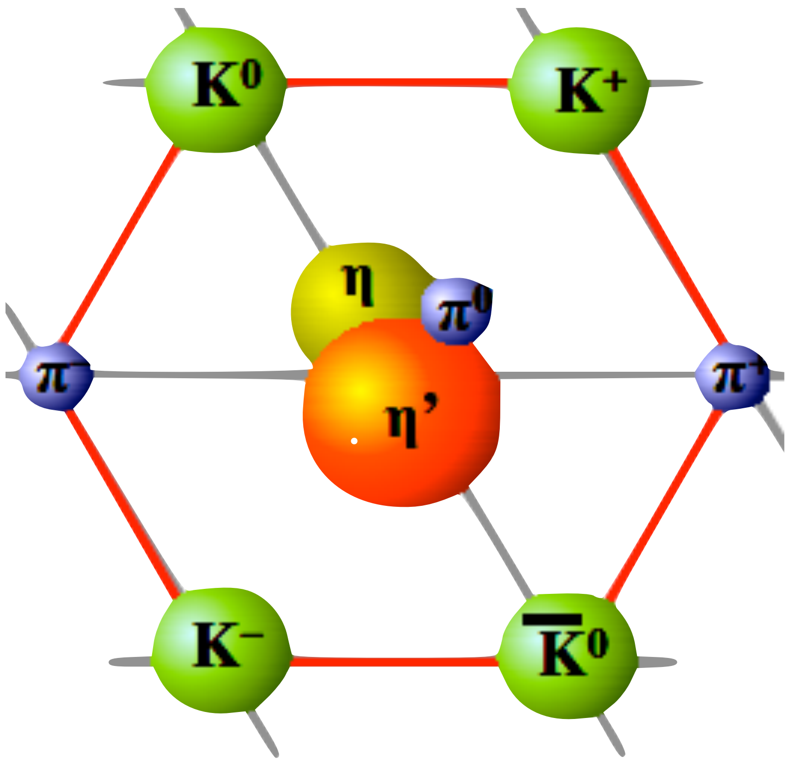

nonet of pseudoscalar mesons

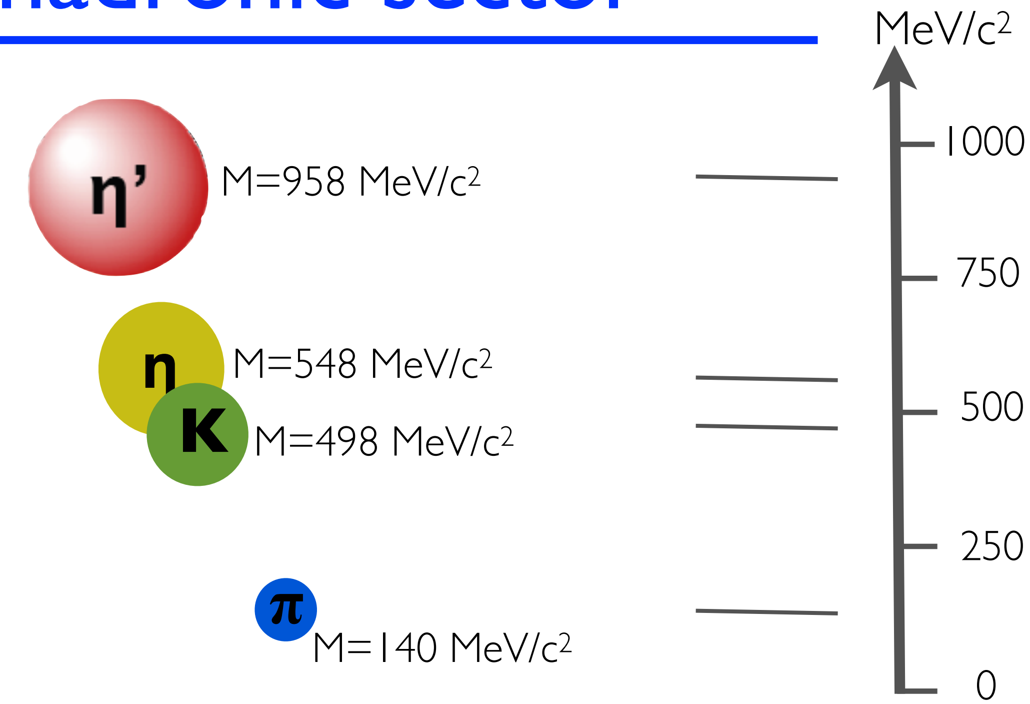

V. Bernard, R.L. Jaffe, U.-G. Meissner, NPB 308 (1988) 753

S. Klimt, M. Lutz, U.Vogel, W.Weise, NPA 516 (1990) 429

H. Nagahiro, D. Jido, H. Fujioka, K. Itahashi, S. Hirenzaki, PRC87 (2013) 045201

mass as a result of symmetry breaking

partial restoration of chiral symmetry predicted to occur in a nucleus $\Longrightarrow$ impact on meson masses ??

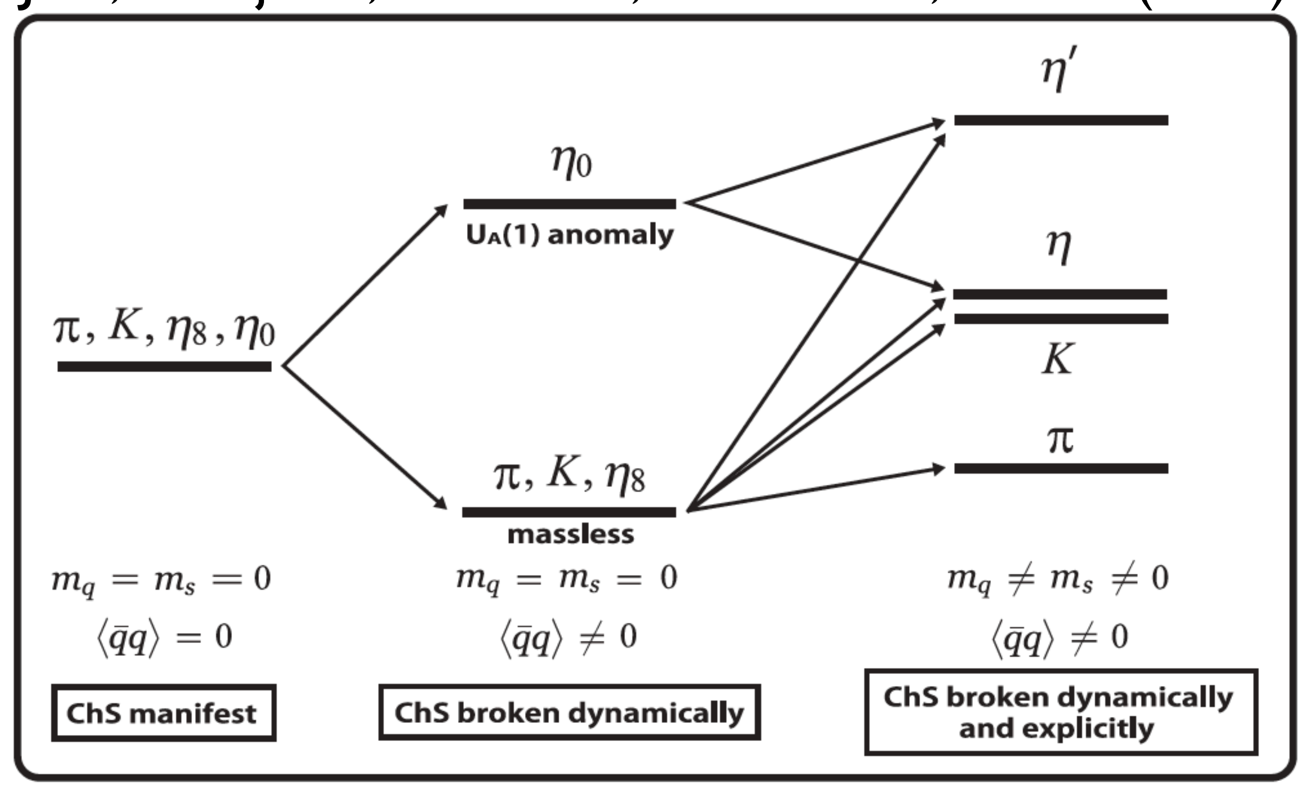

symmetry breaking

partial symmetry restoration

Predictions for in-medium changes

η,η'

NJL-model

H. Nagahiro et al.,
PRC 74 (2006) 045203

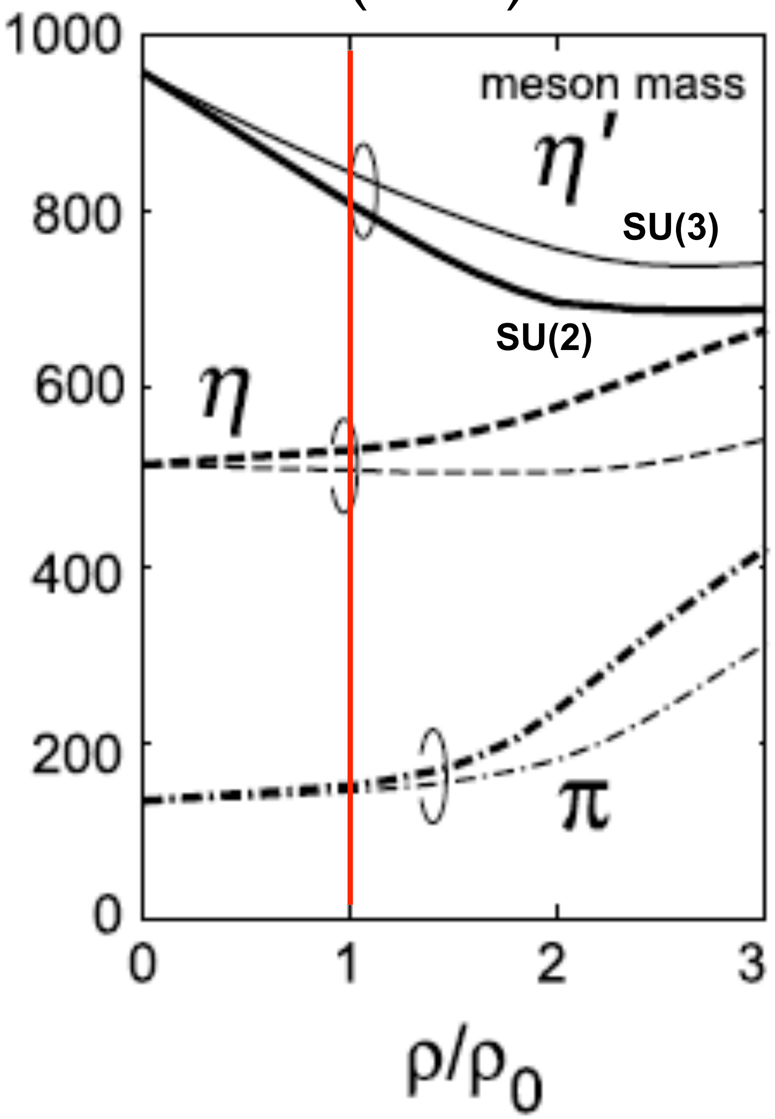

$\Delta m_{\eta'}(\rho_0) \approx -150$ MeV
$\Delta m_{\eta}(\rho_0) \approx +20$ MeV

K+, K-

RMF-approach

J.Schaffner-Bielich et al.,
Nucl. Phys. A625 (1997) 325

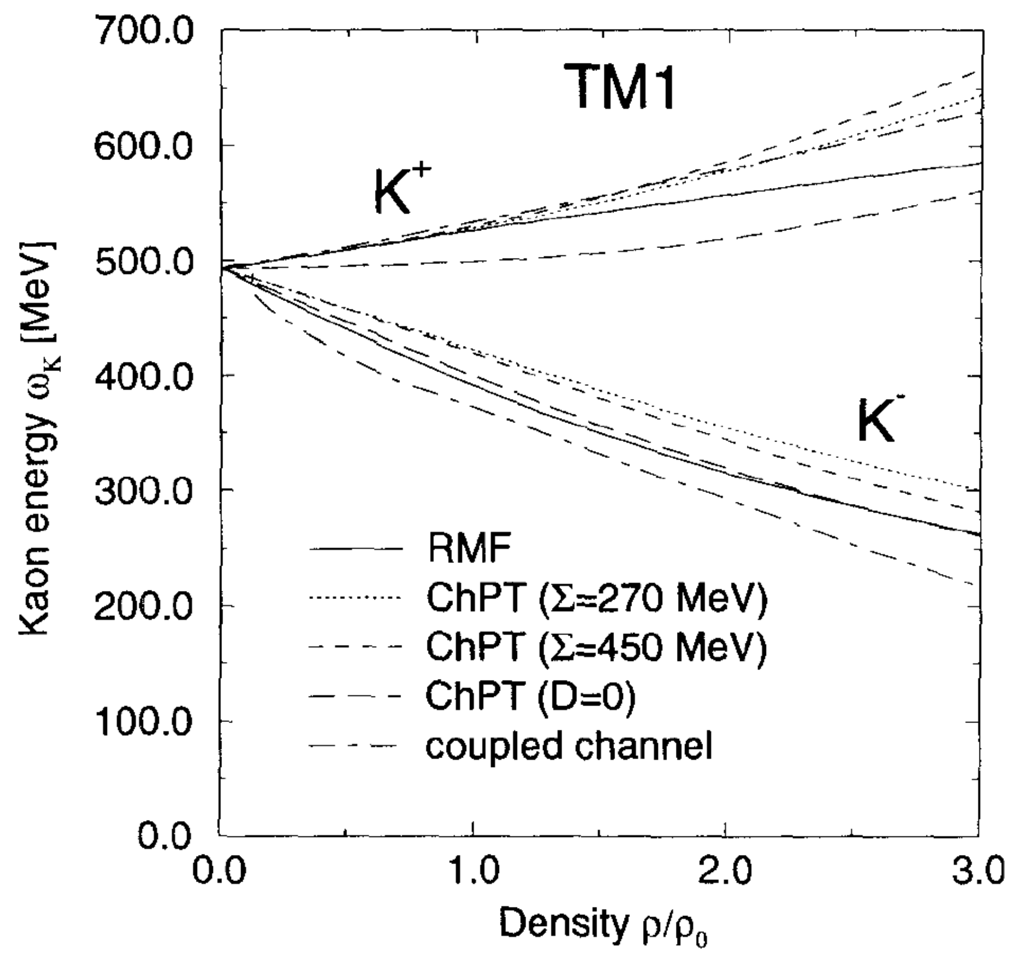

$\Delta m_{K^+}(\rho_0) \approx +30$ MeV
$\Delta m_{K^-}(\rho_0) \approx -100$ MeV

ρ,ω,Φ

QCD sum rules

T. Hatsuda, S. Lee
PRC46 (1992)R34

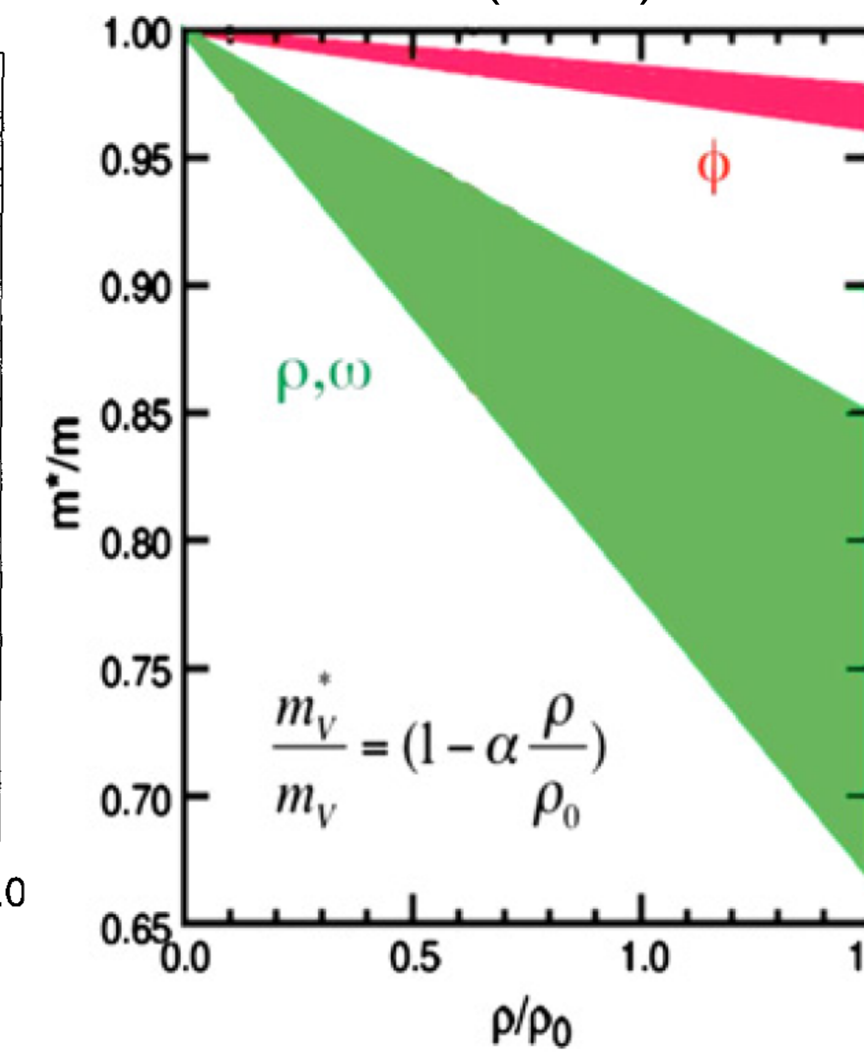

$$\frac{m_V^*}{m_V} = \left(1 - \alpha \frac{\rho}{\rho_0}\right)$$

$\Delta m_{\rho}(\rho_0) \approx -(80\text{-}160)$ MeV
$\Delta m_{\omega}(\rho_0) \approx -(80\text{-}160)$ MeV
$\Delta m_{\Phi}(\rho_0) \approx -(20\text{-}30)$ MeV

Predictions for in-medium broadening

in the nuclear medium mesons have additional "decay"- options
they can be removed by inelastic reactions, e.g. ω N → π N
→shorter lifetime →larger in-medium width

ω

unitary coupled channel
effective Lagrangian model

P. Mühlich et al.,
NPA 780 (2006) 187

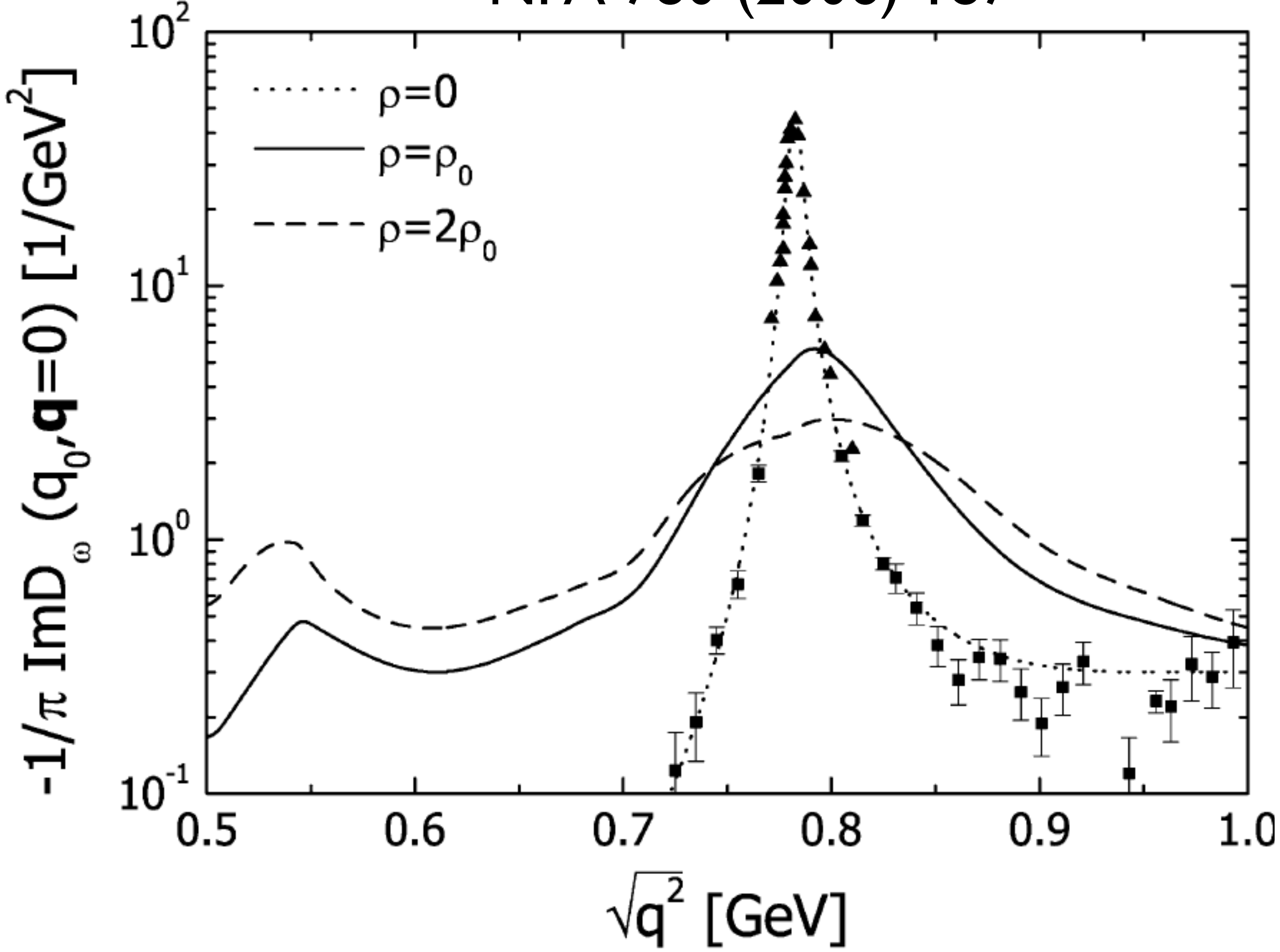

$\Gamma_\omega(\rho=\rho_0) \approx 60$ MeV

Φ

chiral-SU(3)
effective field theory

P. Gubler, W. Weise
PLB 751 (2015) 396

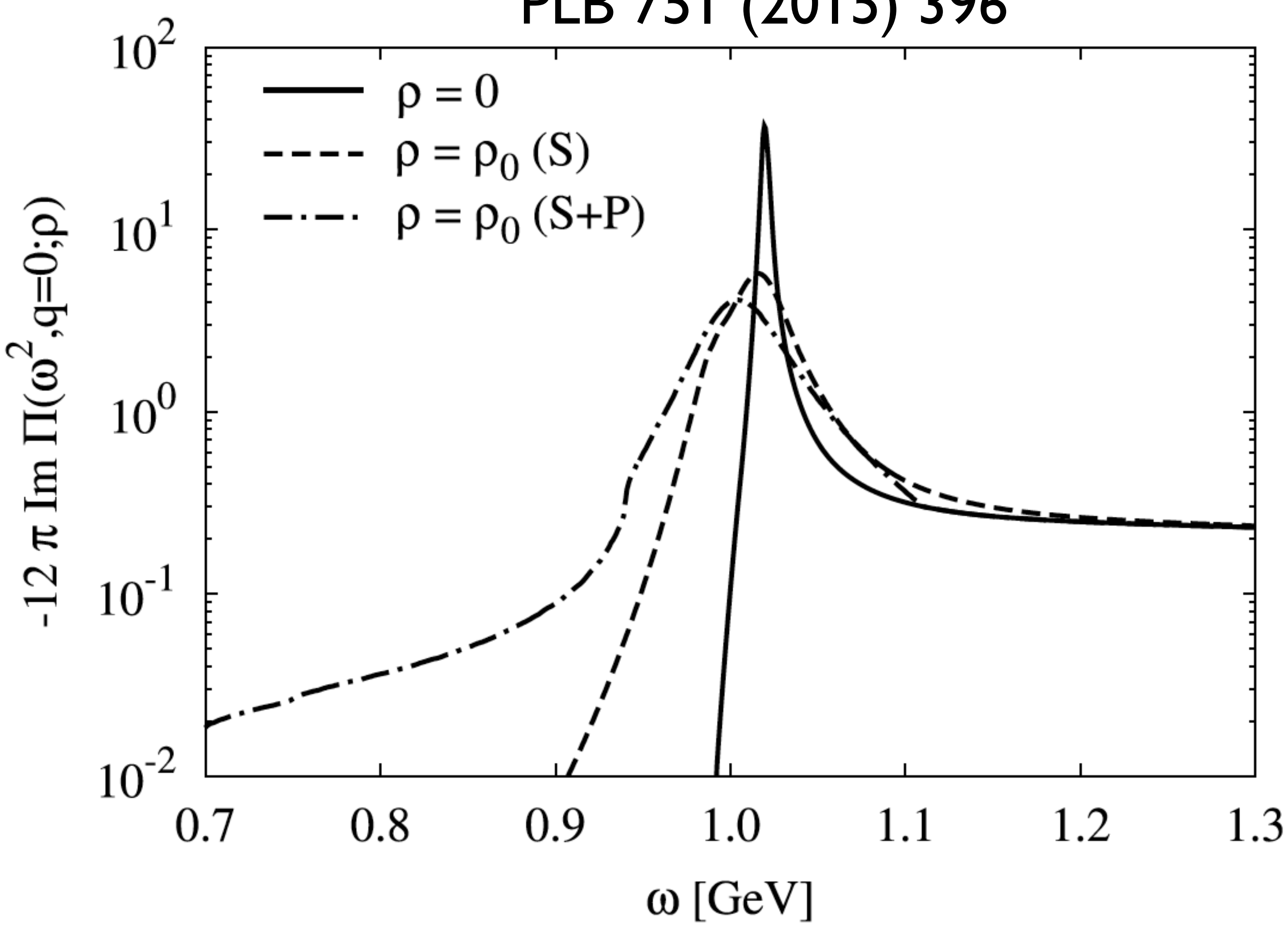

$\Gamma_\Phi(\rho=\rho_0) \approx 45$ MeV

From theoretical predictions to experimental observables

calculations of meson spectral functions assume:

- infinitely extended nuclear matter in equilibrium at ρ, T = const.;
- meson at rest in nuclear medium

From theoretical predictions to experimental observables

calculations of meson spectral functions assume:

- infinitely extended nuclear matter in equilibrium at ρ, T = const.;
- meson at rest in nuclear medium

theoretical predictions ⇨ experimental observables

From theoretical predictions to experimental observables

calculations of meson spectral functions assume:

- infinitely extended nuclear matter in equilibrium at ρ, T = const.;
- meson at rest in nuclear medium

transport calculations (GiBUU, HSD, UrQMD, JAM,…) are needed for comparison with experiment !!!

theoretical predictions ⇨ transport calculations ⇨ experimental observables

- initial state effects: absorption of incoming beam particles
- non equilibrium effects: varying density and temperature
- absorption and regeneration of mesons in the nuclear medium
- fraction of decays inside of the nuclear environment
- final state interactions: distortion of momenta of decay products

II.
Meson line shape analysis
(sensitive to nuclear density at the decay point)

problems in line shape analysis

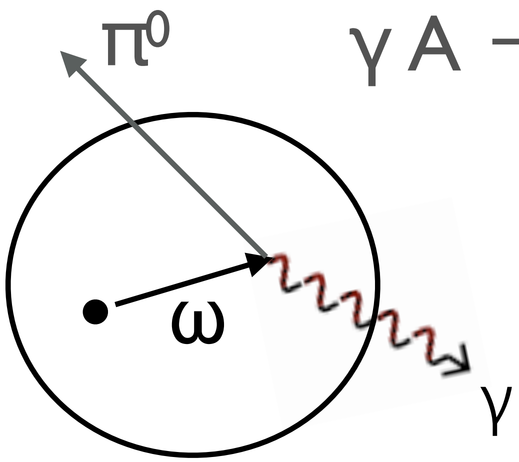

$\gamma A \rightarrow \omega X$

$\hookrightarrow \pi^0 \gamma$

$$m = \sqrt{(p_1+p_2)^2}$$

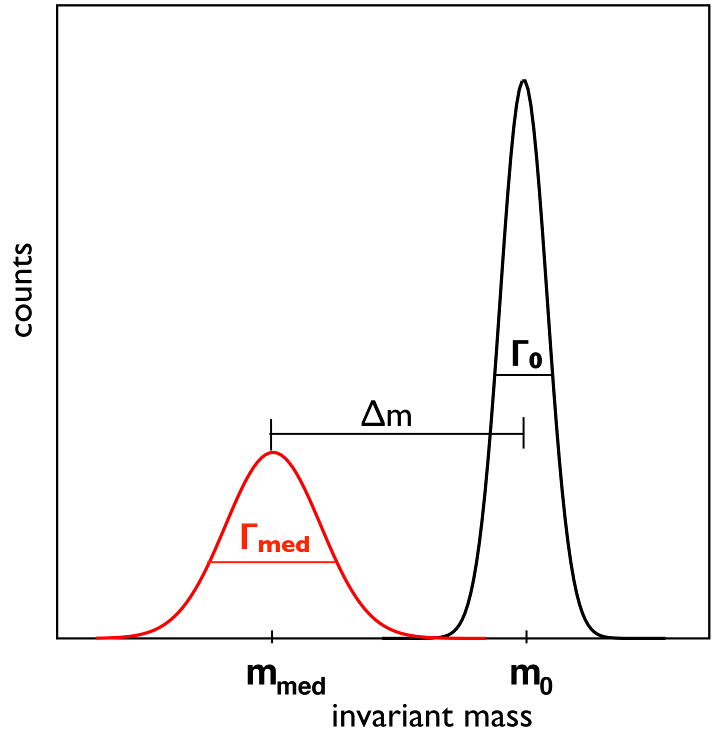

problems in line shape analysis

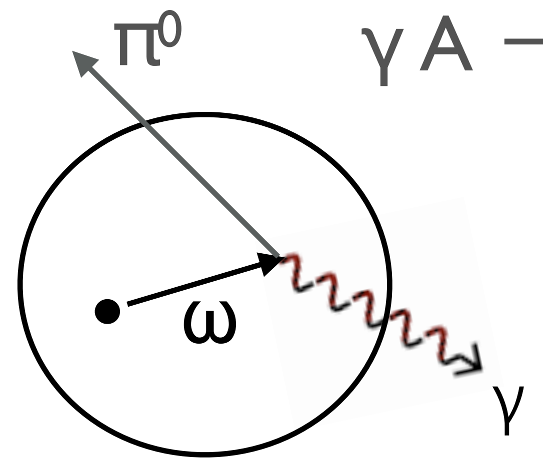

$\gamma A \rightarrow \omega X$
$\quad \hookrightarrow \pi^0 \gamma$

$$m = \sqrt{(p_1+p_2)^2}$$

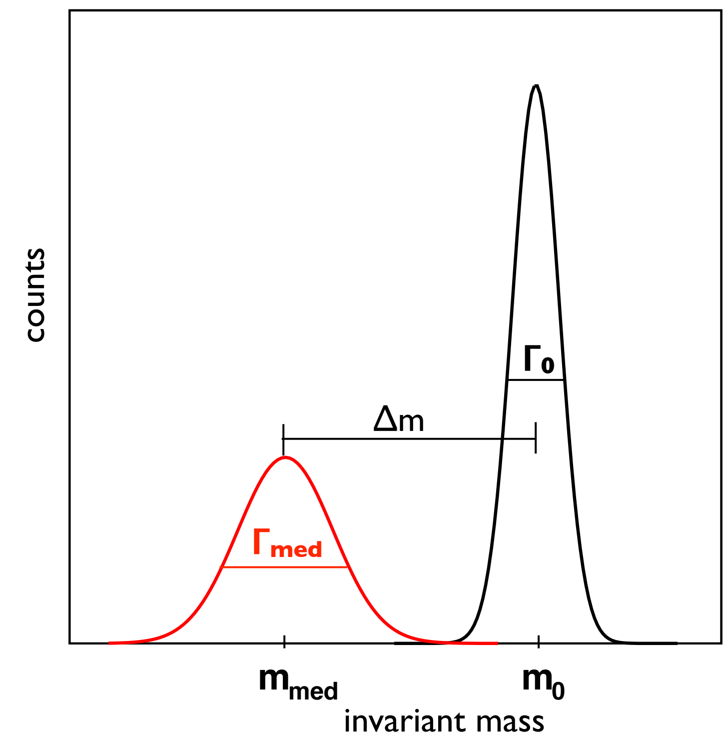

three effects limit the sensitivity:

1.) only fraction of decays occur within the nucleus:
decay length $s = \gamma \cdot \beta\tau = \frac{p}{m} \cdot \tau$
$s_\omega = 22$ fm >> $R_{nucleus}$ for $\frac{p}{m} \approx 1.0$

2.) in-medium decays occur over wide range of nuclear densities (nuclear density profile)

3.) additional complication for $\omega \rightarrow \pi^0\gamma$: observation of in-medium decays hampered by π^0 absorption

GiBUU simulation:

$\Delta m/m = -16\%$; $\Gamma_{coll} = 140$ MeV; $\sigma_{res}/m = 3\%$

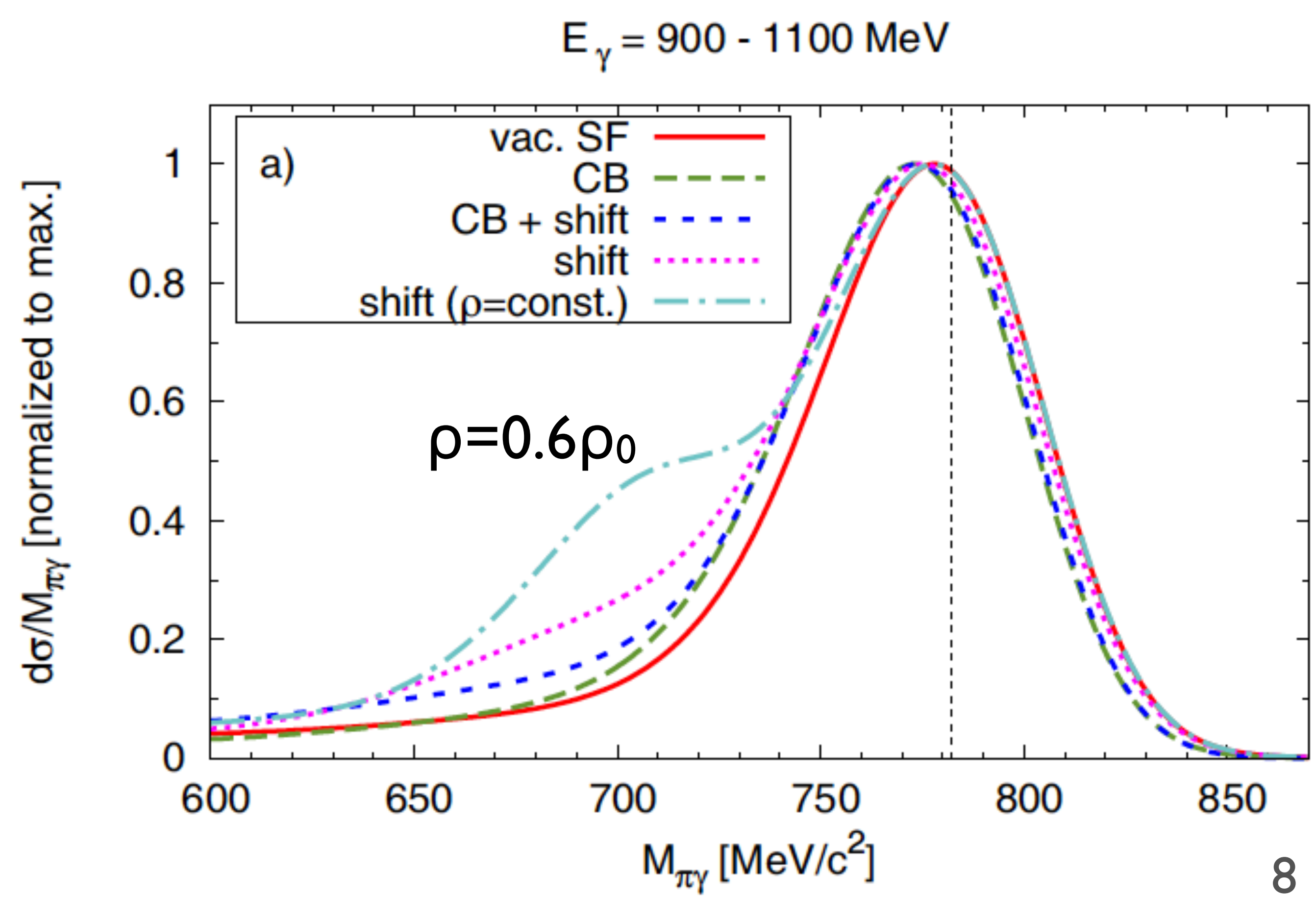

ω line shape in $\omega \rightarrow \pi^0\gamma$

$\gamma A \rightarrow \omega X$; E_γ= 900-1300 MeV   M.Thiel et al., EPJA 49 (2013)132

line shapes for LH_2, C, Nb

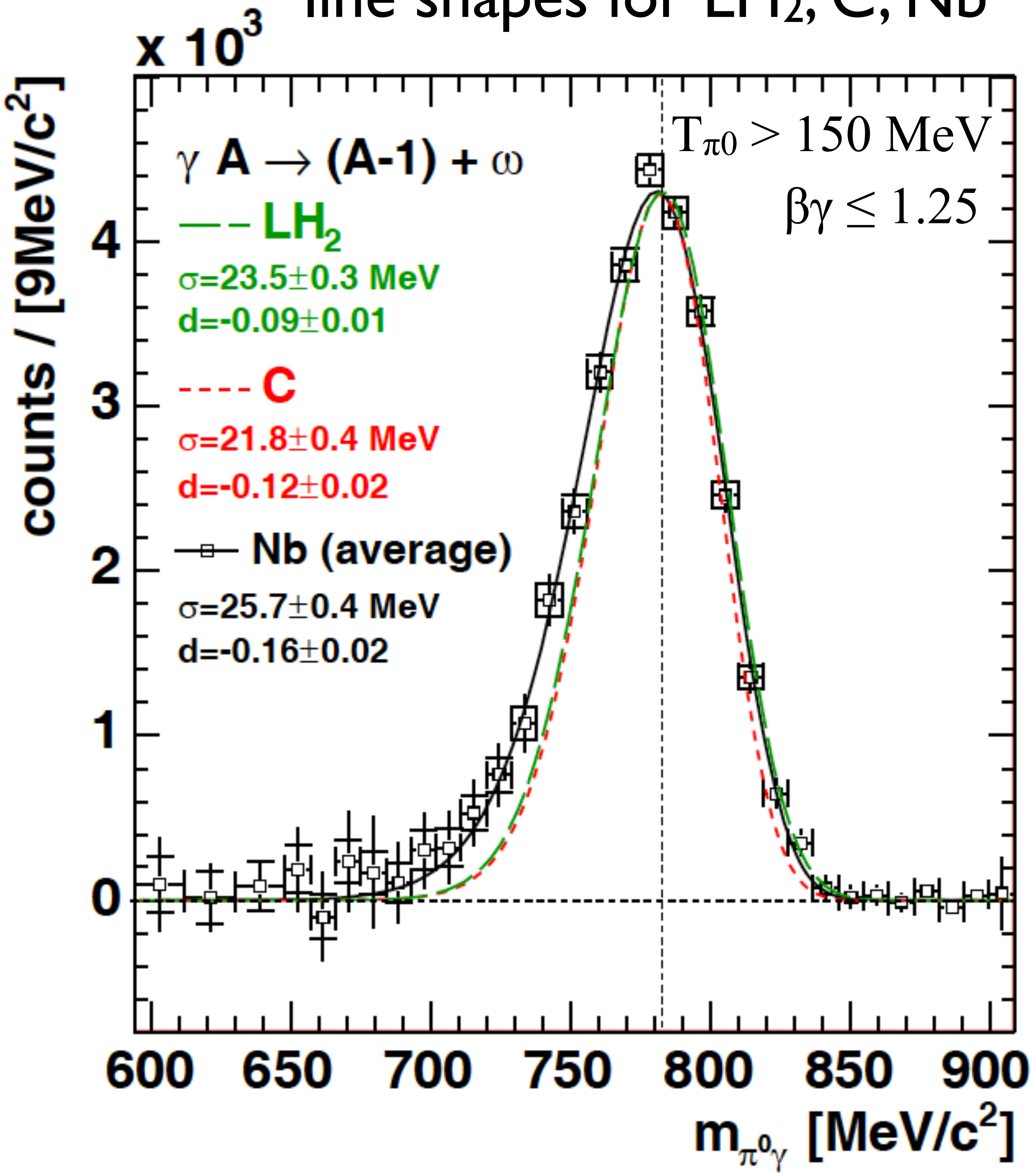

signal broader for Nb
than for LH_2, C

comparison with GiBUU simulations

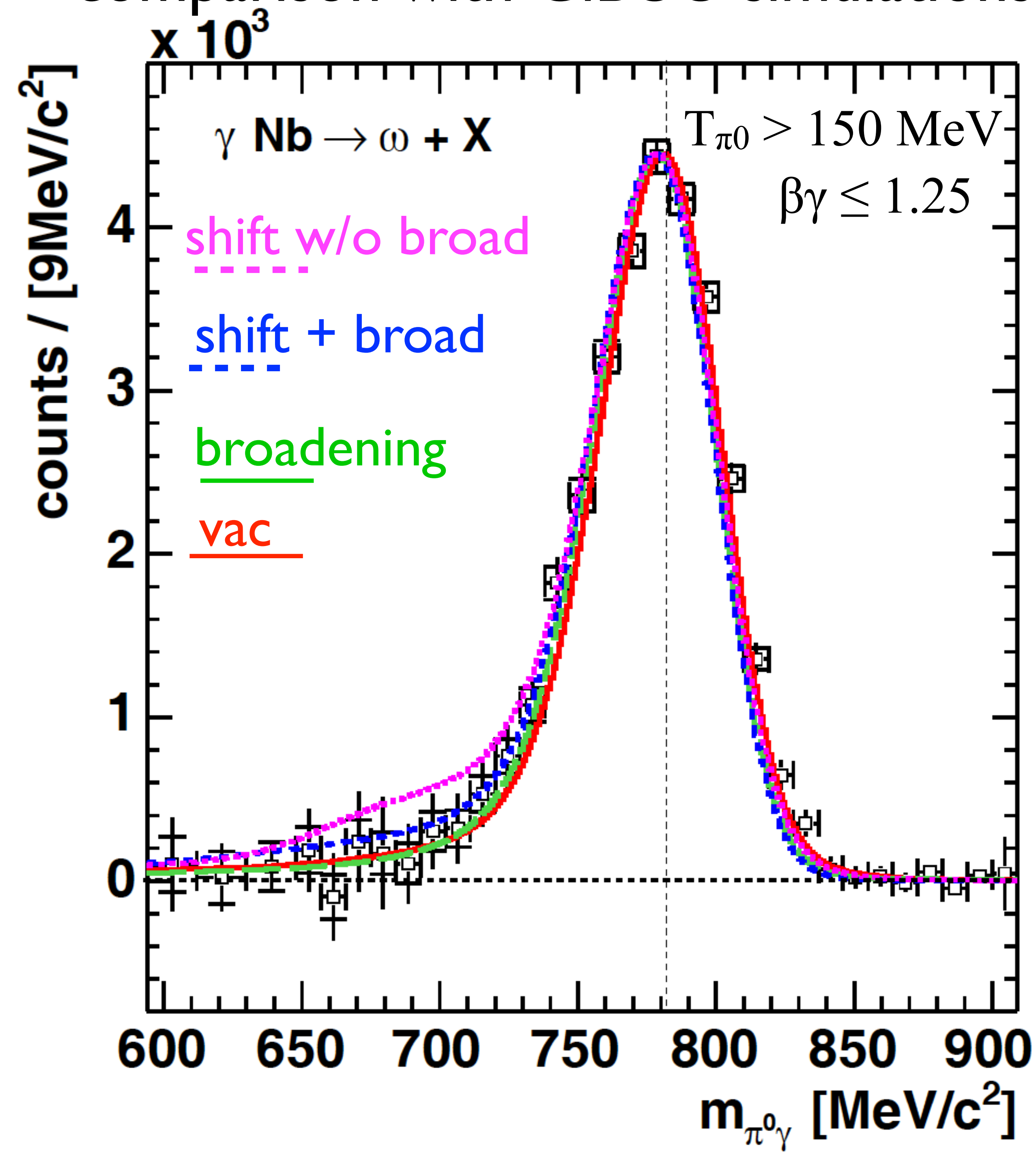

statistics not sufficient to
differentiate various scenarios

Line shape analysis: Φ meson

p + C, Cu →Φ + X @12 GeV

KEK E325: R.Muto et al. PRL 98 (2007) 042501

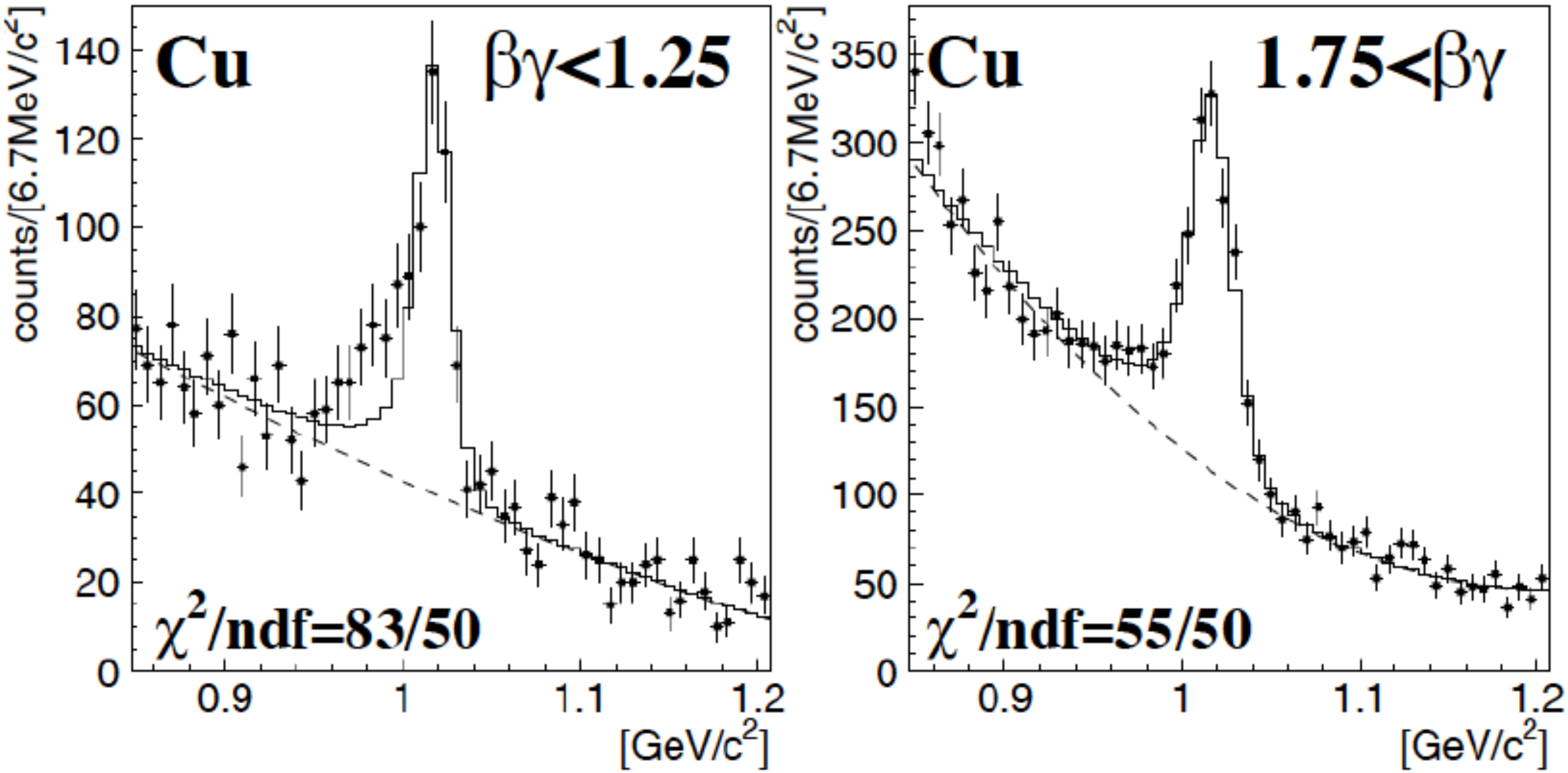

deviation from expected line shape for slow Φs with βγ < 1.25

$V_0 = \Delta m\ (\rho=\rho_0) = (35\pm7)$ MeV; $W(\rho=\rho0) = 7^{+4}_{-3}$ MeV

$\phi \rightarrow e^+e^-$ decays

Janus Weil (Univ. Frankfurt): J-PARC workshop 2015

GiBUU simulation: p + Pb 30 GeV (E16)

to enhance in-medium decays select low momentum ϕ mesons: $\beta\gamma < 0.5$

mass shift 3.4% + broadening by 3.6

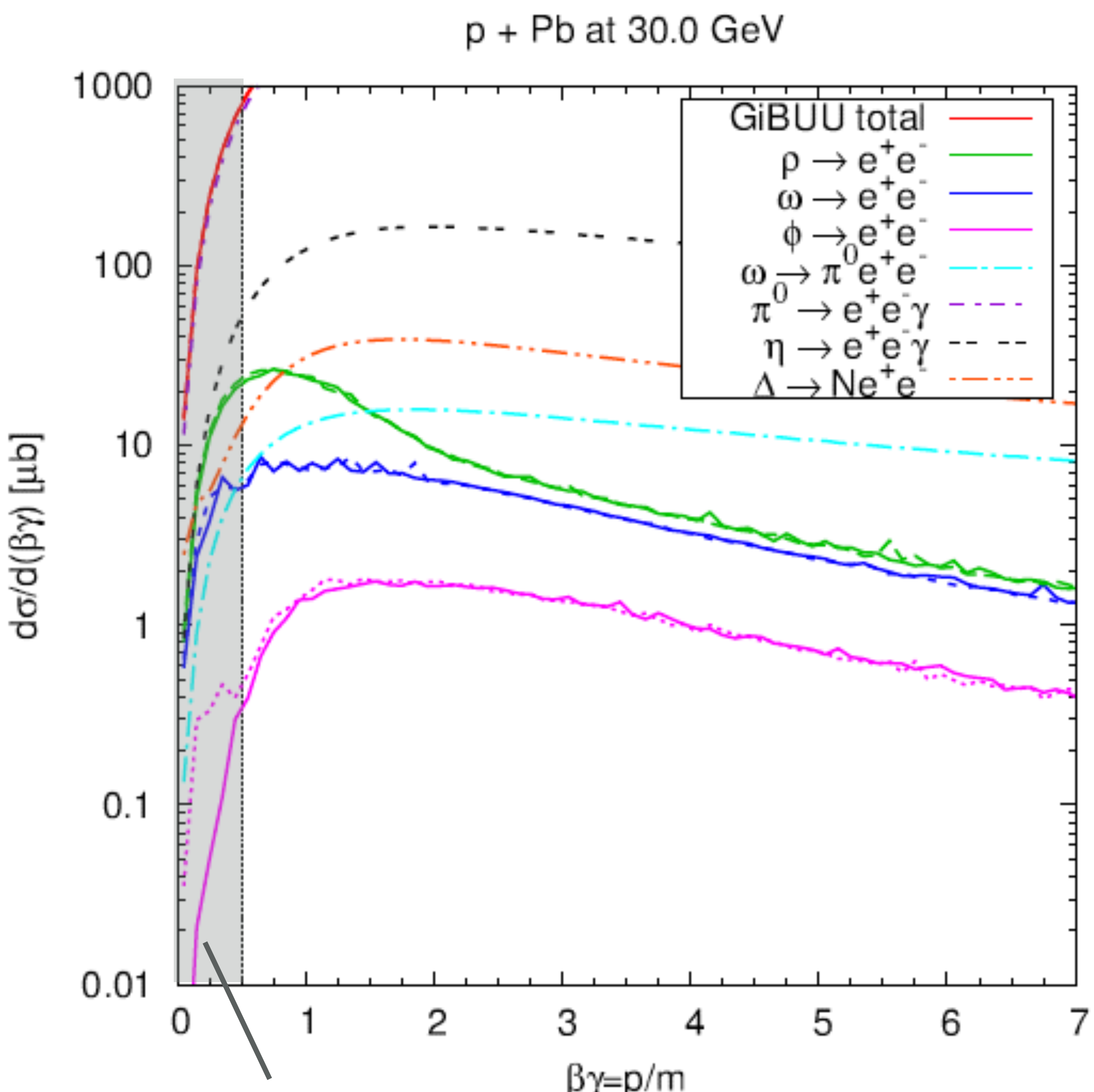

$\beta\gamma < 0.5$

tiny fraction of Φ mesons going backwards in cm; almost at rest in lab

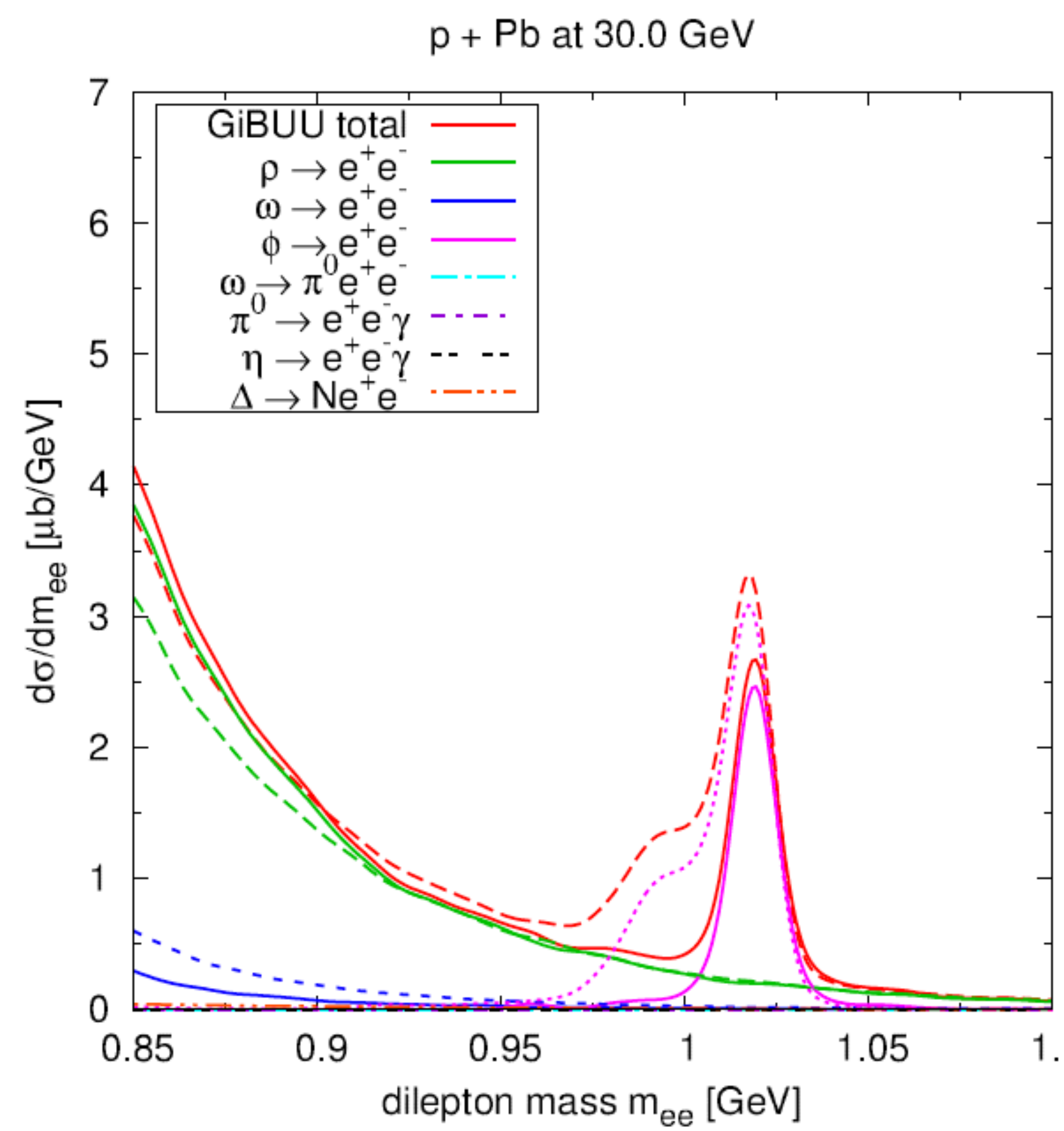

E16 experiment: S. Yokkaichi et al.

$p + A \rightarrow \Phi + X$ at 30 GeV

III.
Meson-nucleus potential from measuring excitation functions, momentum distributions and transparency ratios

(sensitive to nuclear density at the production point)

Meson-nucleus potential

H. Nagahiro, S. Hirenzaki, PRL 94 (2005) 232503

$$U(r) = V(r) + i\,W(r)$$

attractive ?
repulsive ?

absorption

$$V(r) = \Delta m(\rho_0) \cdot \rho(r)/\rho_0$$

$$W(r) = -\Gamma_0/2 \cdot \rho(r)/\rho_0$$
$$= -1/2 \cdot \hbar c \cdot \rho(r) \cdot \sigma_{inel} \cdot \beta$$

Meson-nucleus potential

H. Nagahiro, S. Hirenzaki, PRL 94 (2005) 232503

$$U(r) = V(r) + i\,W(r)$$

attractive ?
repulsive ?

absorption

$$V(r) = \Delta m(\rho_0) \cdot \rho(r)/\rho_0$$

$$W(r) = -\Gamma_0/2 \cdot \rho(r)/\rho_0$$
$$= -1/2 \cdot \hbar c \cdot \rho(r) \cdot \sigma_{inel} \cdot \beta$$

- excitation function
- momentum distribution

- transparency ratio measurement

$$T_A = \frac{\sigma_{\gamma A \to \eta' X}}{A \cdot \sigma_{\gamma N \to \eta' X}}$$

D. Cabrera et al., NPA733 (2004)130

Determining the real part of the meson-nucleus potential from excitation functions and momentum distributions

sensitive to nuclear density at the production point

excitation function

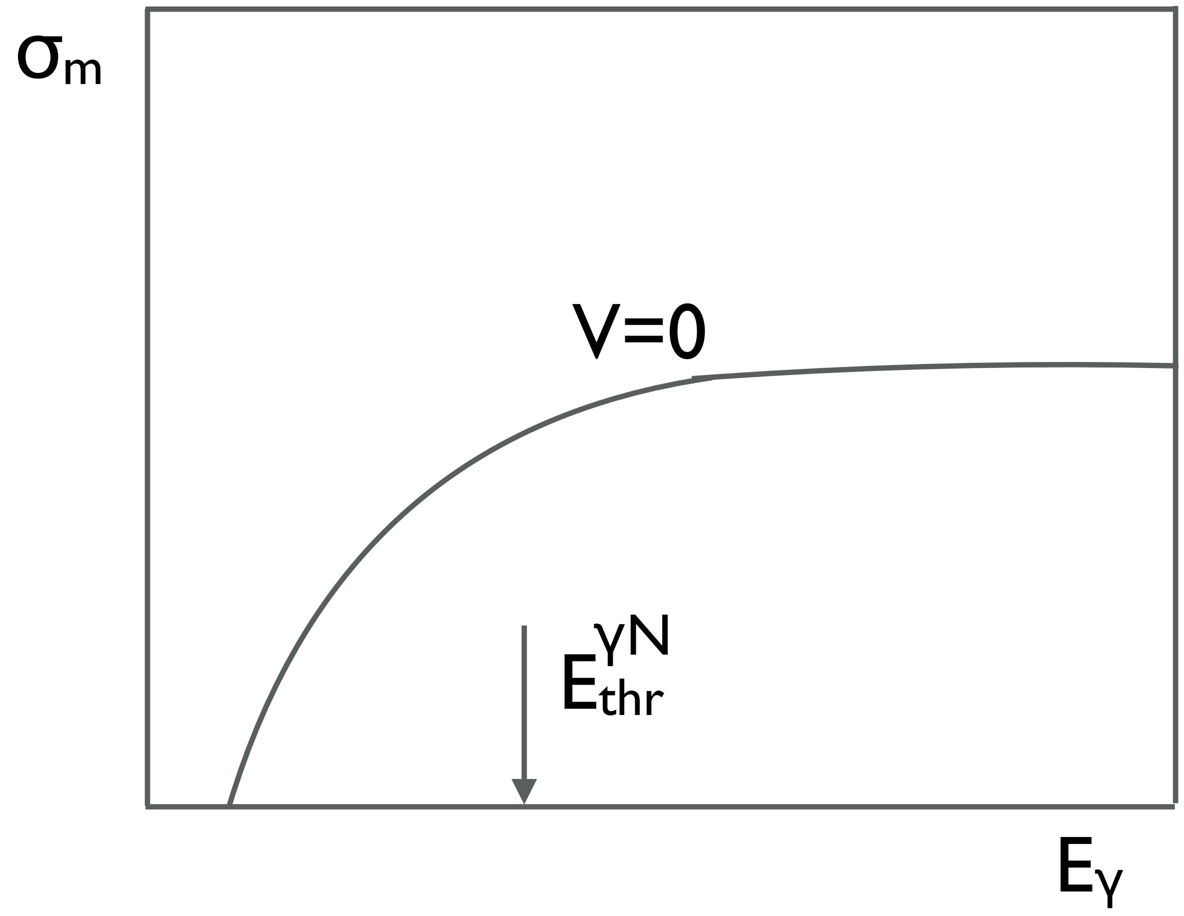

Determining the real part of the meson-nucleus potential from excitation functions and momentum distributions

sensitive to nuclear density at the production point

excitation function

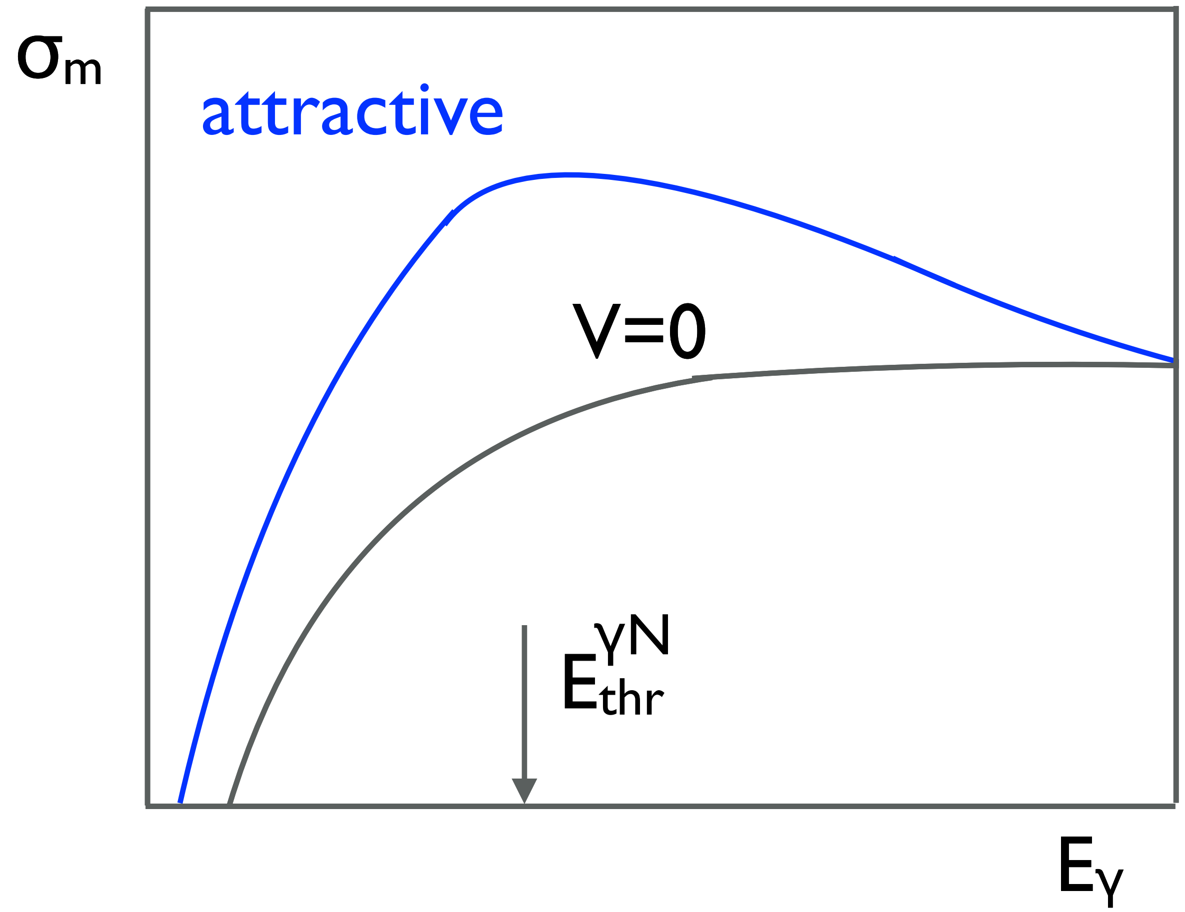

attractive interaction → mass drop →
lower threshold → larger phase space→
larger cross section

Determining the real part of the meson-nucleus potential from excitation functions and momentum distributions

sensitive to nuclear density at the production point

excitation function

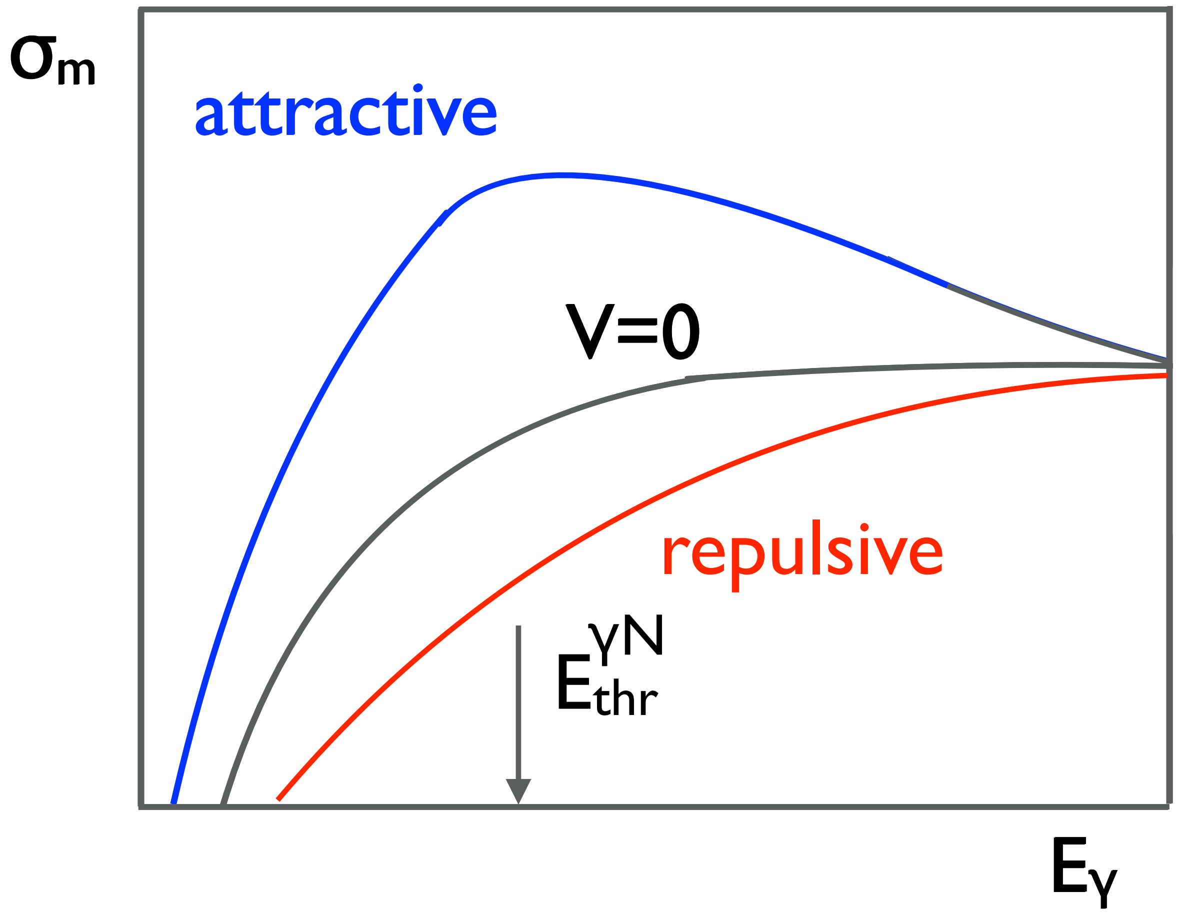

attractive interaction → mass drop → lower threshold → larger phase space→ larger cross section

repulsive interaction → mass increase → higher threshold → smaller phase space→ smaller cross section

Determining the real part of the meson-nucleus potential from excitation functions and momentum distributions

sensitive to nuclear density at the production point

excitation function

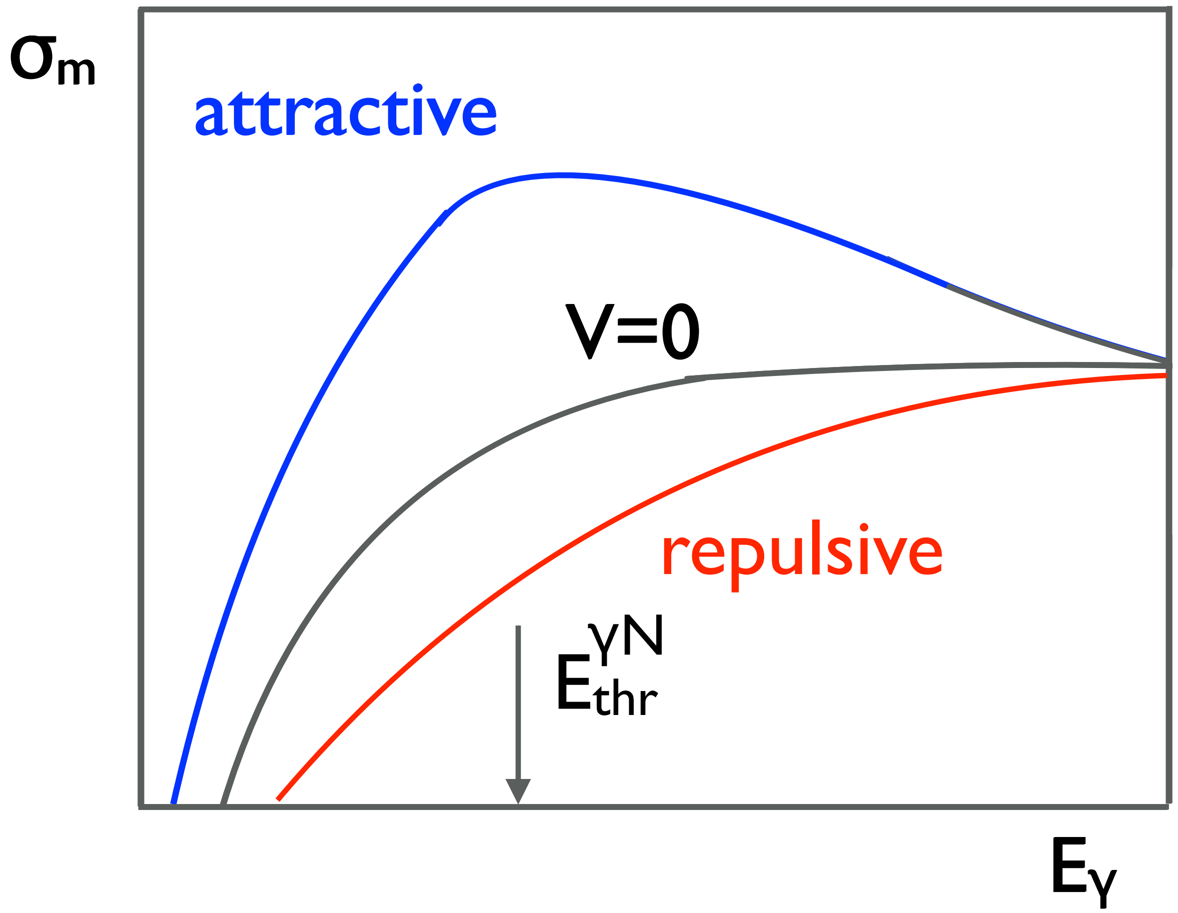

momentum distribution

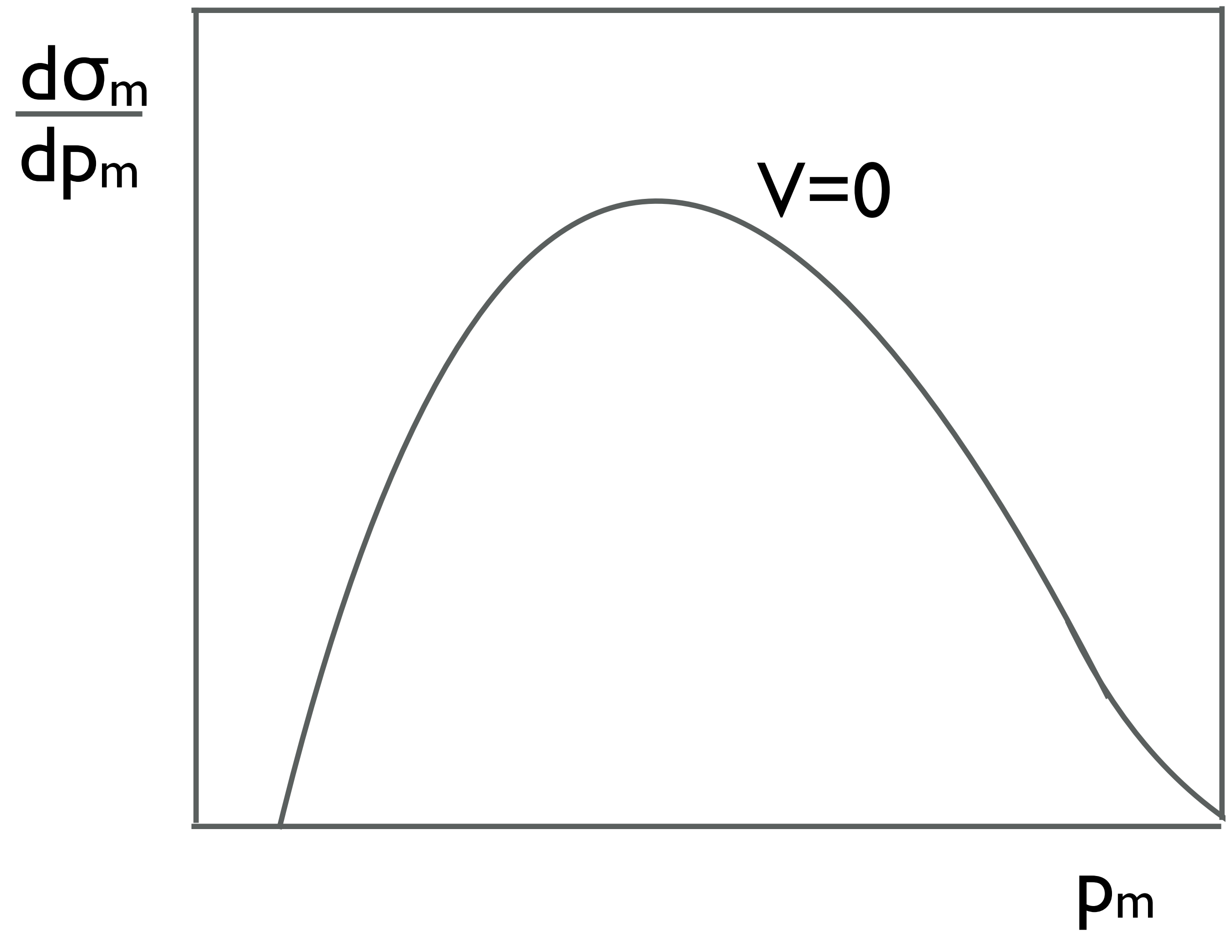

attractive interaction → mass drop → lower threshold → larger phase space→ larger cross section

repulsive interaction → mass increase → higher threshold → smaller phase space→ smaller cross section

Determining the real part of the meson-nucleus potential from excitation functions and momentum distributions

sensitive to nuclear density at the production point

excitation function

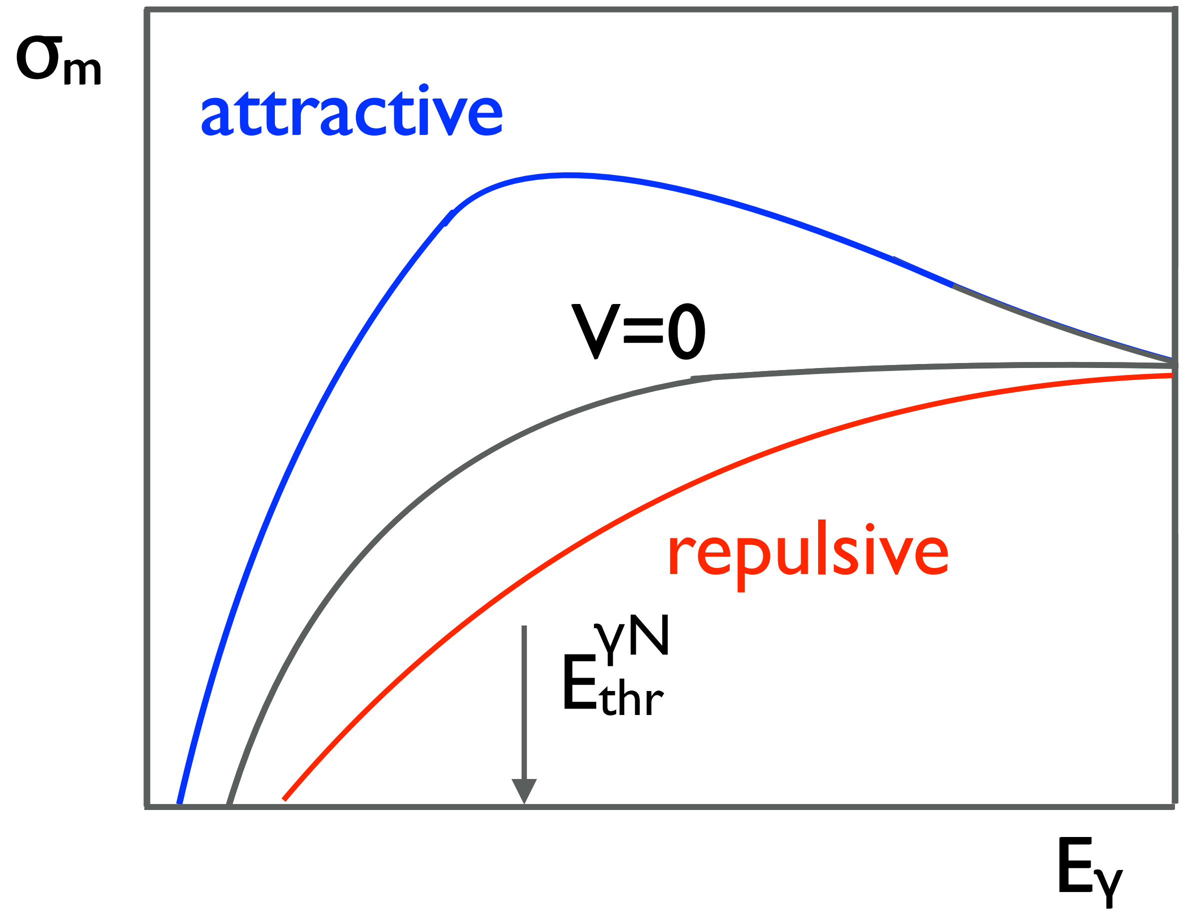

momentum distribution

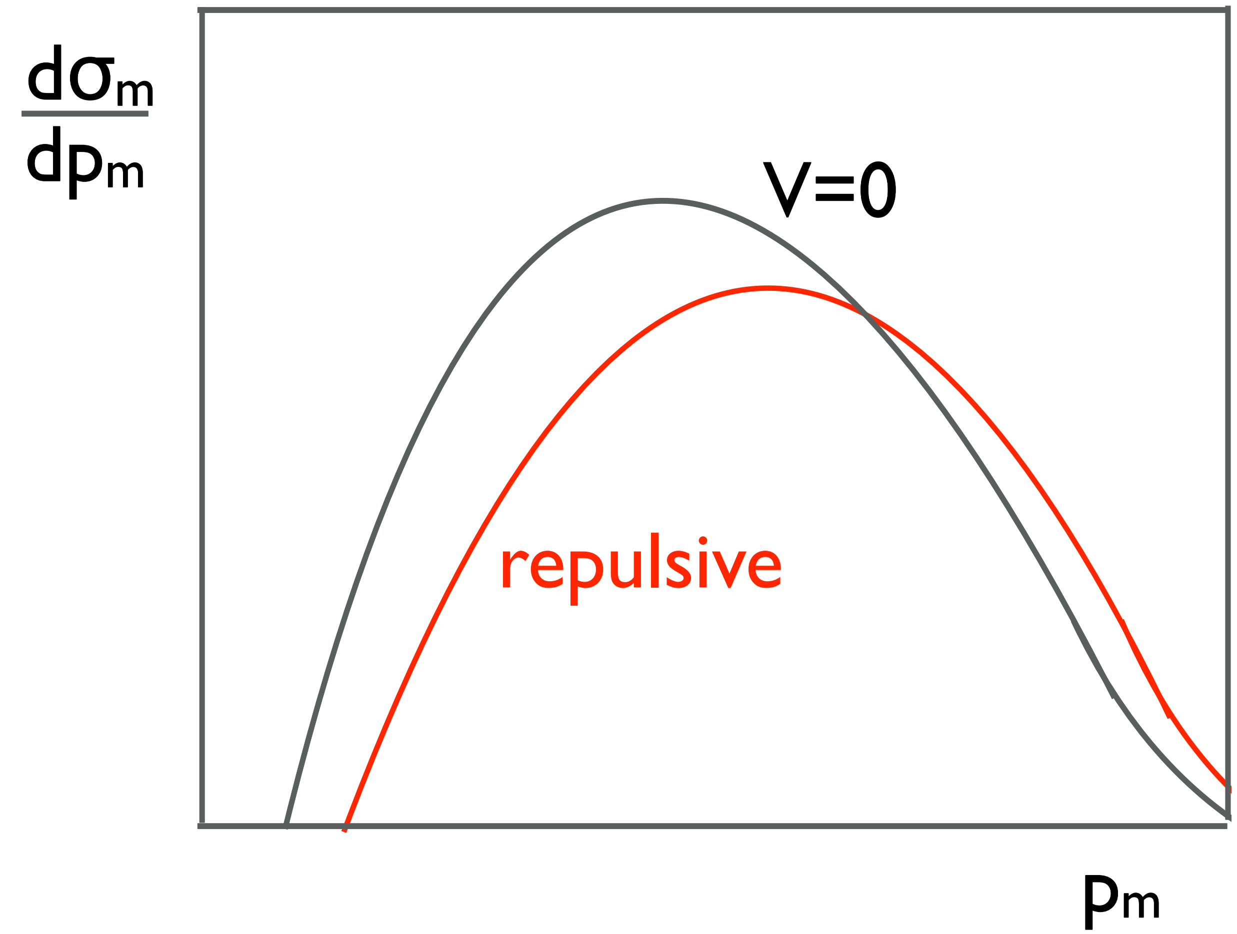

attractive interaction → mass drop → lower threshold → larger phase space→ larger cross section

repulsive interaction → mass increase → higher threshold → smaller phase space→ smaller cross section

repulsive interaction → extra kick → shift to higher momenta

Determining the real part of the meson-nucleus potential from excitation functions and momentum distributions

sensitive to nuclear density at the production point

excitation function

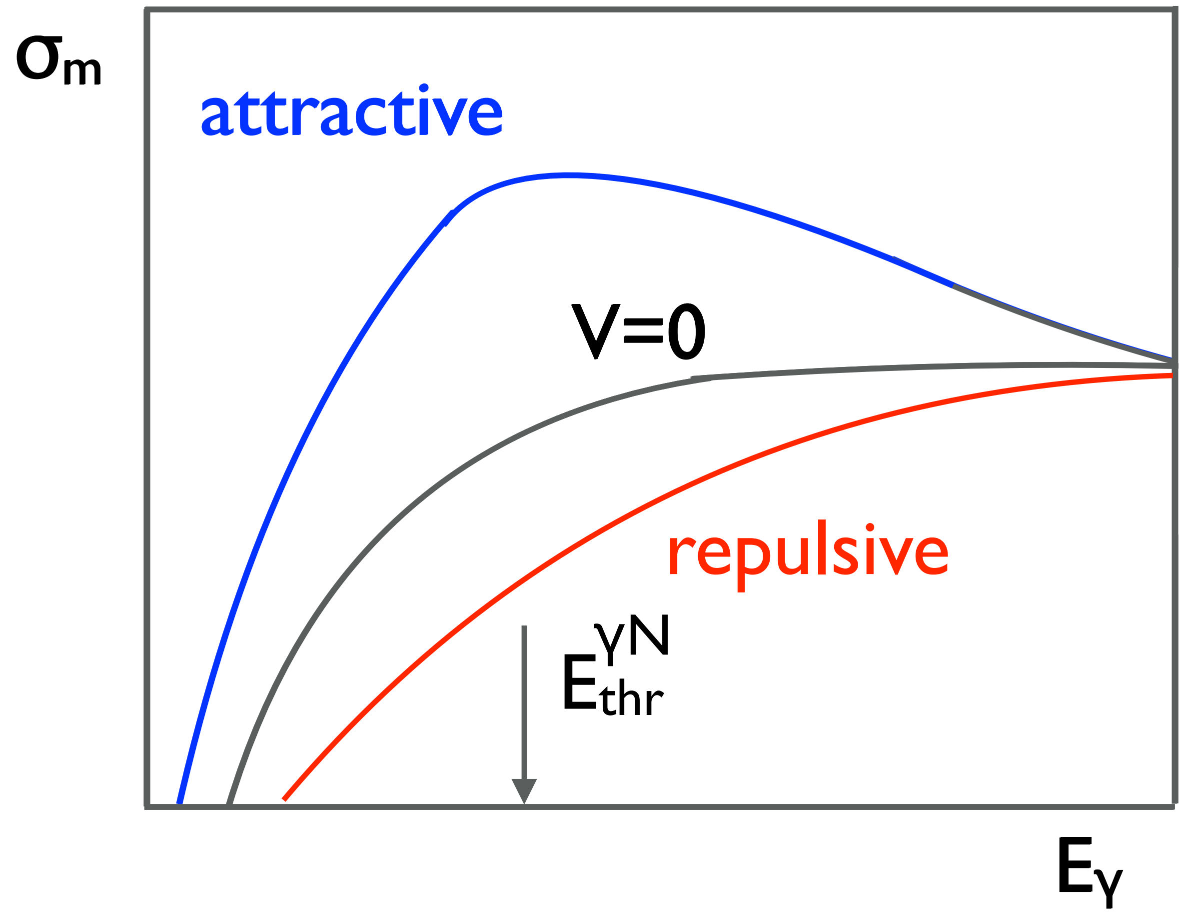

momentum distribution

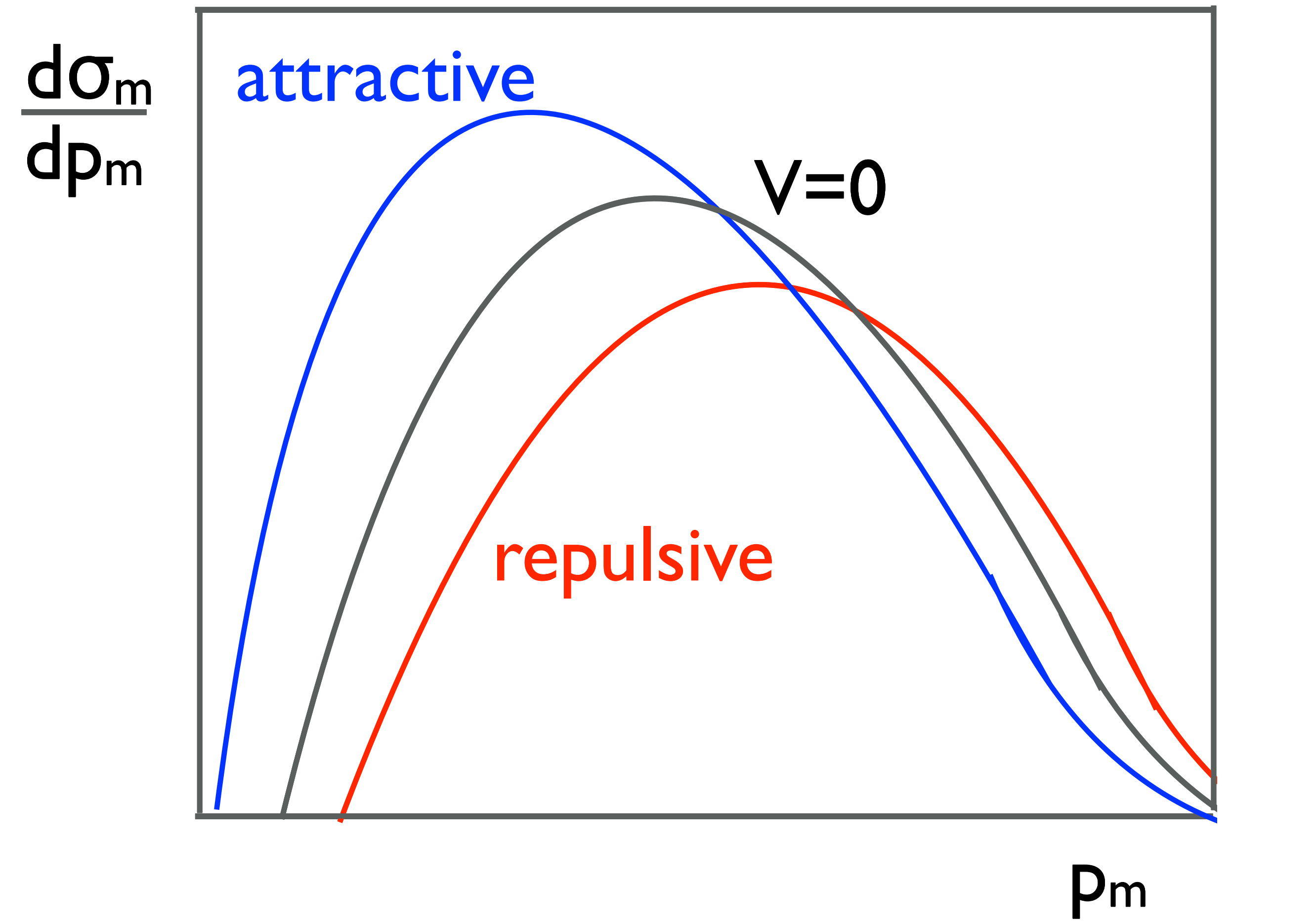

attractive interaction → mass drop → lower threshold → larger phase space→ larger cross section

repulsive interaction → mass increase → higher threshold → smaller phase space→ smaller cross section

repulsive interaction → extra kick → shift to higher momenta

attractive interaction → meson slowed down → shift to lower momenta

Determining the real part of the meson-nucleus potential from excitation functions and momentum distributions

sensitive to nuclear density at the production point

excitation function

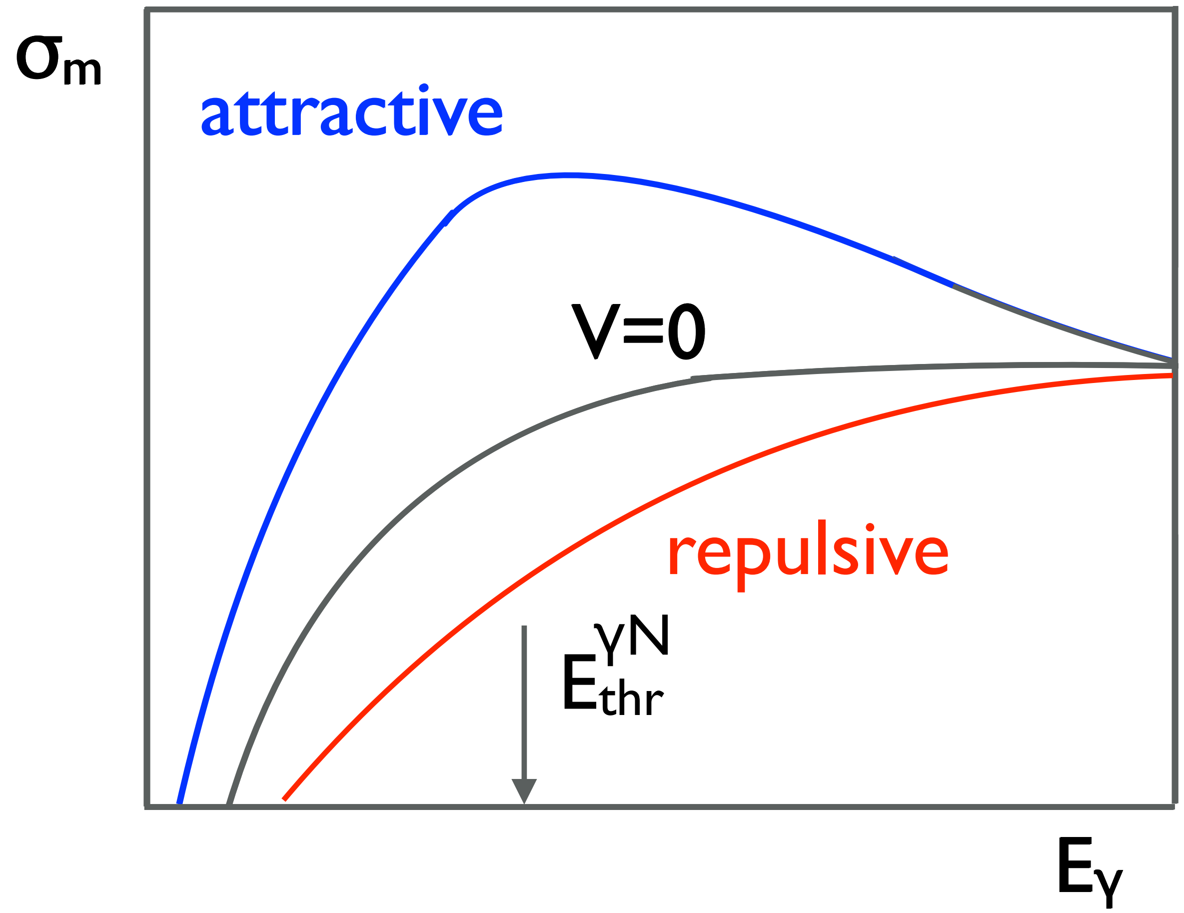

momentum distribution

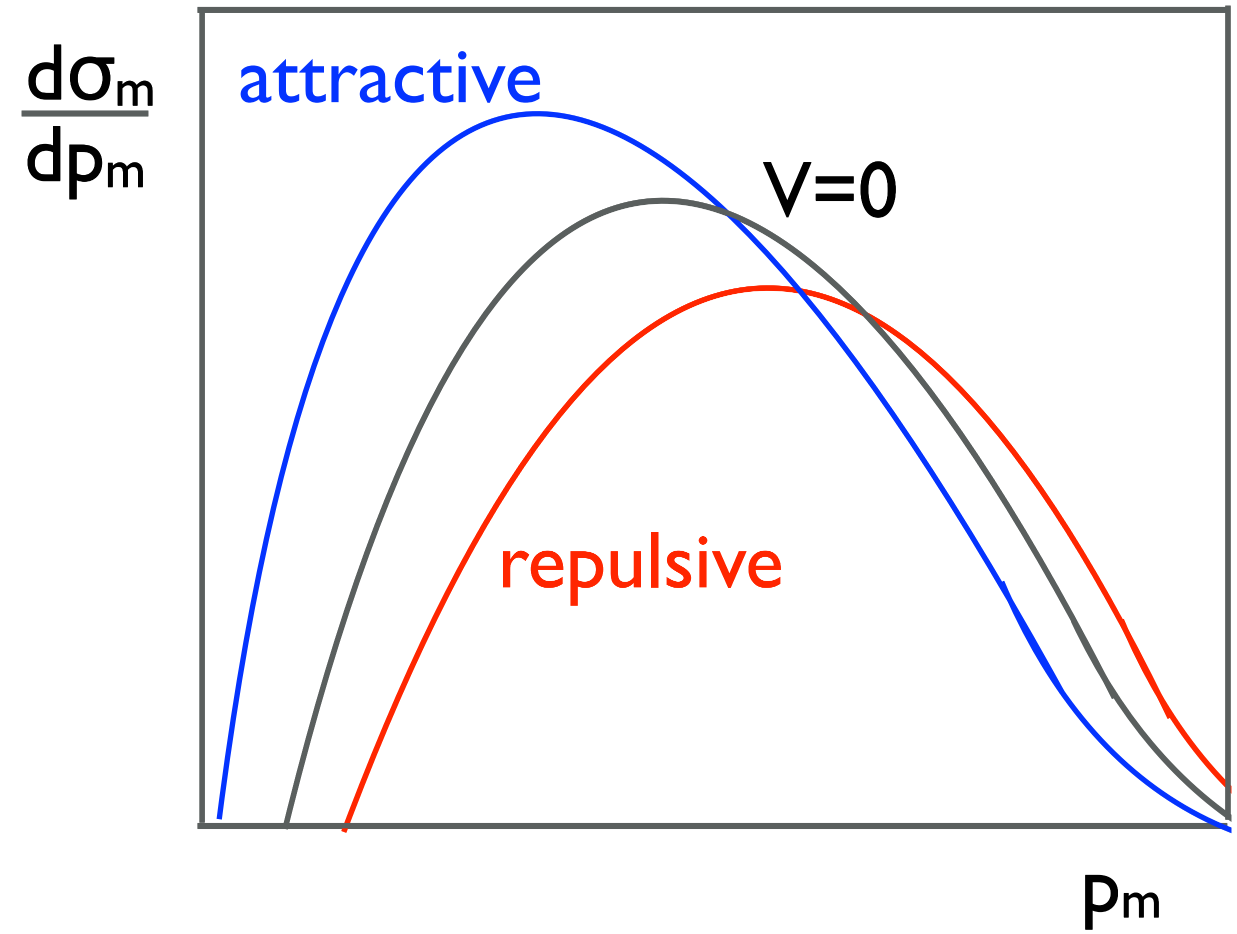

attractive interaction → mass drop → lower threshold → larger phase space→ larger cross section

repulsive interaction → mass increase → higher threshold → smaller phase space→ smaller cross section

repulsive interaction → extra kick → shift to higher momenta

attractive interaction → meson slowed down → shift to lower momenta

quantitative analysis requires transport model or collision model calculations

test of method

Coulomb interaction among charged pions and the fireball in heavy-ion collisions

Eur. Phys. J. A 56 (2020) 259

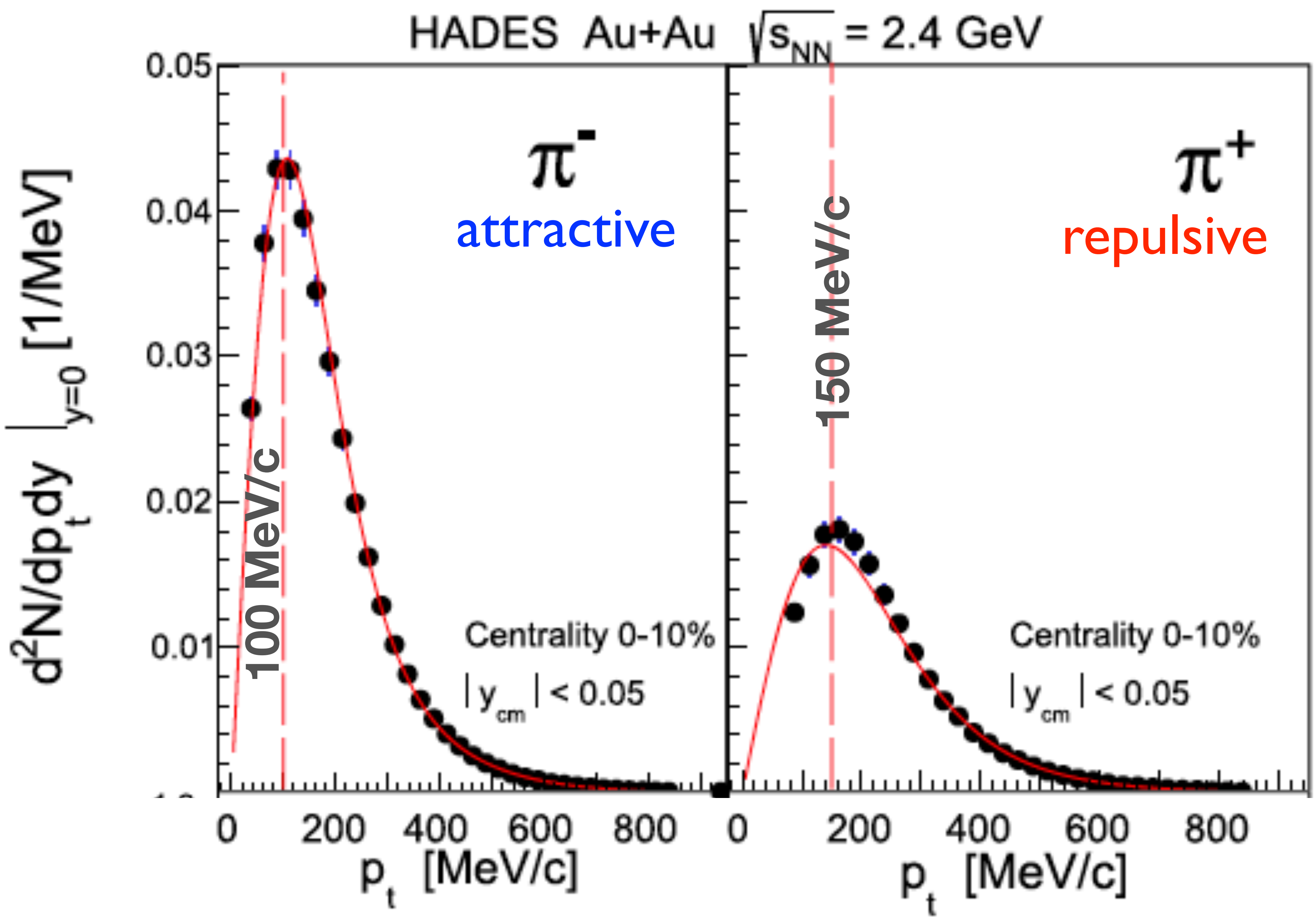

spectrum shifted to smaller (larger) momenta for π^+ (π^-) mesons

$V_c \approx 15$ MeV; paper in preparation

Determining the imaginary part of the meson-nucleus potential from transparency ratio measurements

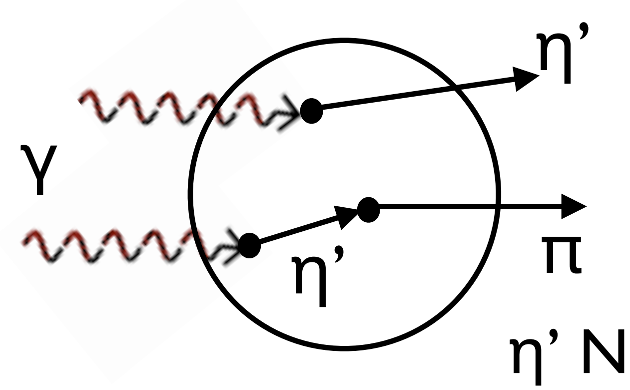

η' N → π N

$$T_A = \frac{\sigma_{\gamma A \to \eta' X}}{A \cdot \sigma_{\gamma N \to \eta' X}}$$

D. Cabrera et al., NPA733 (2004)130

transport model calculation: GiBUU

P. Mühlich and U. Mosel, NPA 773 (2006) 156

$\gamma A \to \omega X$ at E_γ=1.5 GeV

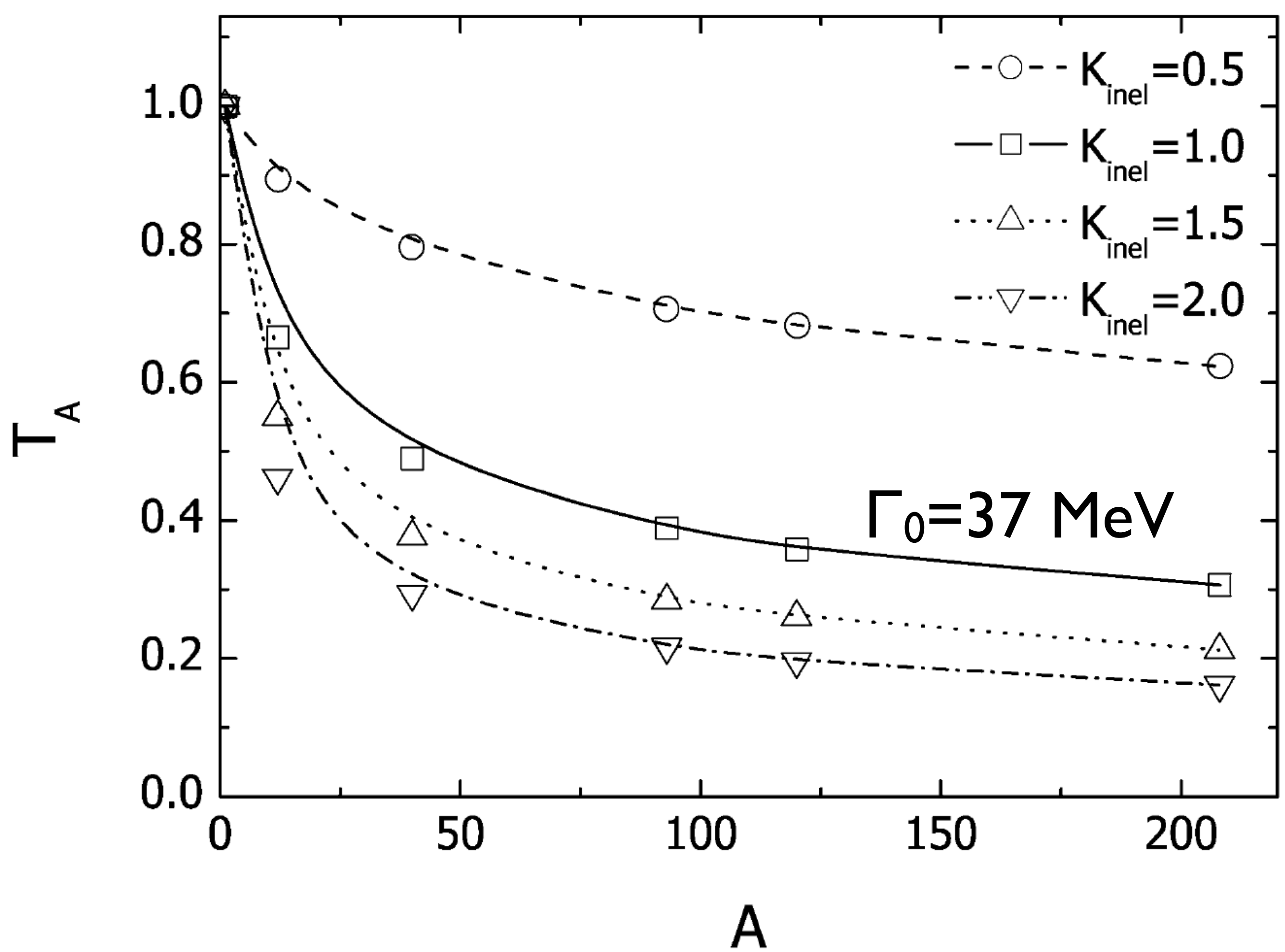

collision model calculation

E. Ya. Paryev, J. Phys.G 40 (2013)025201

$\gamma A \to \eta' X$ at E_γ=1.9 GeV

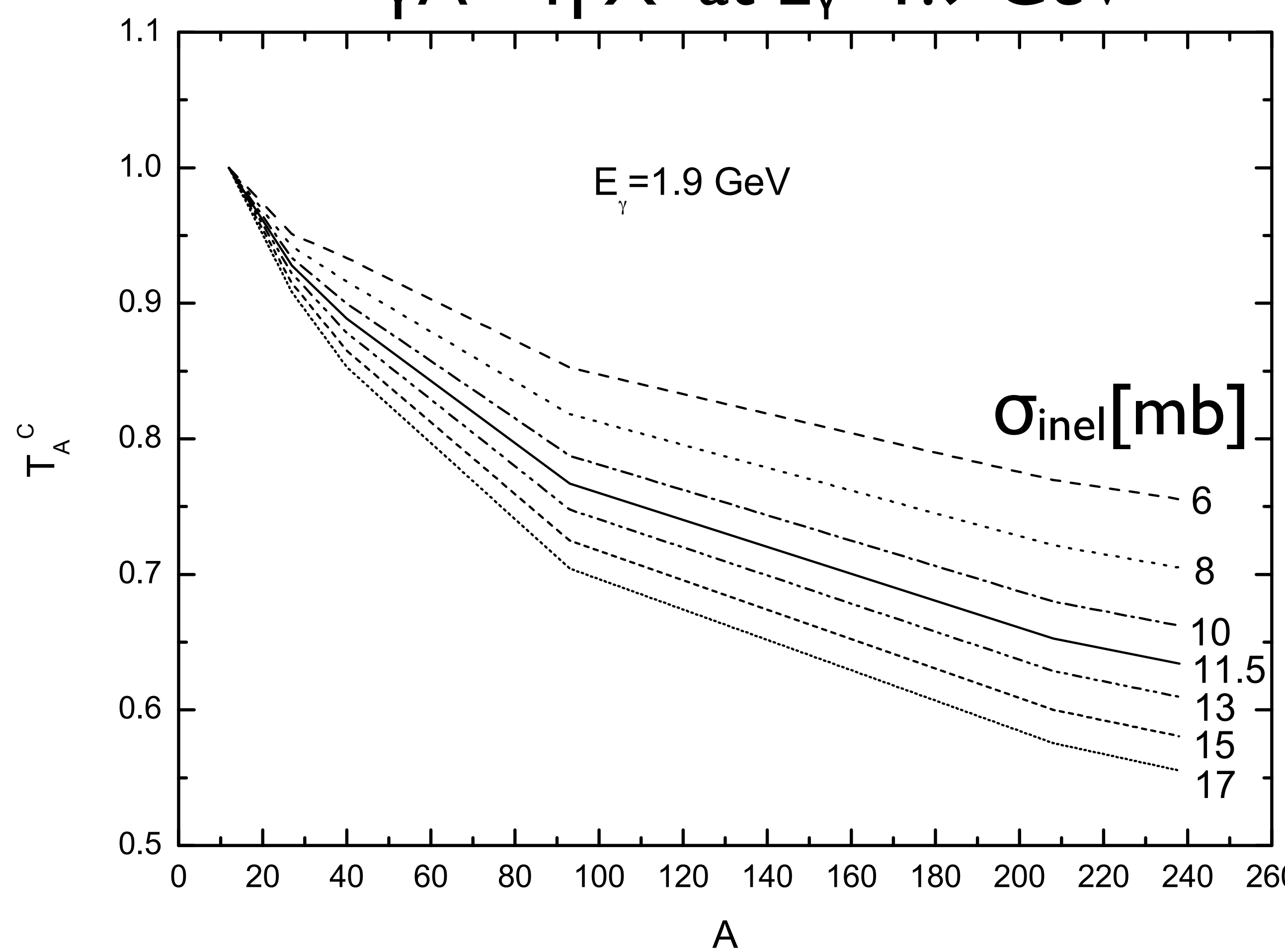

$$W(\rho=\rho_0) = -\Gamma/2\ (\rho=\rho_0) = -1/2 \cdot \hbar c \cdot \rho_0 \cdot \sigma_{inel} \cdot \beta$$

Determining the real part and imaginary part of the ω-nucleus potential from measurement of excitation function and transparency ratio

<u>real part</u> from excitation function

V. Metag et al., Prog. Part. Nucl. Phys. 67 (2012) 530

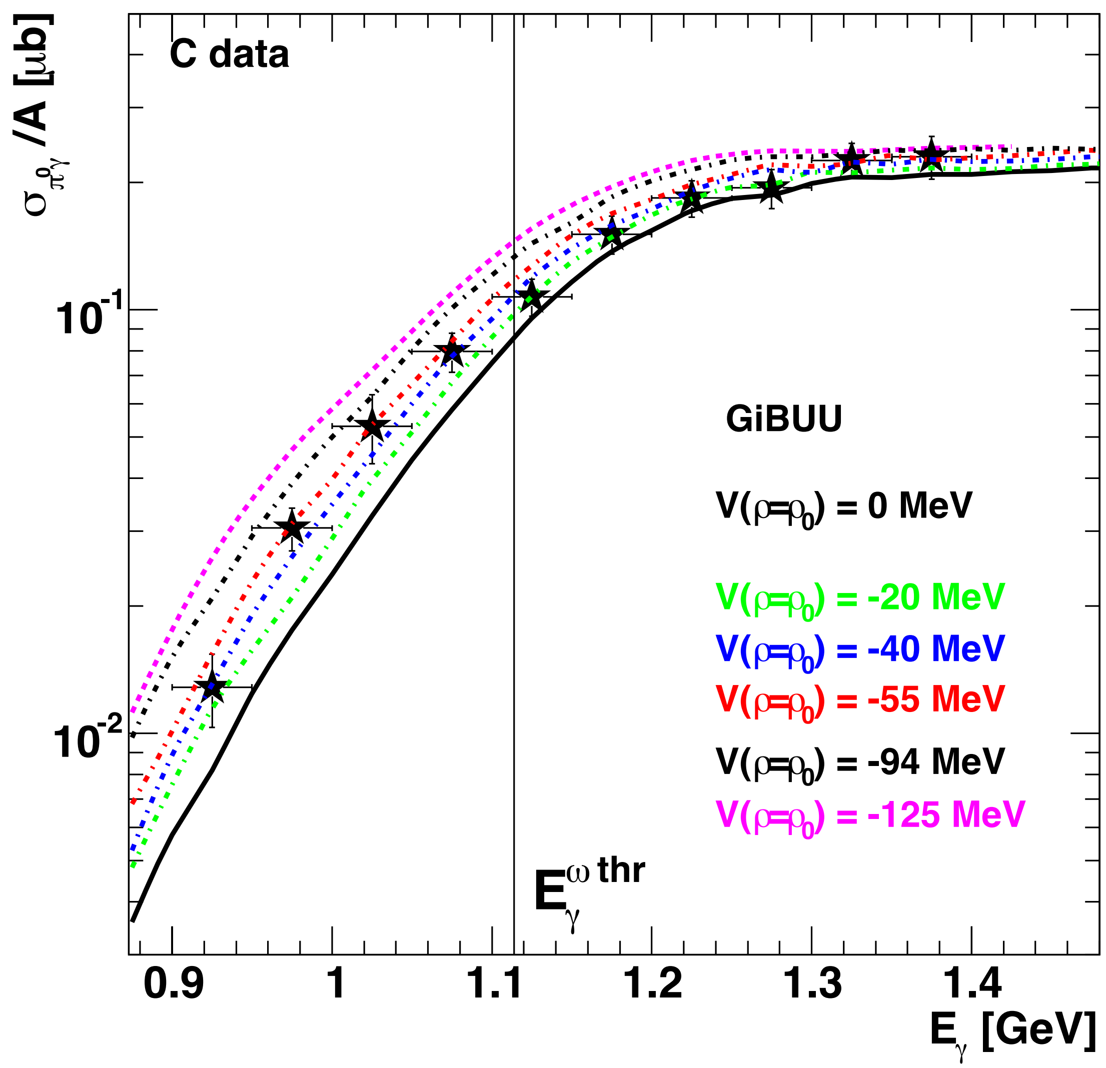

including information from momentum distributions (S. Friedrich et al. PLB 736 (2014) 26)

$V_{\omega A}(\rho=\rho_0)$ = - (29±19(stat)± 20(syst)) MeV

<u>imaginary part</u> from transparency ratio

$$T_A = \frac{\sigma_{\gamma A \to \omega X}}{A \cdot \sigma_{\gamma N \to \omega X}}$$

ω

M. Kotulla et al., PRL 100 (2008) 192302
PRL 114 (2015) 199903

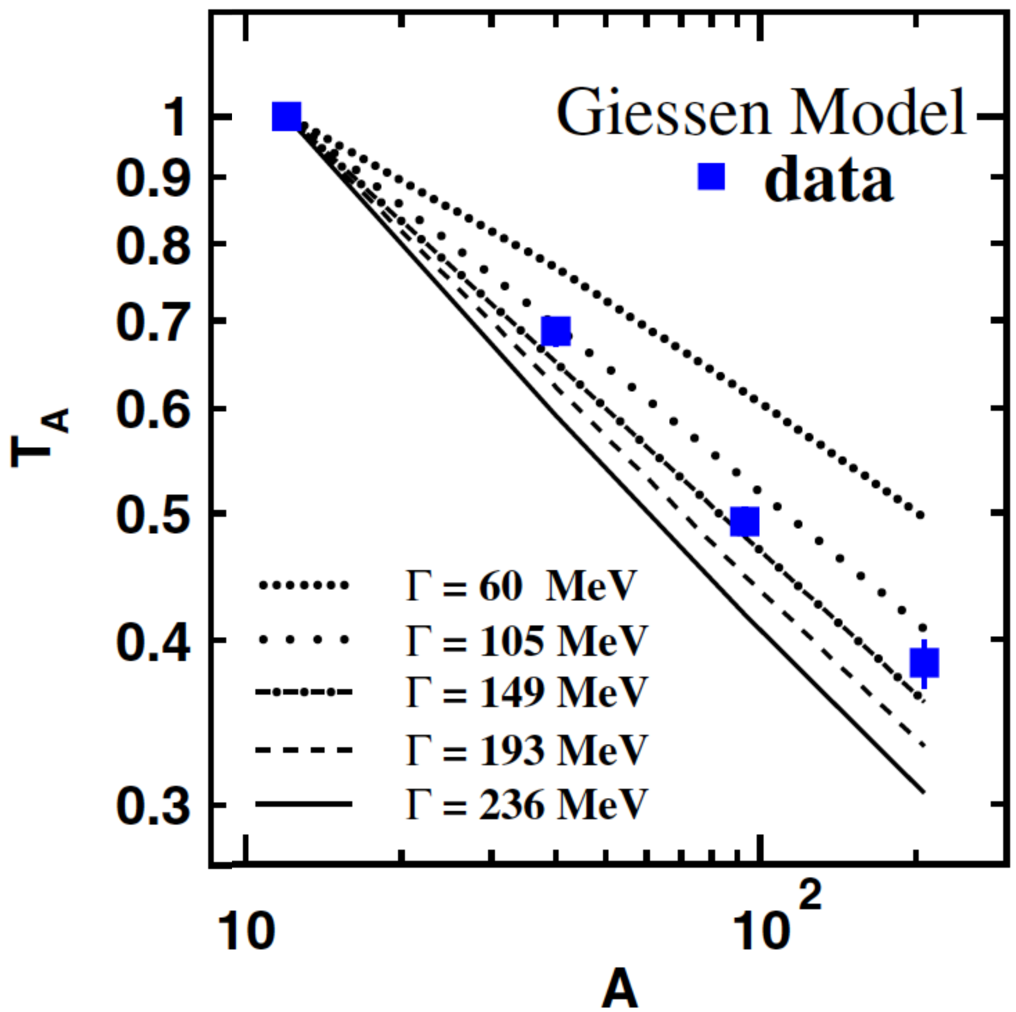

Γ(ρ=ρ0) ≈ 120 MeV

Determining the real part and imaginary part of the ω-nucleus potential from measurement of excitation function and transparency ratio

<u>real part</u> from excitation function

V. Metag et al., Prog. Part. Nucl. Phys. 67 (2012) 530

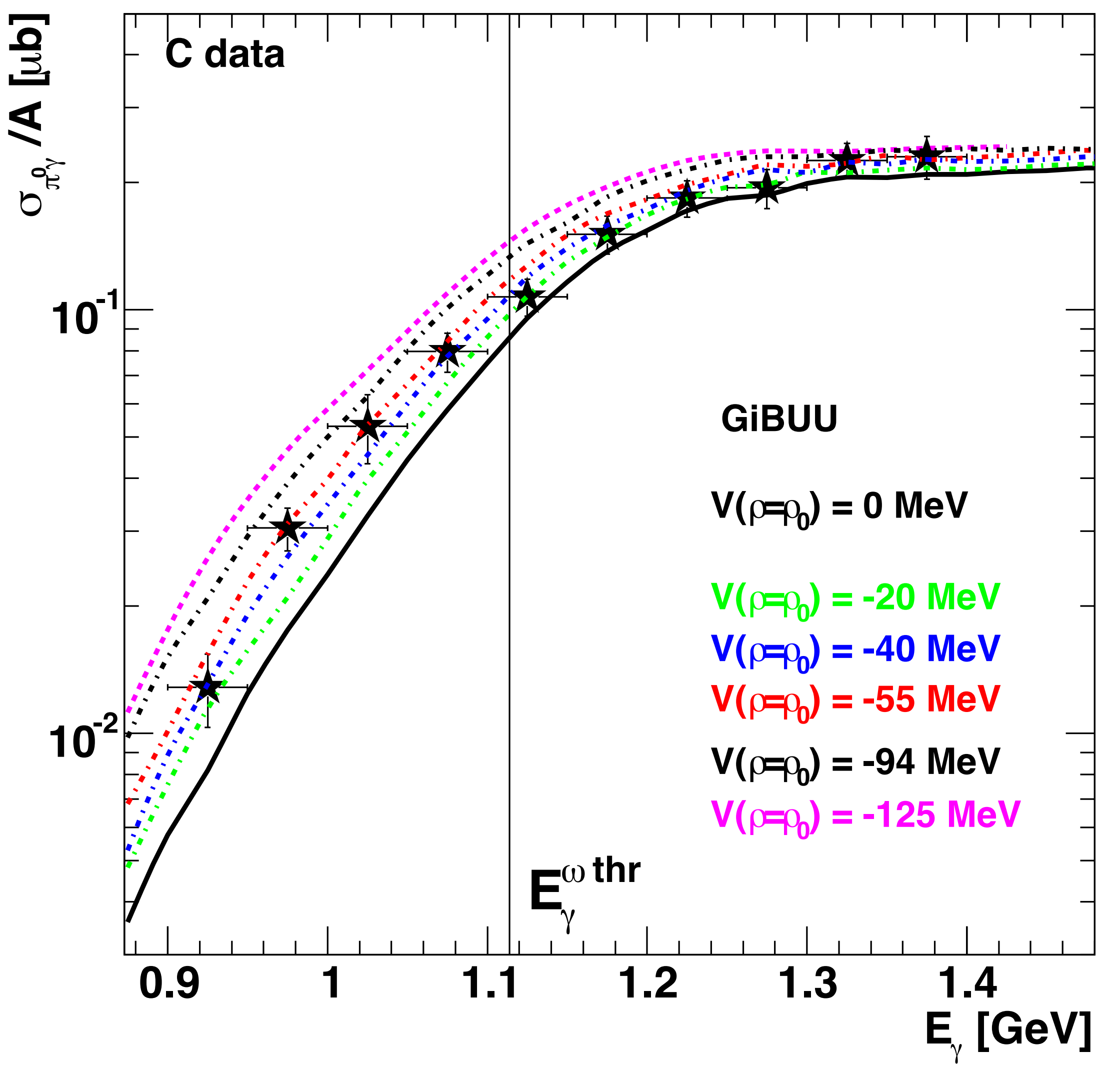

including information from momentum distributions (S. Friedrich et al. PLB 736 (2014) 26)

$V_{\omega A}(\rho=\rho_0) = -(29\pm19(stat)\pm20(syst))$ MeV

<u>imaginary part</u> from transparency ratio

$$T_A = \frac{\sigma_{\gamma A\rightarrow\omega X}}{A\cdot\sigma_{\gamma N\rightarrow\omega X}}$$

ω

S. Friedrich et al. EPJA 52 (2016) 297

momentum dependence of W

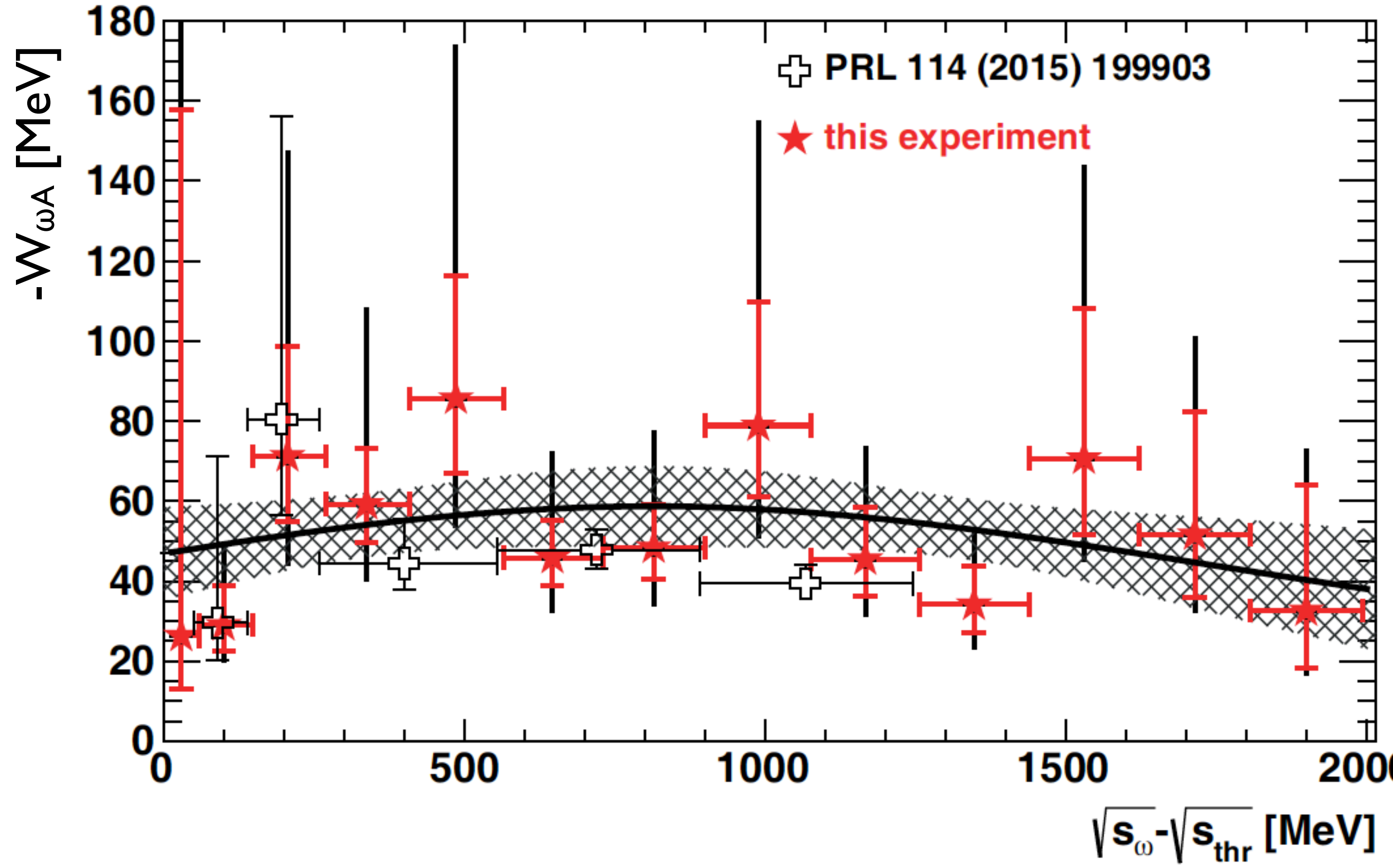

$W_{\omega A}(p_\omega=0) = -(48\pm12(stat)\pm9(syst))$ MeV

|V| ≤ |W| !! ω no good candidate for meson-nucleus bound states !!

Determining the real part of the η'-nucleus potential from measurement of excitation function and momentum distributions

CBELSA/TAPS @ ELSA

$\gamma\, C \rightarrow \eta' X$

data: M. Nanova et al., PLB 727 (2013) 417

calc.: E. Paryev, J. Phys. G 40 (2013) 025201

η'

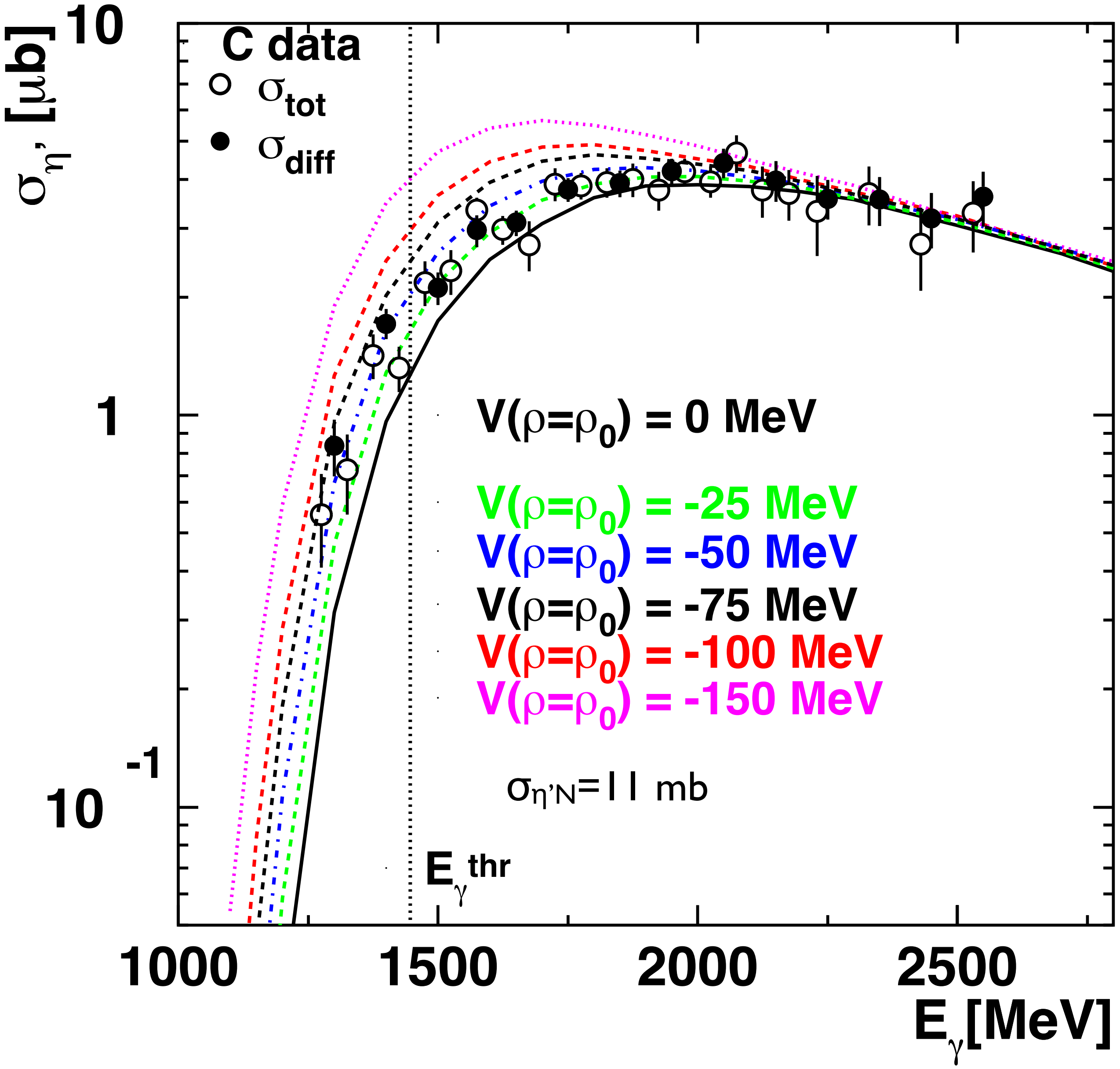

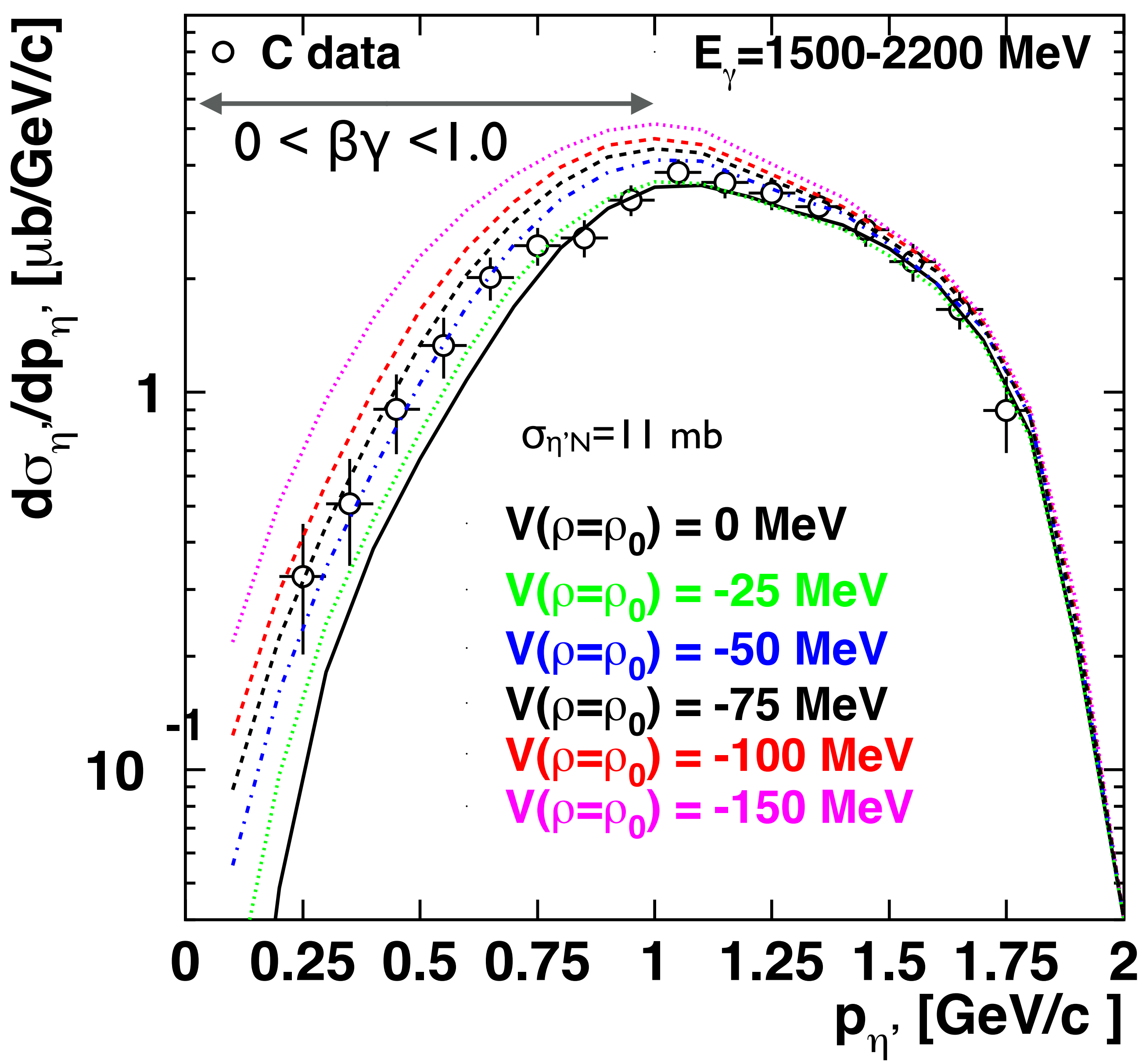

$V_{\eta'}(\rho=\rho_0) = -(40\pm6)$ MeV $V_{\eta'}(<p_{\eta'}>\approx1.1\ \mathrm{GeV/c};\rho=\rho_0) = -(32\pm11)$ MeV

data disfavour strong mass shifts

Determining the imaginary part of the η' - nucleus potential from transparency ratio measurements

η'

$$T_A = \frac{\sigma_{\gamma A \to \eta' X}}{A \cdot \sigma_{\gamma N \to \eta' X}}$$

mass dependence of T_A

M. Nanova et al., PLB 710 (2012) 600

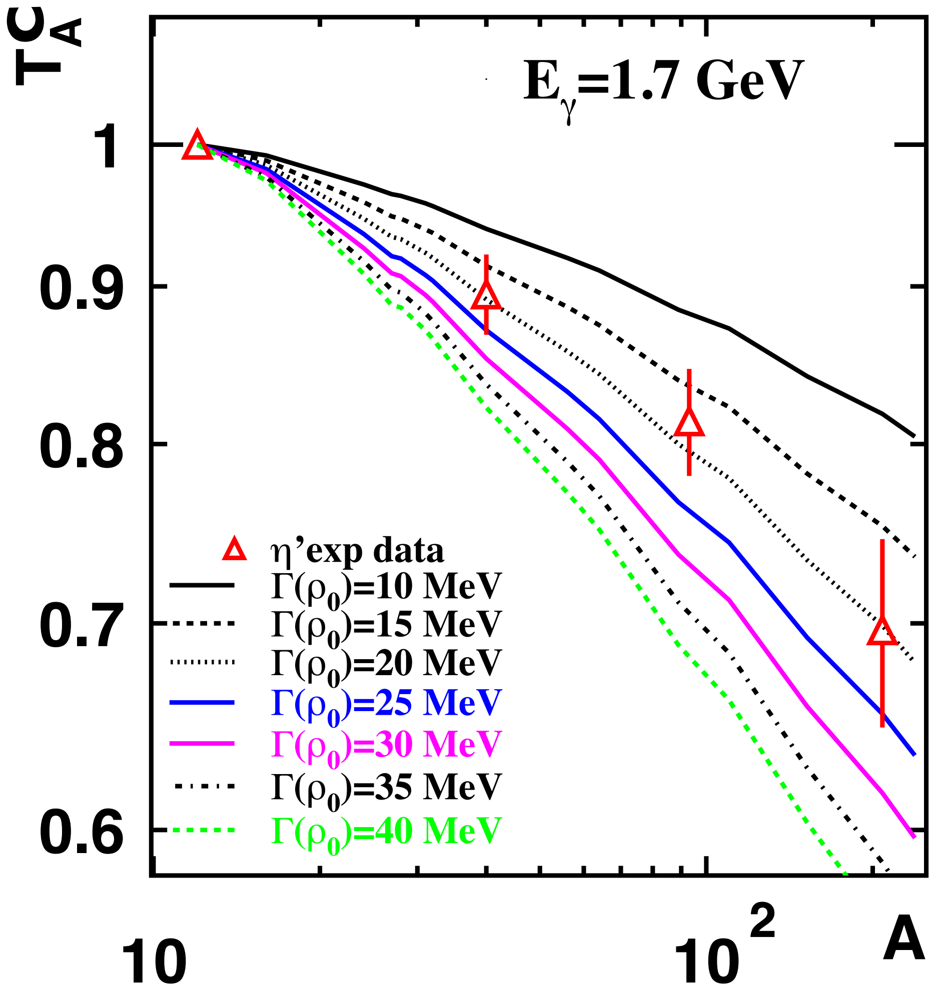

$\Gamma_{\eta'}(\rho=\rho_0)$ =15-25 MeV

momentum dependence of W_0

S. Friedrich et al., EPJA 52 (2016) 297

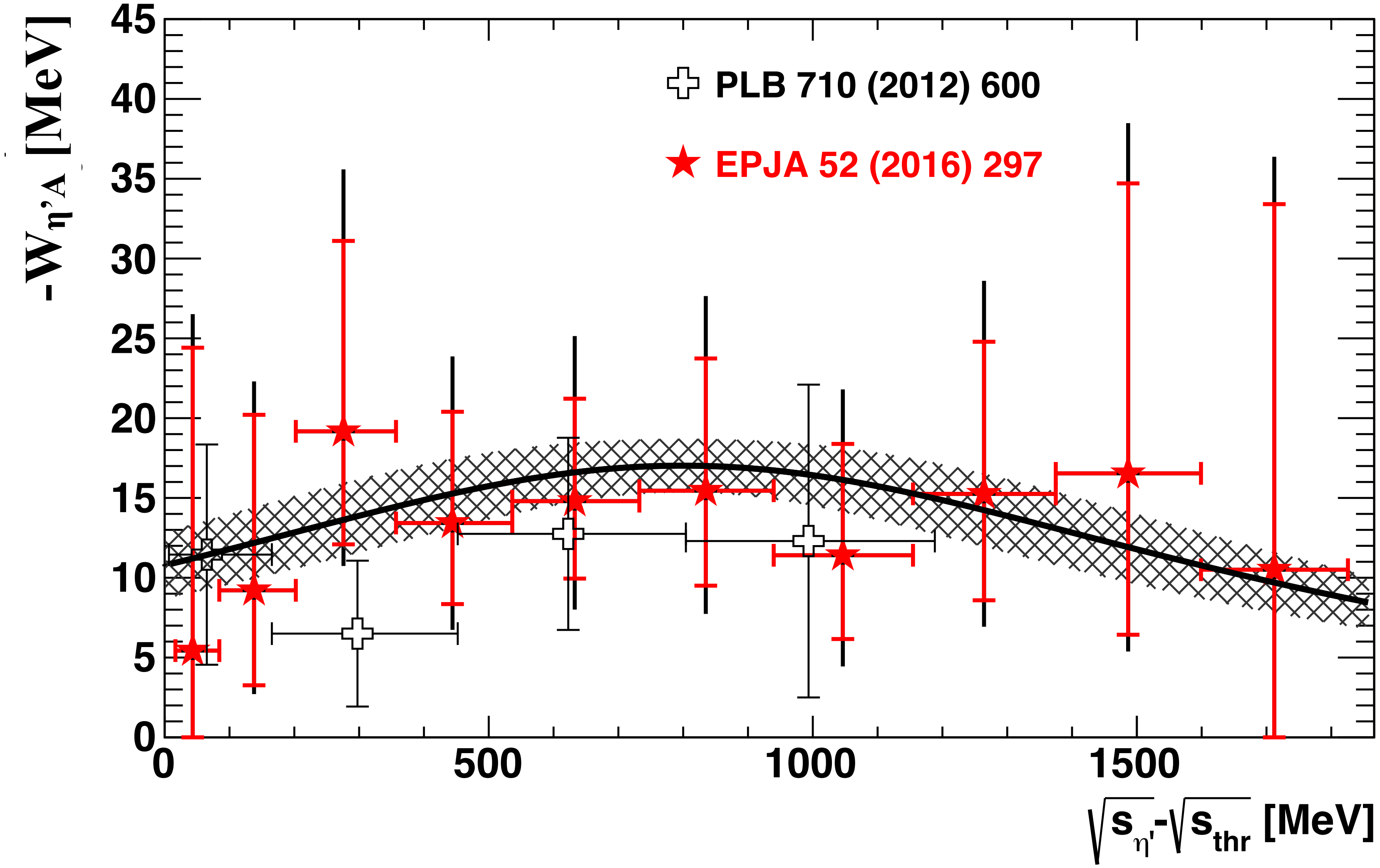

$$W_0 = \text{Im } U(\rho=\rho_0, p_{\eta'}=0) = -[13\pm3(\text{stat})\pm3(\text{syst})] \text{ MeV}$$

Real and imaginary part of the η' - nucleus potential

η'

M. Nanova et al., PLB 727 (2013) 417
M. Nanova et al., PRC 94 (2016) 025205
M. Nanova et al., EPJ A 54 (2018) 182
S. Friedrich et al., EPJA 52 (2016) 297

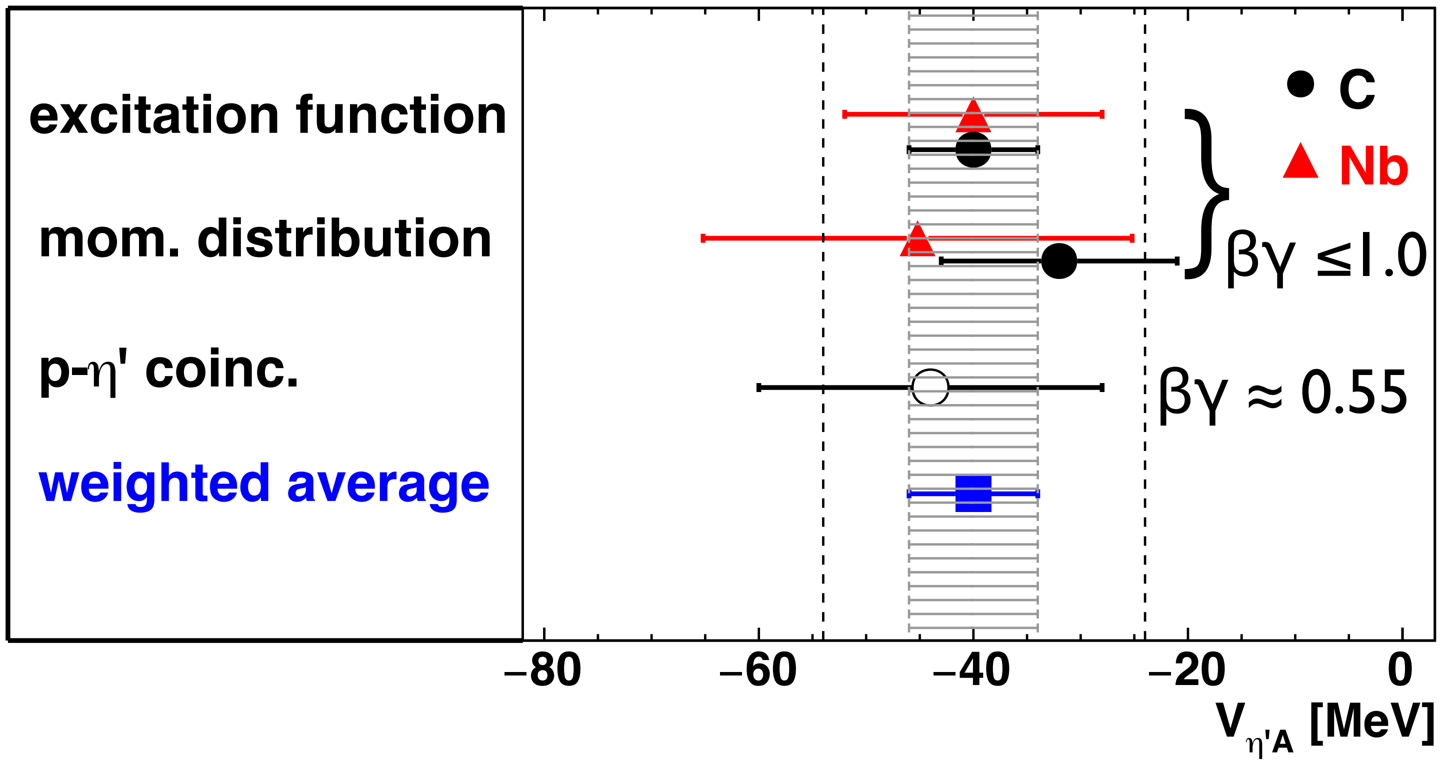

$V_0 = \Delta m(\rho=\rho_0) = -$ [40±(stat)±15(syst)] MeV

$W_0 = \mathrm{Im}\, U(\rho=\rho_0, p_{\eta'}\approx 0) = -$ [13±3(stat)±3(syst)] MeV

observed mass shift in agreement with QMC model predictions

S. Bass and T. Thomas, PLB 634 (2006) 368

Real and imaginary part of the η' - nucleus potential

η'

M. Nanova et al., PLB 727 (2013) 417
M. Nanova et al., PRC 94 (2016) 025205
M. Nanova et al., EPJ A 54 (2018) 182
S. Friedrich et al., EPJA 52 (2016) 297

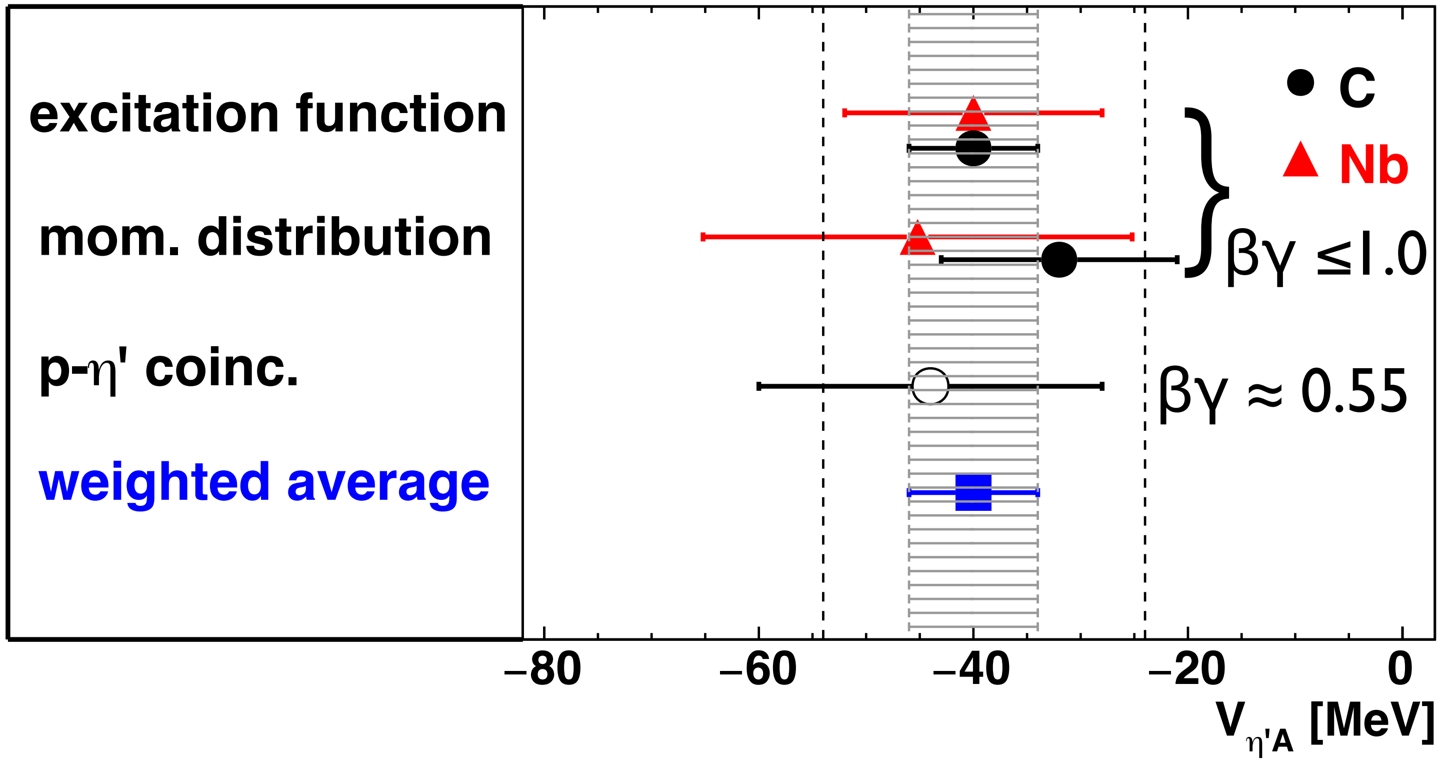

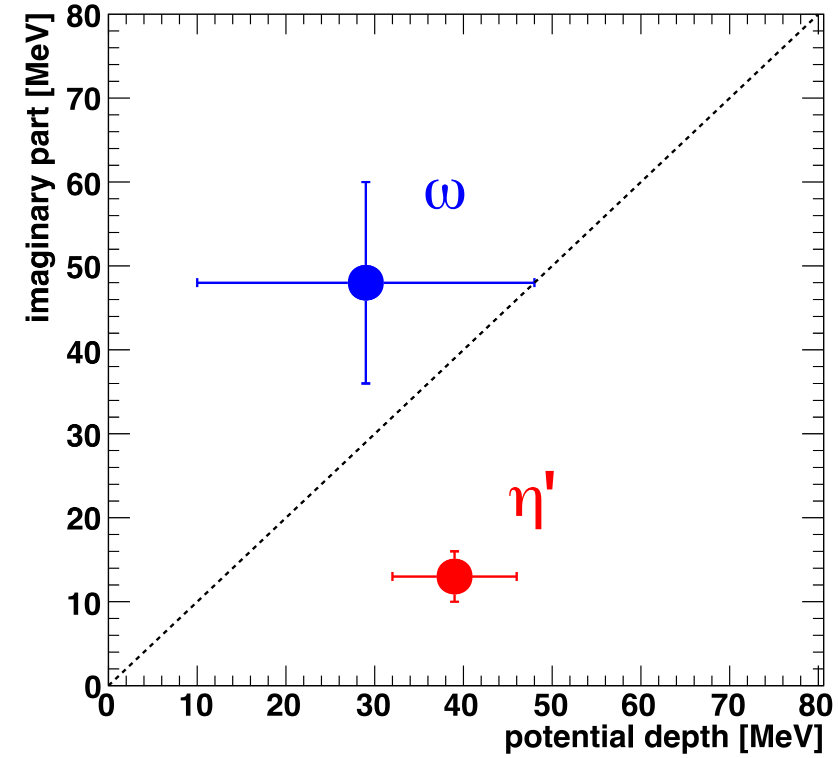

$V_0 = \Delta m(\rho=\rho_0) = -$ [40±(stat)±15(syst)] MeV

$W_0 = \mathrm{Im}\, U(\rho=\rho_0, p_{\eta'}\approx 0) = -$ [13±3(stat)±3(syst)] MeV

ω: $|V_0| \lesssim |W_0|$

η: $|V_0| >> |W_0|$

observed mass shift in agreement with QMC model predictions

S. Bass and T. Thomas, PLB 634 (2006) 368

η': $|V_0| >> |W_0|$ → better candidate for search for meson-nucleus bound states than the ω meson!

Determining the real part of the K⁰-nucleus potential from measurement of momentum distributions

K^0

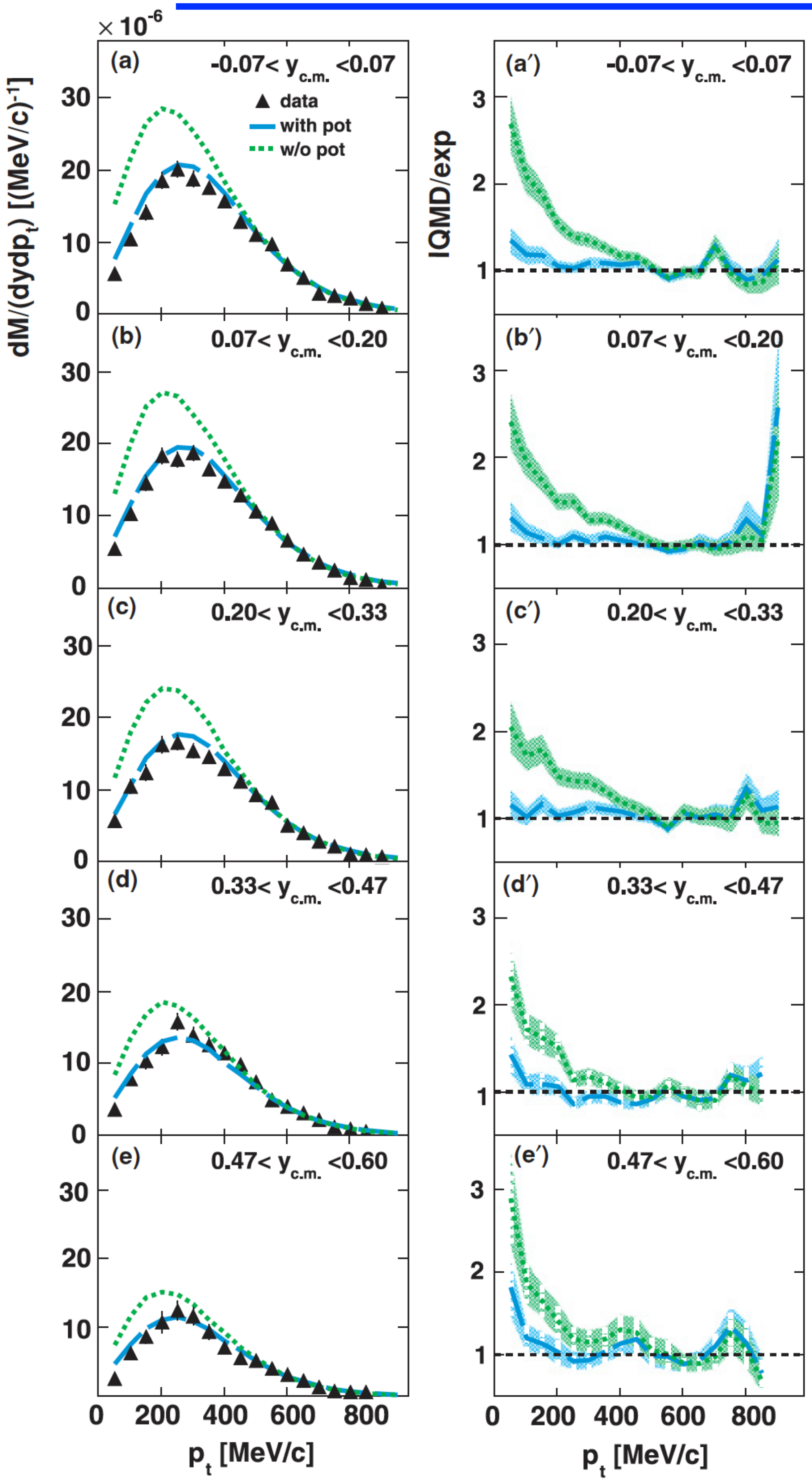

HADES: Ar + KCl at 1.756 AGeV

G. Agakishiev et al., PRC90 (2014) 054906

K^0 transverse momentum spectra compared to IQMD transport calculations without potential (green dotted) and with repulsive potential of +46 MeV (blue dashed curve)

V ≈+ 40 MeV

$\phi \rightarrow K^+K^-$ decays

HADES: π^- + C,W at p_π = 1.7 GeV/c

J. Adamczweski-Musch et al., PRL 123 (2019) 022002

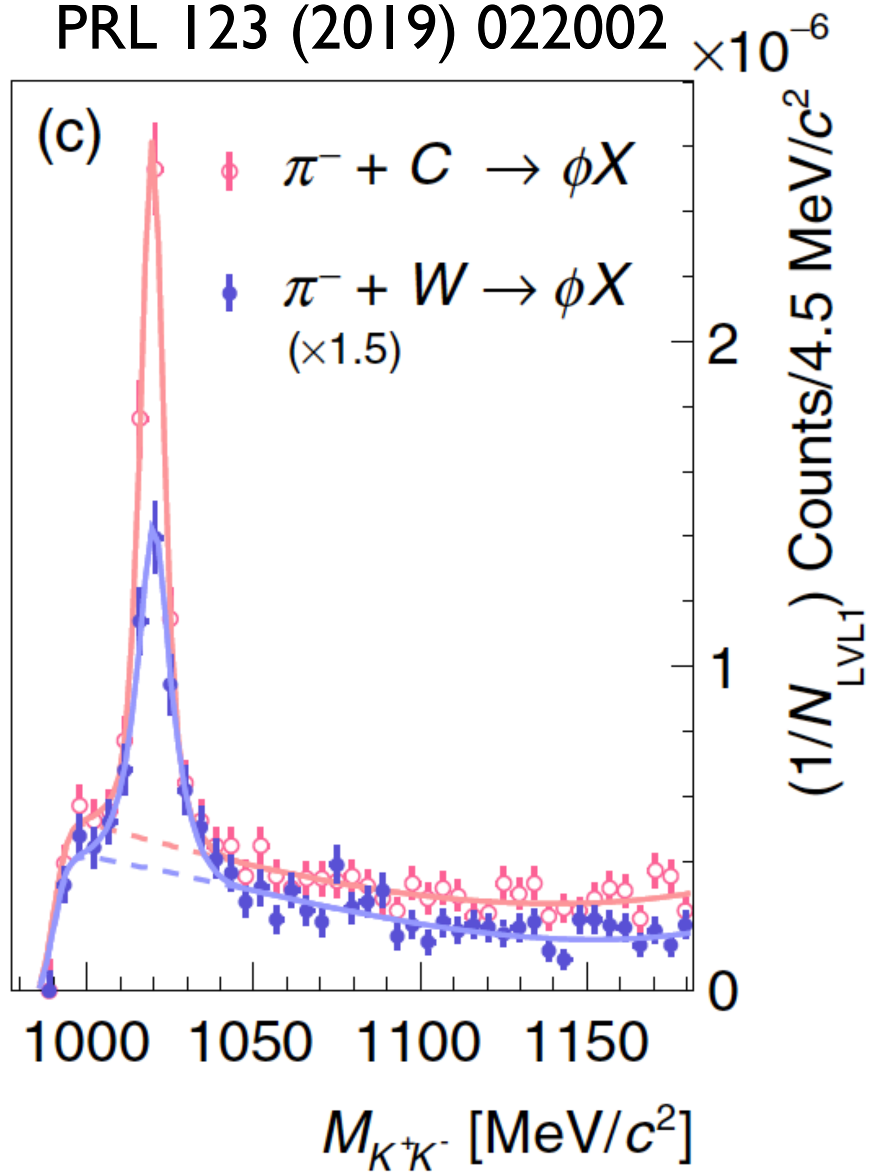

$(K^-/K^+)_W/(K^-/K^+)_C = 0.32\pm0.01$

→ strong K^- absorption

$(\Phi/K^-)_C = 0.55\pm0.04 \approx (\Phi/K^-)_W = 0.63\pm0.06$

→ sizeable Φ absorption

$$T = \frac{12}{184} \bullet \frac{\sigma_W^\Phi}{\sigma_C^\Phi} = 0.18\pm0.02\pm0.01^{+0.04}_{-0.043}$$

E. Ya. Paryev, Chin. Phys. C 42 (2018) 084101 and priv. com.

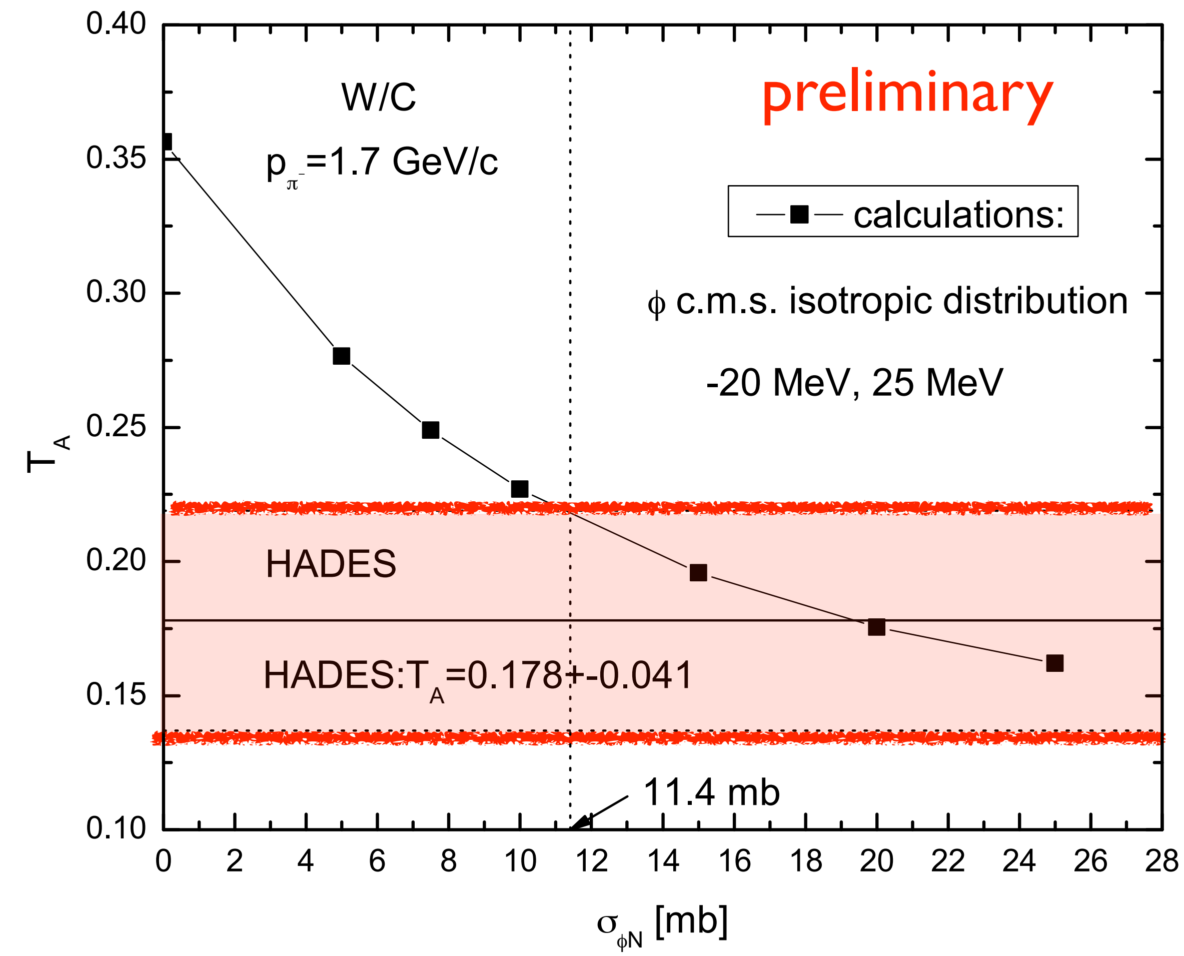

$\sigma_{abs}^\Phi \approx$ 20 mb; $W(\rho=\rho_0) \approx$ -20 MeV

earlier determinations of σ_{abs}^Φ

LEPS: (35^{+17}_{-11}) mb; ANKE: (15-25) mb

The meson-nucleus potential $U(\rho_0) = V(\rho_0) + i\,W(\rho_0)$

V. Metag, M. Nanova and E.Ya. Paryev, Prog. Part. Nucl. Phys.97 (2017) 199

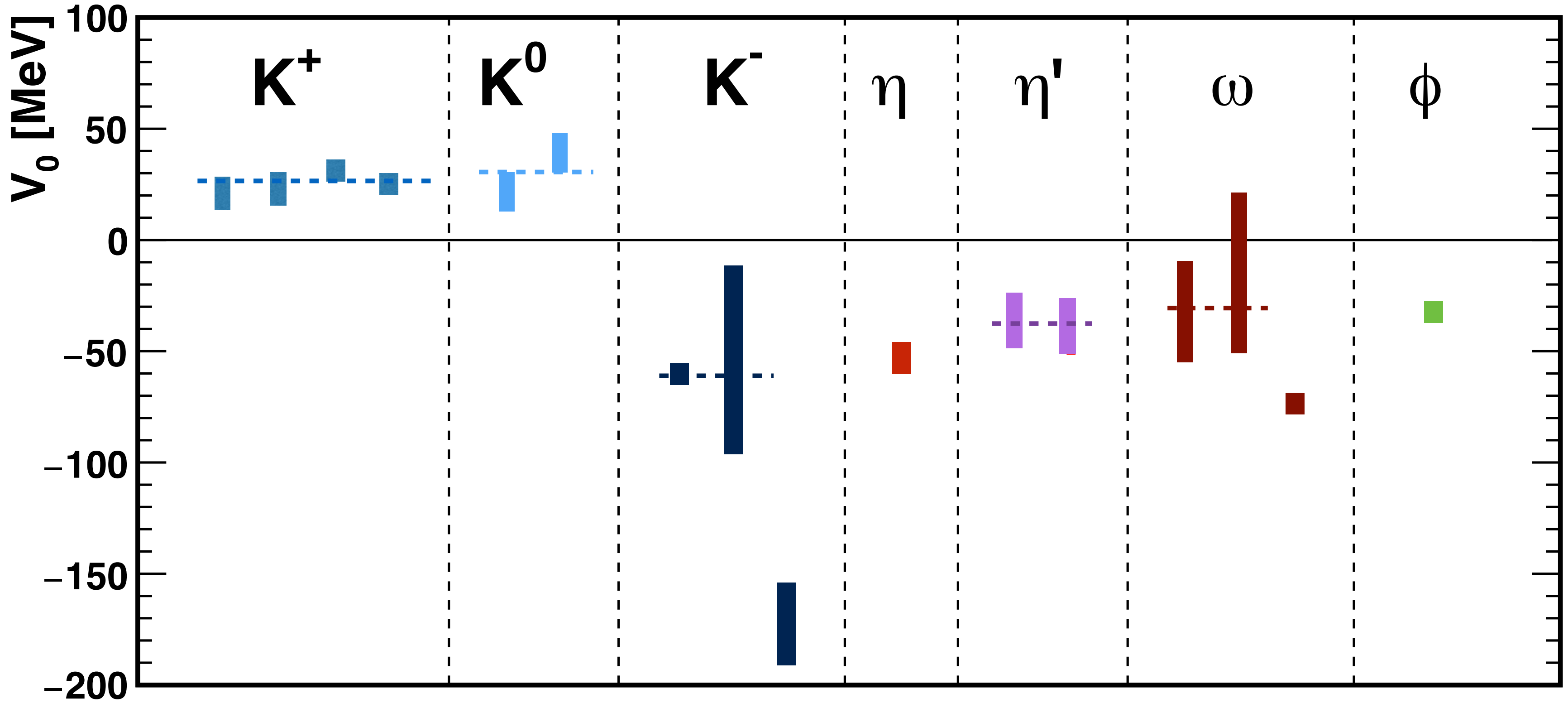

real potential $V(\rho_0)$

K^+, K^0 : 20-40 MeV; repulsive
K^- : - (30 - 100) MeV
η, η', ω, Φ : - (20 - 50) MeV

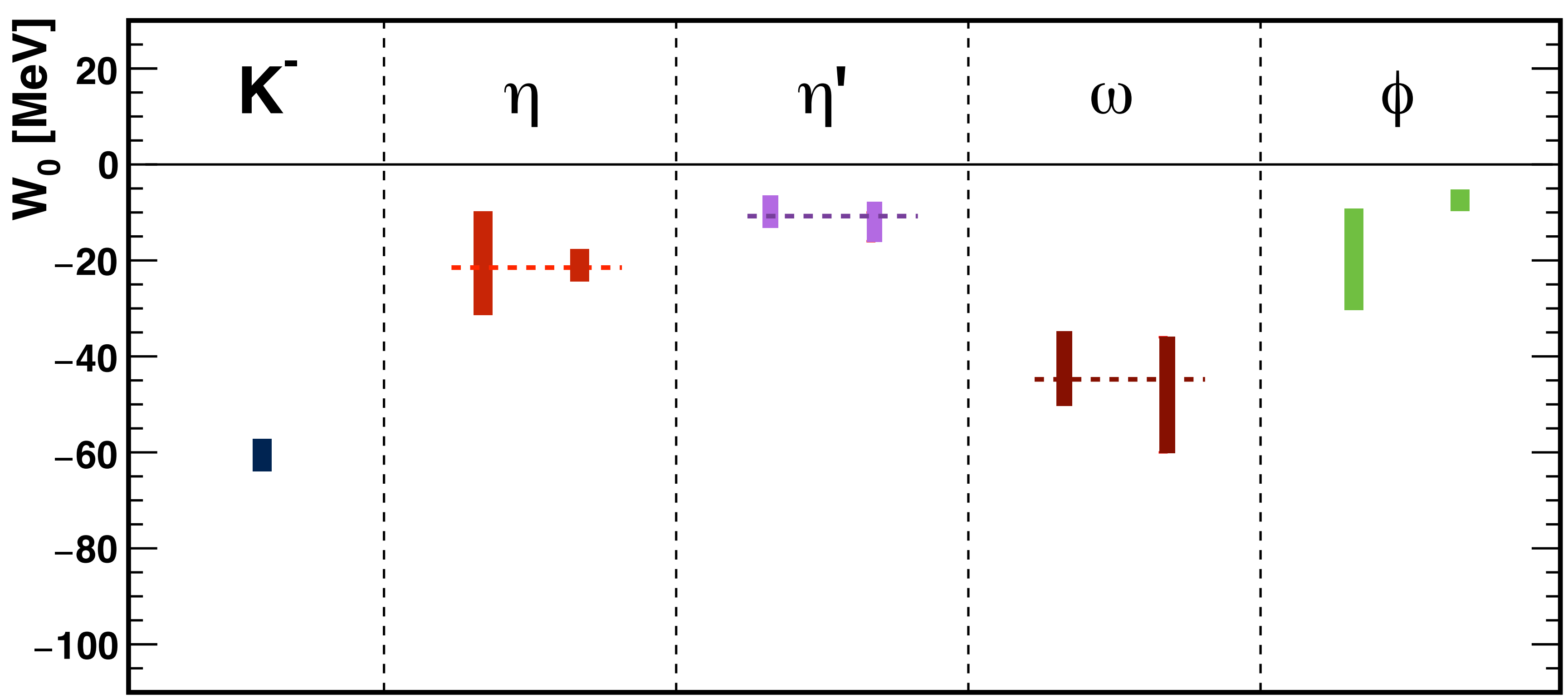

imaginary potential $W(\rho_0)$

η' : ≈ -10 MeV
η, Φ : ≈ - 20 MeV
ω : ≈ - 40 MeV quite broad
K^- : ≈ - 60 MeV very broad

η' promising candidate for mesic state: $|W_0| \approx 13$ MeV $\ll |V_0| \approx 40$ MeV

IV.
Information on meson - nucleus interaction from meson-nucleus bound states

Search for η’ - nucleus bound states in $^{12}C(p,d)\eta' X$

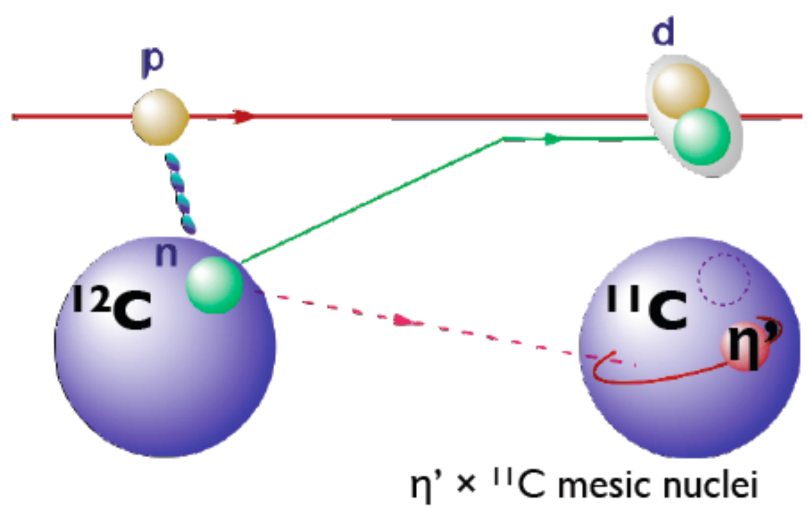

recoilless production in $^{12}C(p,d)$ reaction

PRiME collaboration (2012)

K. Itahashi et al., Exp. S 437

theoretical expectation

H. Nagahiro et al., PRC 87(2013) 045201

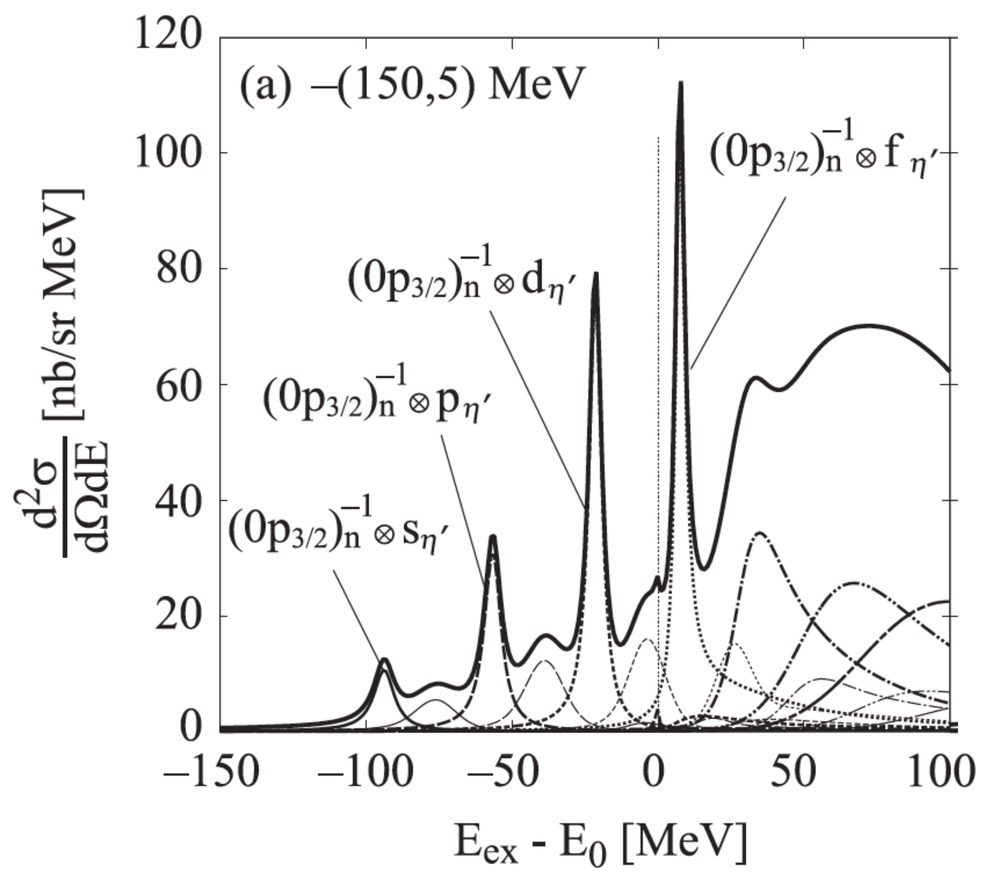

Search for η' - nucleus bound states in $^{12}C(p,d)\eta' X$

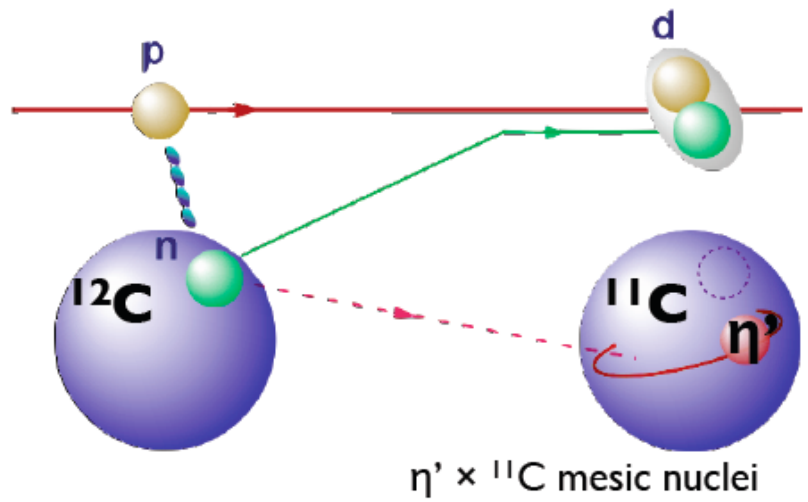

recoilless production in ^{12}C(p,d) reaction

PRiME collaboration (2012)

K. Itahashi et al., Exp. S 437

Y.K. Tanaka et al., PRL 117 (2016) 202501

Y.K. Tanka et al., PRC 97 (2018) 015202

theoretical expectation

H. Nagahiro et al., PRC 87(2013) 045201

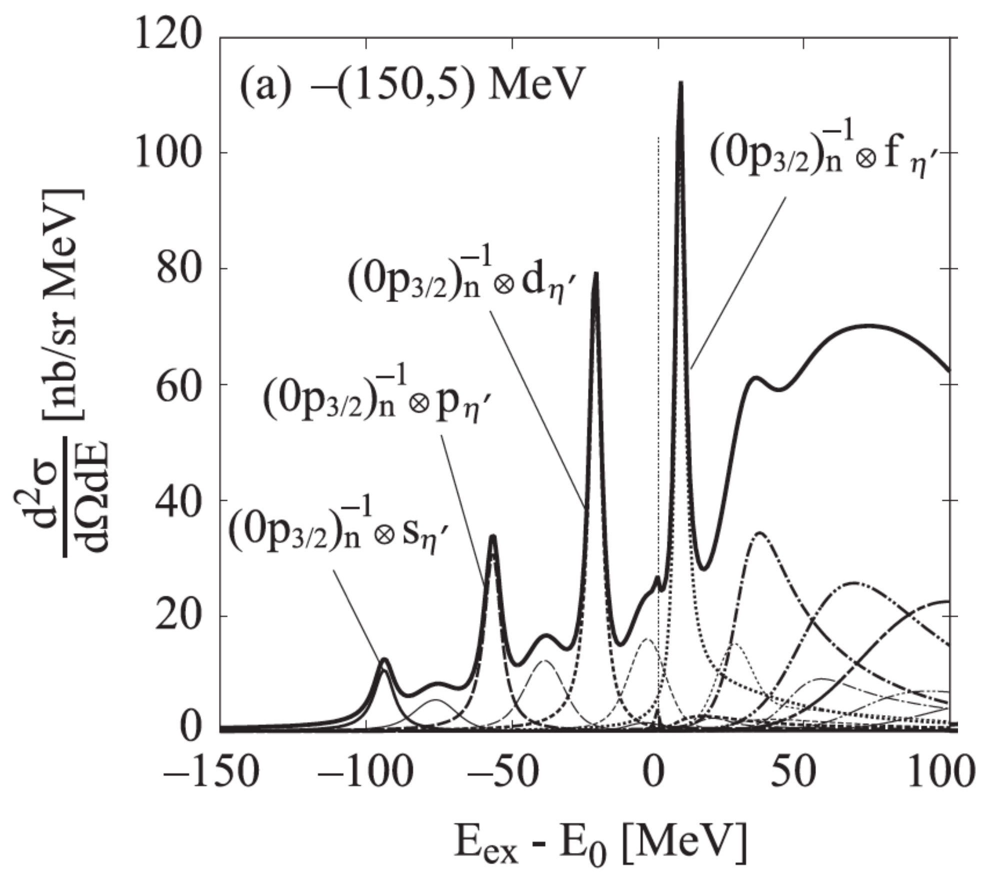

^{12}C(p,d) near η' - threshold

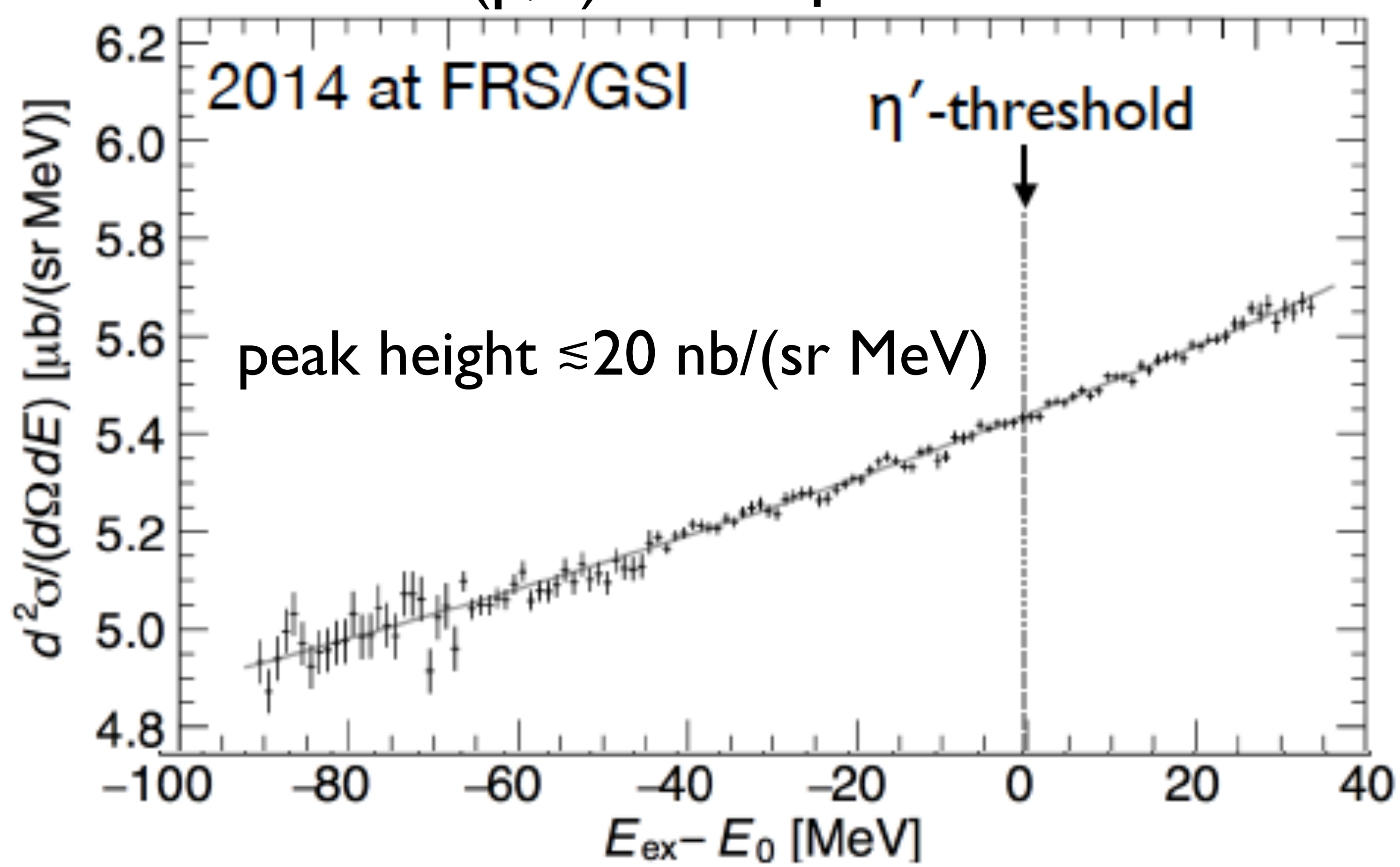

high statistical sensitivity sets constraints on η'-^{11}C interaction: $|V_0| < 100$ MeV

Search for η' - nucleus bound states in $^{12}C(p,d)\eta' X$

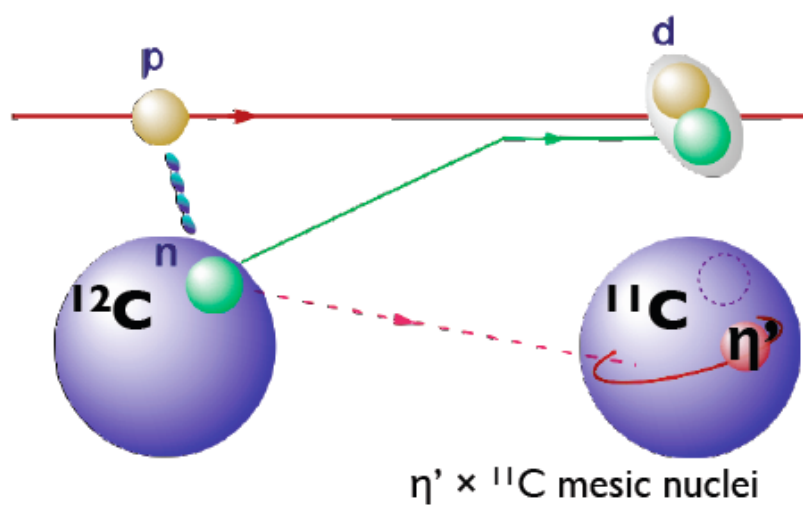

recoilless production in $^{12}C(p,d)$ reaction

PRiME collaboration (2012)

K. Itahashi et al., Exp. S 437

Y.K. Tanaka et al., PRL 117 (2016) 202501

Y.K. Tanka et al., PRC 97 (2018) 015202

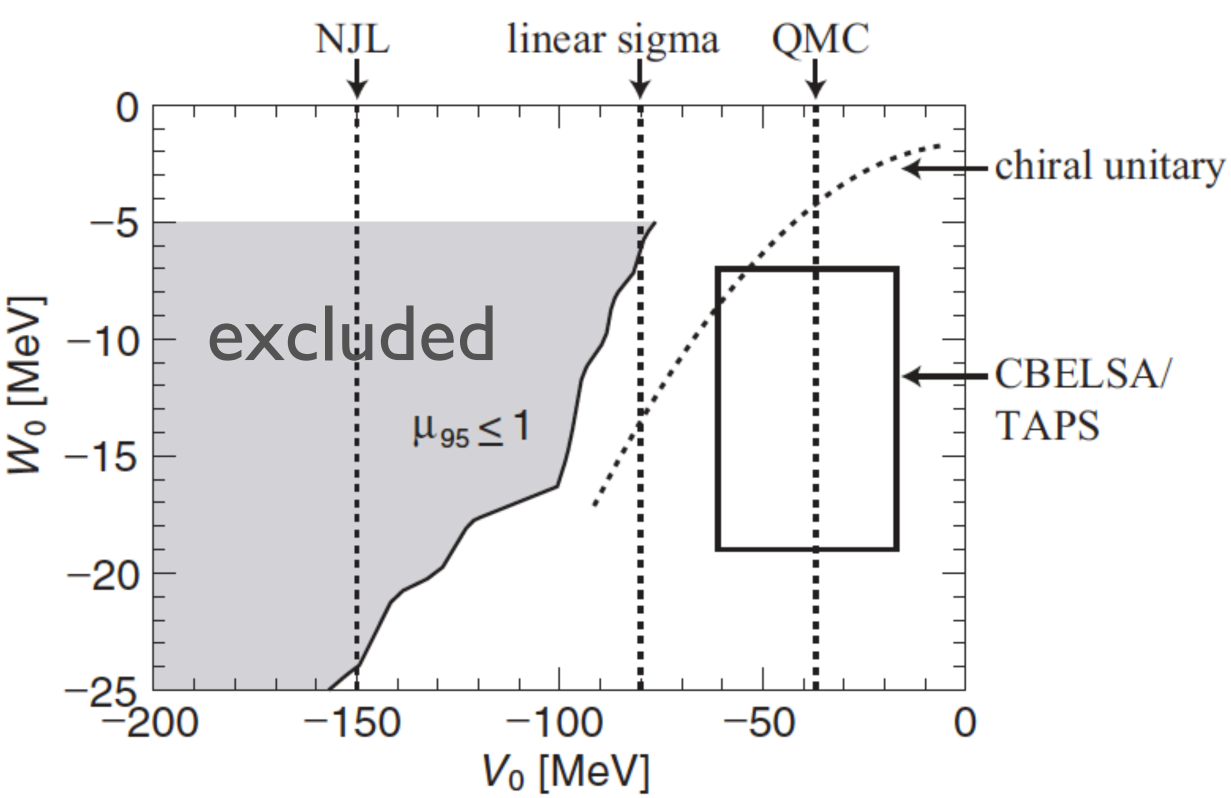

$^{12}C(p,d)$ near η' - threshold

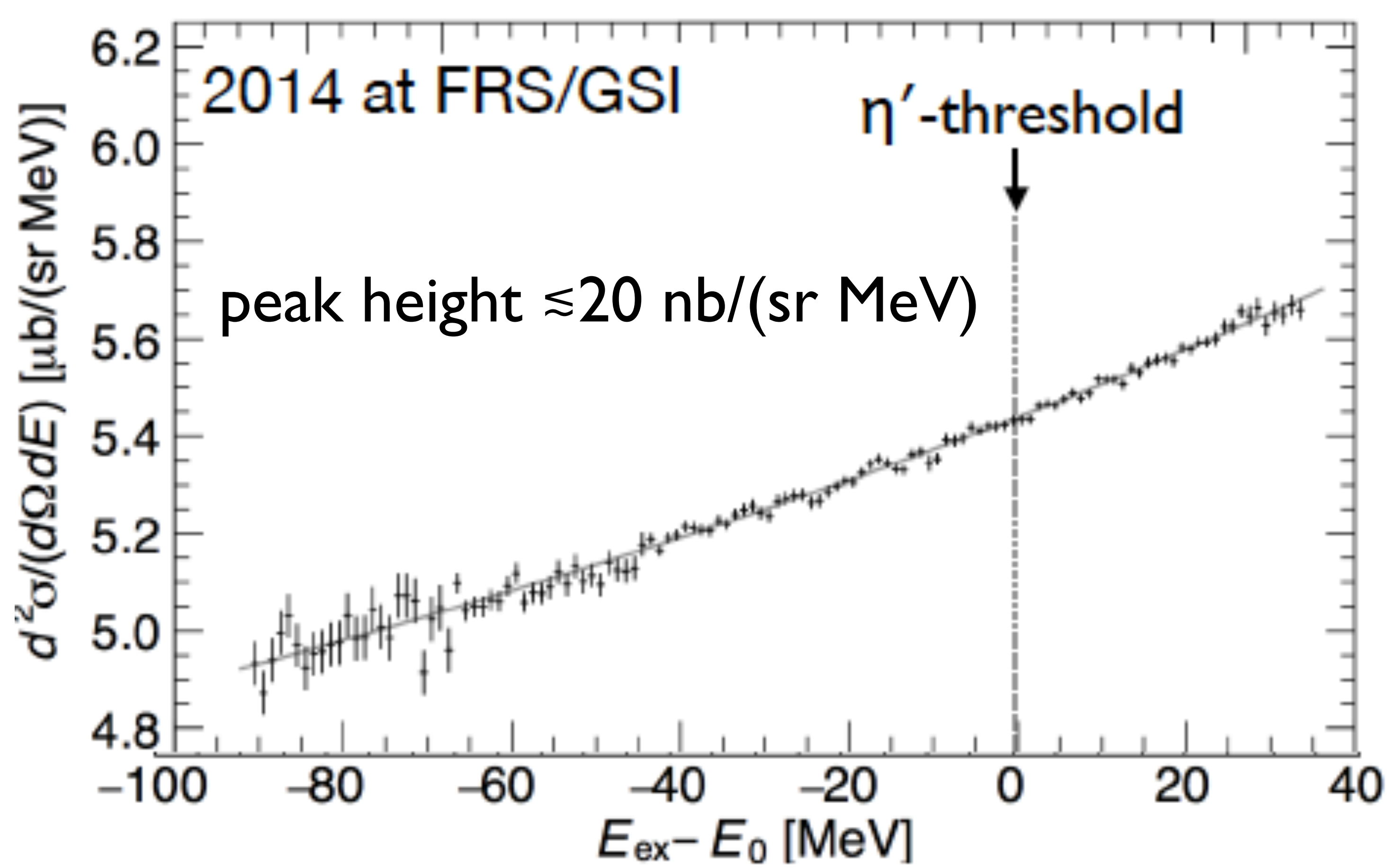

high statistical sensitivity sets constraints on η'-^{11}C interaction:

improved experiment detecting formation and decay of mesic state ongoing

Search for η' mesic states in $^{12}C(\gamma,p)$ reaction

N. Tomida et al. PRL 124 (2020) 202501

$\gamma + {}^{12}C \rightarrow p_f + \eta' \otimes {}^{11}B$

$\eta' + p \rightarrow \eta + p_s$

p_f = forward going proton

p_s= sideward going proton

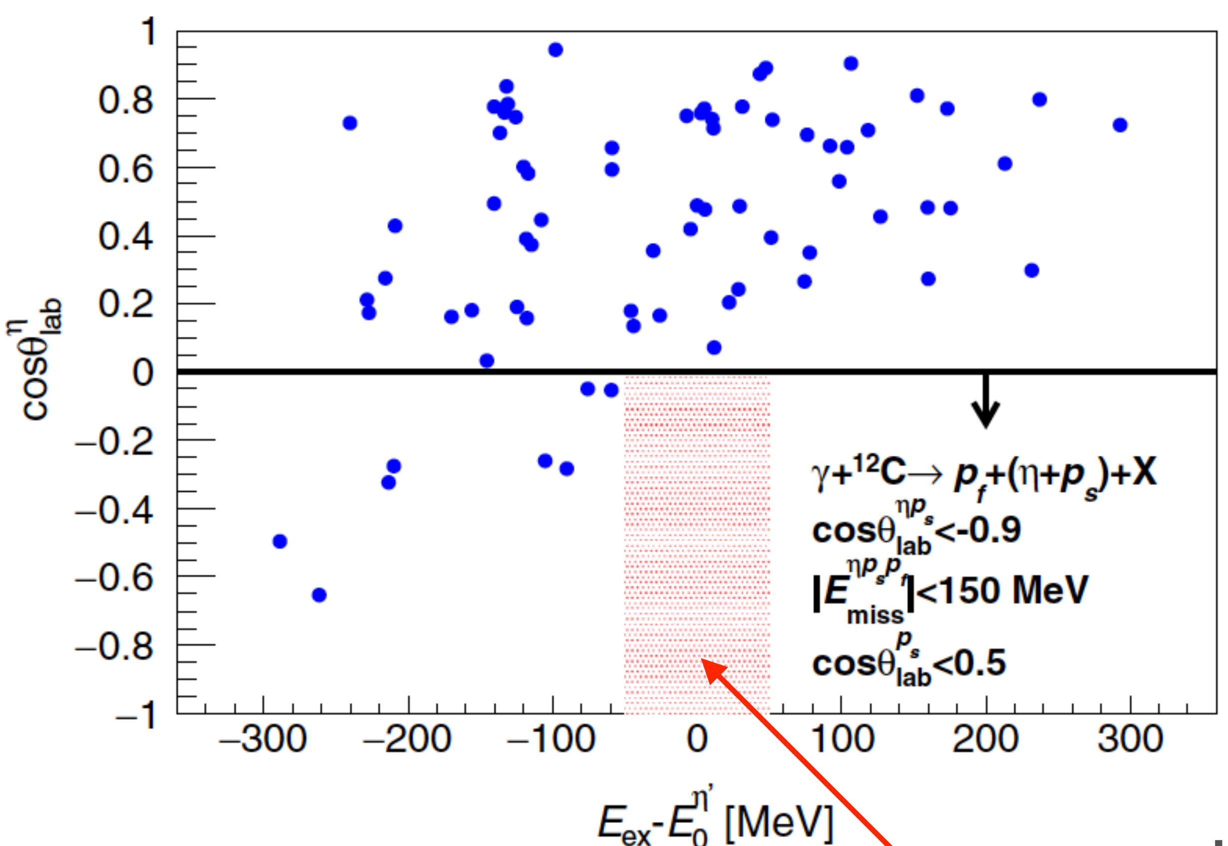

simultaneous measurement of forward going proton (production of mesic state) and almost back-to-back (η, p_s) pair (decay of mesic state)

upper limit for branching ratio BR(η'N→ηN) ≈ 24% for V_0= -100 MeV

≈ 80% for V_0= -20 MeV

these limits questioned in H. Fujioka et al. PRL126 (2021) 019201

Search for η-d mesic states in $\gamma\, d \rightarrow \pi^0\, \eta\, d$ reaction

T. Ishikawa et al., PRC 104 (2021) L052201; arXiv:2111.01388

coherent $\pi^0\,\eta$ photoproduction off nuclei

forward going high momentum π takes over most of the beam momentum so that low energy η can couple to the intact nucleus

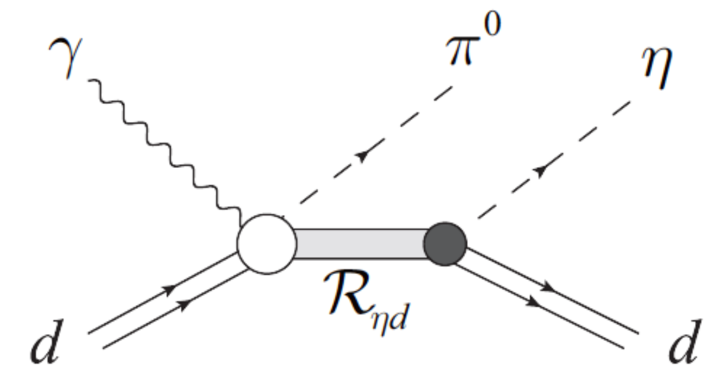

resonance like structure in $M_{\eta d}$ observed near threshold (more pronounced at lower E_γ)

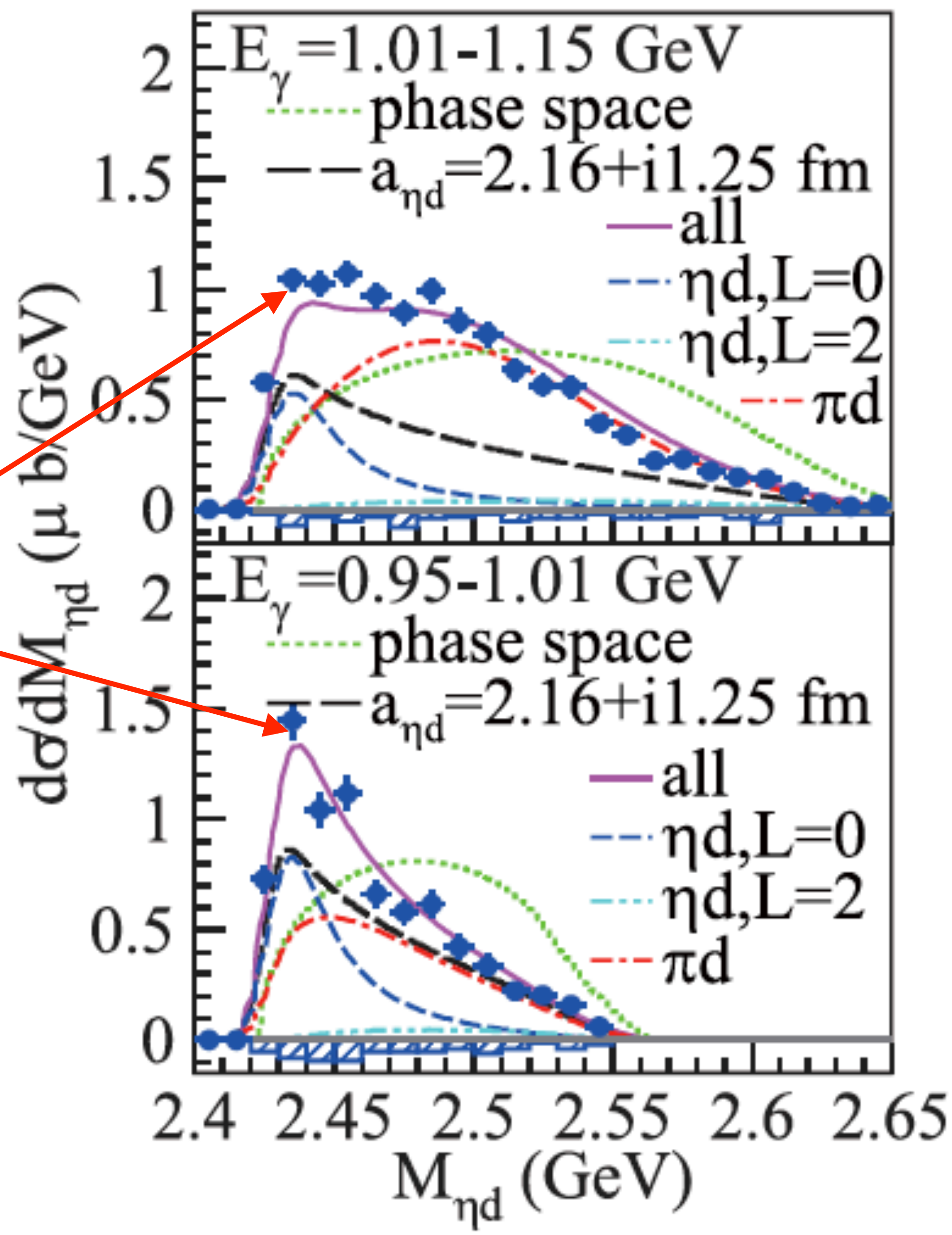

mass = $(2.427^{+0.013}_{-0.006})$ GeV

$m_\eta + m_d$ = 2.4235 GeV

width = $0.029^{+0.006}_{-0.029}$ GeV

isoscalar 1^- ηNN bound state or virtual ηd state

ηd scattering length:

$a_{\eta d} = \pm(0.7^{+0.8}_{-0.6} + i\,(0.00^{+1.5}_{-0.0}))$ fm

coherent $\gamma A \rightarrow \pi^0 \eta\, A$ promising tool for studying η-A interaction

Search for K⁻pp clusters

J-PARC E15 experiment
M. Iwasaki et al.

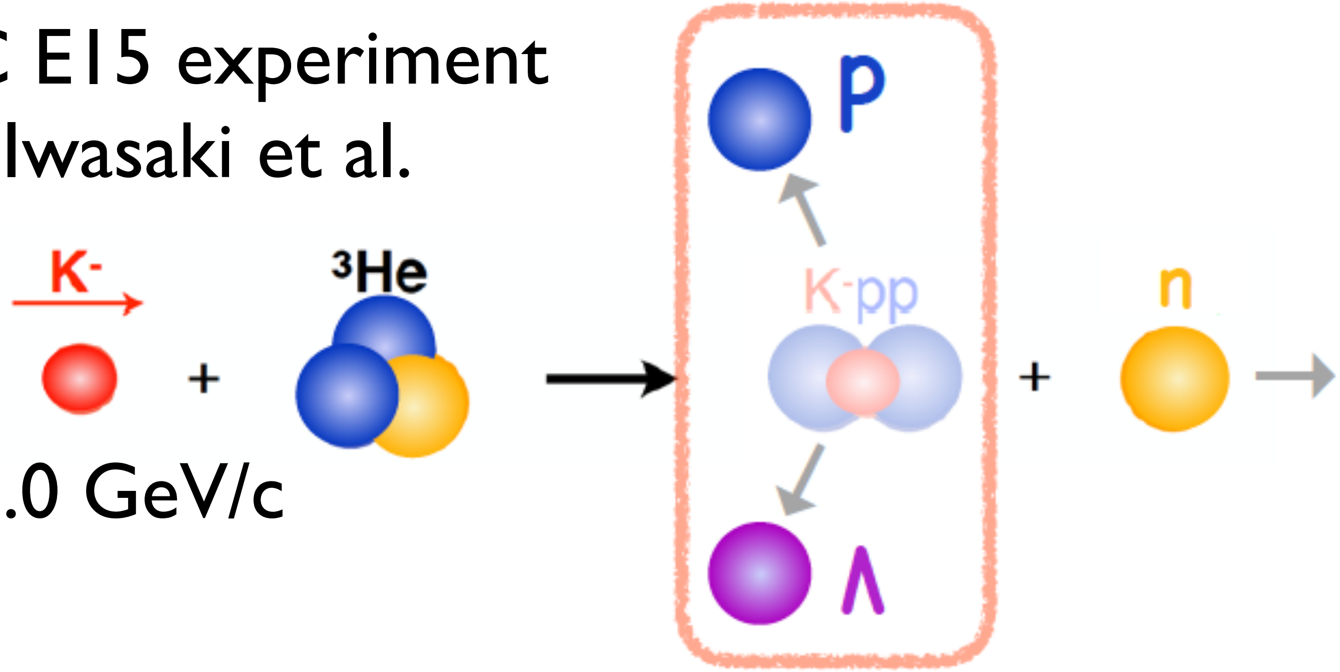

p_{K^-} = 1.0 GeV/c

strategy:
detect Λp pairs from K⁻pp decay in coincidence with forward-going neutron

K⁻pp bound state formed decaying into Λp

BE=(42±3(stat)$^{+3}_{-2}$(syst))MeV

Γ=(100±7(stat)$^{+19}_{-9}$(syst))MeV

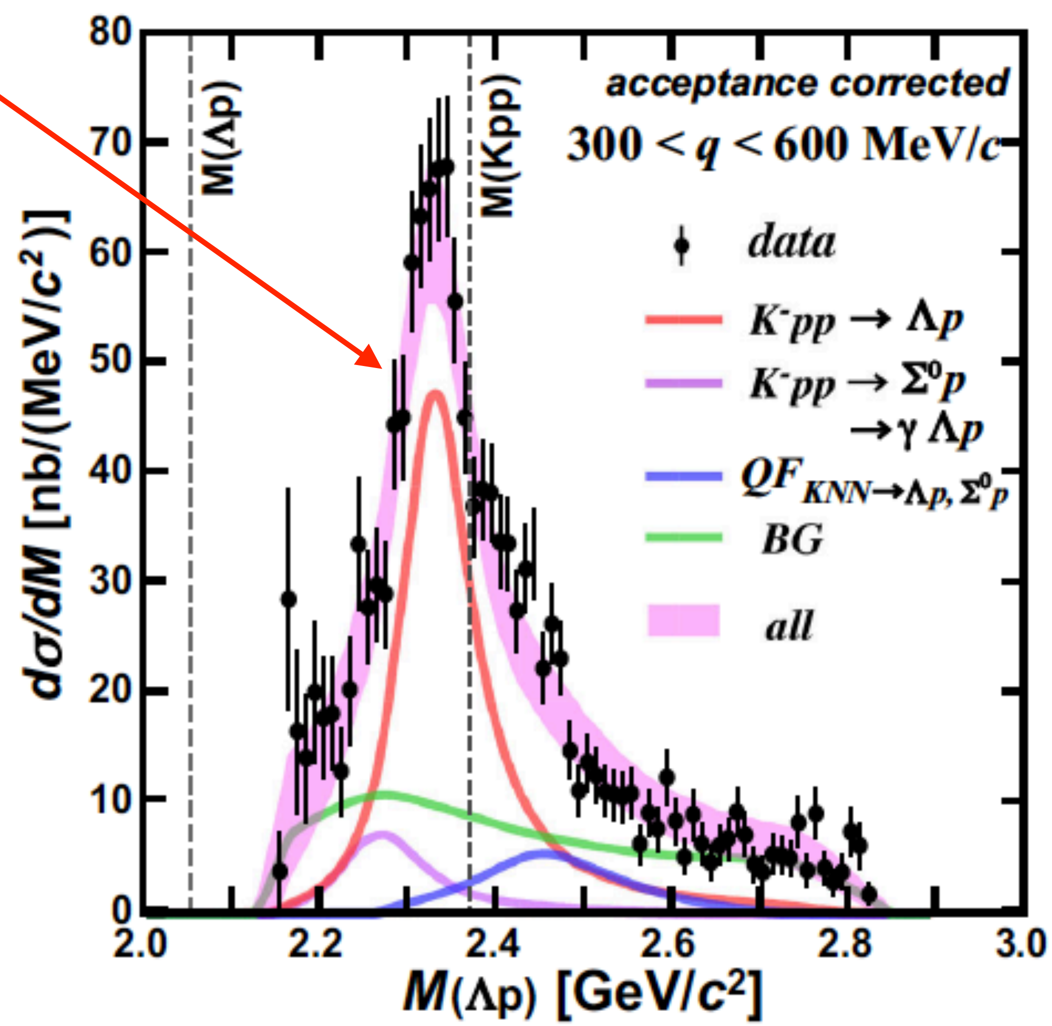

Y. Sada et al., PTEP 2016, 051D01

S. Ajimura et al. Phys. Lett. B 789 (2019) 620

T. Yamaga et al. PRC 102 (2020) 044002

new era of studying kaonic nuclei in J-PARC E80

Summary and conclusions

- mesons change properties in the nuclear medium as predicted theoretically !!
  - mesons masses are lowered for attractive and increased for repulsive meson-nucleus interactions: $m_{K+,K0} \nearrow$; $m_{K^-} \searrow$; $m_{\eta'} \searrow$
  - in-medium lifetimes are shortened by hadronic interactions within the nucleus → in-medium broadening
- experimental approaches:
  - line shape analysis (sensitive to nuclear density at decay point)
  - real and imaginary part of meson-nucleus potentials from excitation functions, momentum distributions and transparency ratios (sensitive to nuclear density at production point; model dependent !)
- model independent information on meson-nucleus potential from observation of meson-nucleus bound states:
  - evidence for existence of virtual ηd state and bound K^-pp cluster
  - studies of kaonic nuclei and search for $\eta' \otimes A$ ongoing
- vivid field: new results are eagerly awaited !!

Back up slides

Line shape analysis

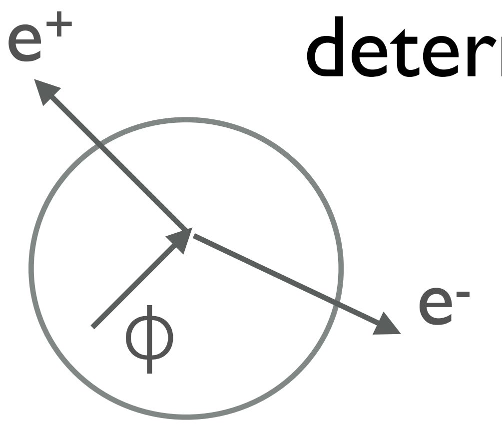

determine mass from in-medium decay:
e.g., $\phi \rightarrow e^+e^-$

$$m = \sqrt{(p_1+p_2)^2}$$

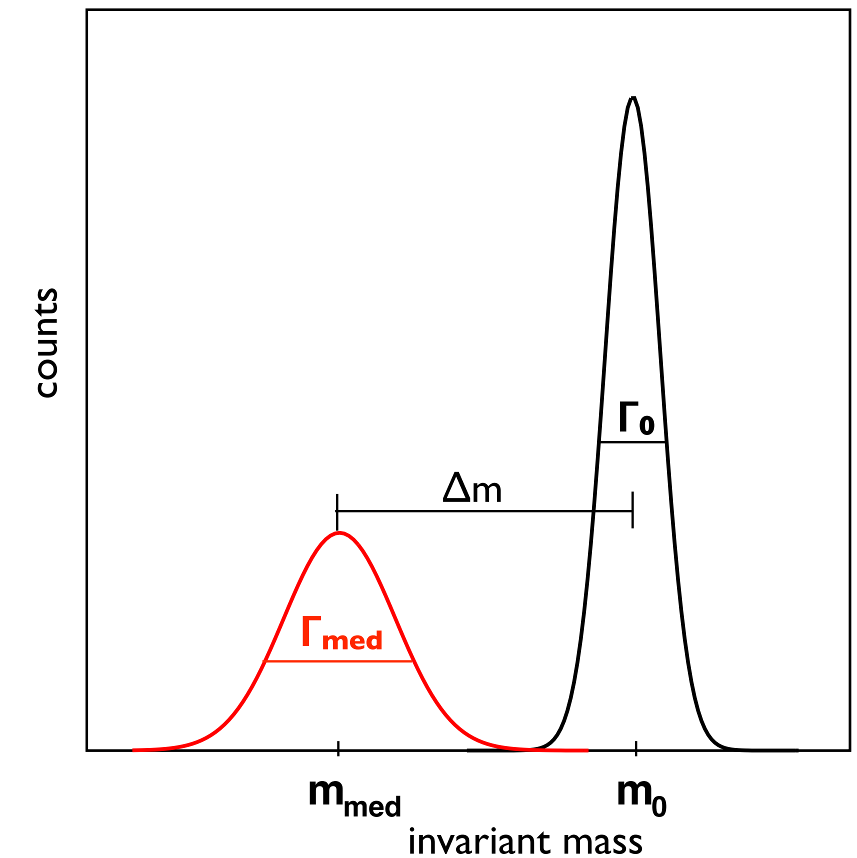

probability for decay:

$$\frac{dP_{decay}}{dl} = \frac{mc}{p} \cdot \frac{1}{\hbar c} \cdot \Gamma_{decay} = 6.5 \cdot 10^{-6}\,/\mathrm{fm}$$

$$\Gamma_{\phi \rightarrow e^+e^-} = 1.3 \cdot 10^{-3}\ \mathrm{MeV} \qquad \left(\text{for } \approx \frac{mc}{p} \approx 1.0\right)$$

$$\frac{P_{decay}}{P_{abs}} \approx 2 \bullet 10^{-5}$$

probability for absorption:

$$\frac{dP_{abs}}{dl} = \sigma_{abs} \cdot \rho(r) = 0.3/\mathrm{fm} \text{ at } \rho=\rho_0$$

$$\sigma_{abs} \approx 20\ \mathrm{mb}$$

50 000 times more likely
to get absorbed than to decay

more favourable decay/absorption ratio only at lower densities near the surface where in-medium modifications are reduced

sensitive to nuclear density at decay point !!

Determining the real part of the K⁻ -nucleus potential from momentum distributions

p + C, Cu, Ag, Au → $K^+ K^-$ +X

$K^+ K^-$ - pairs not from Φ decay

ANKE: Yu. T. Kiselev et al., PRC92 (2015) 065201

K-

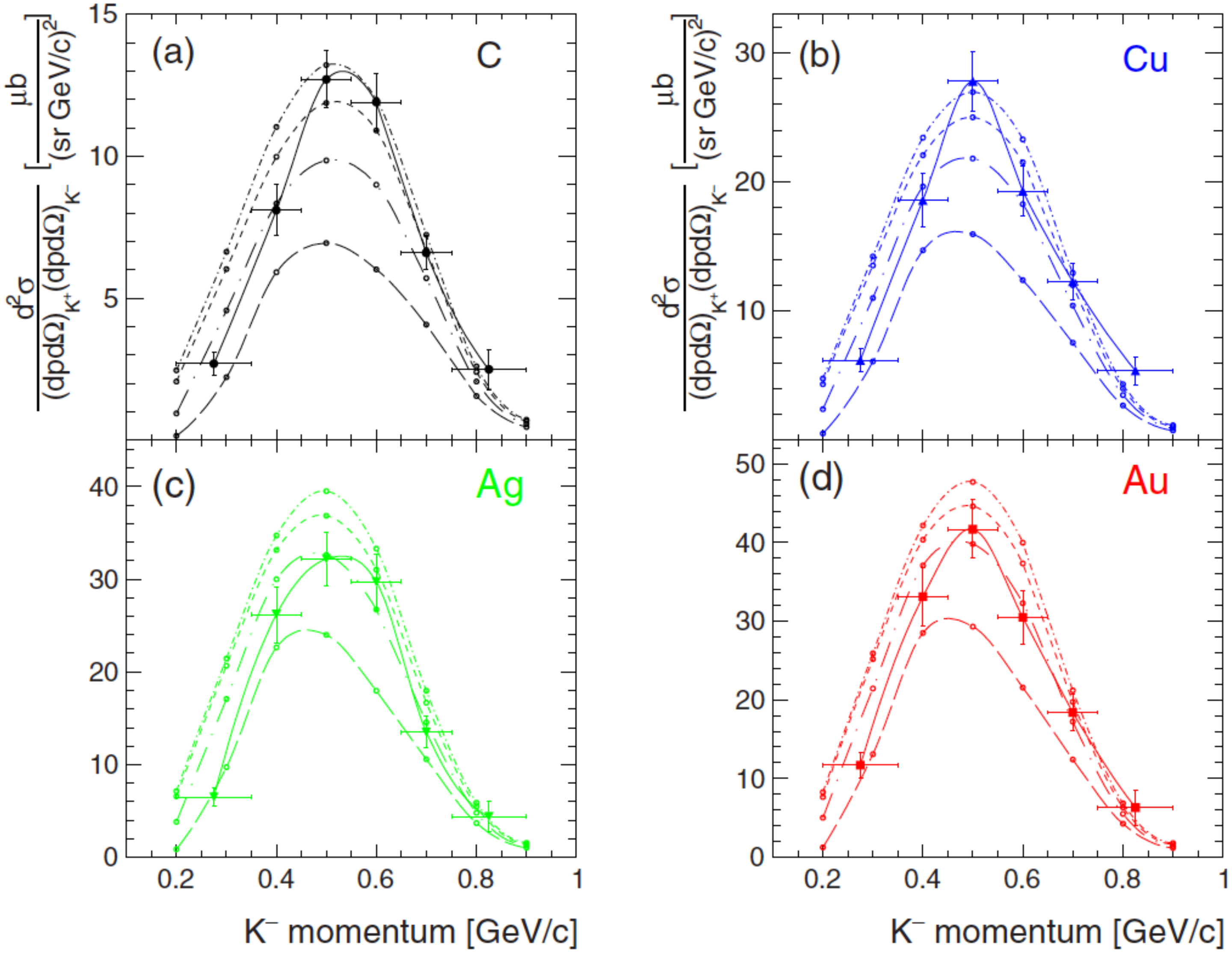

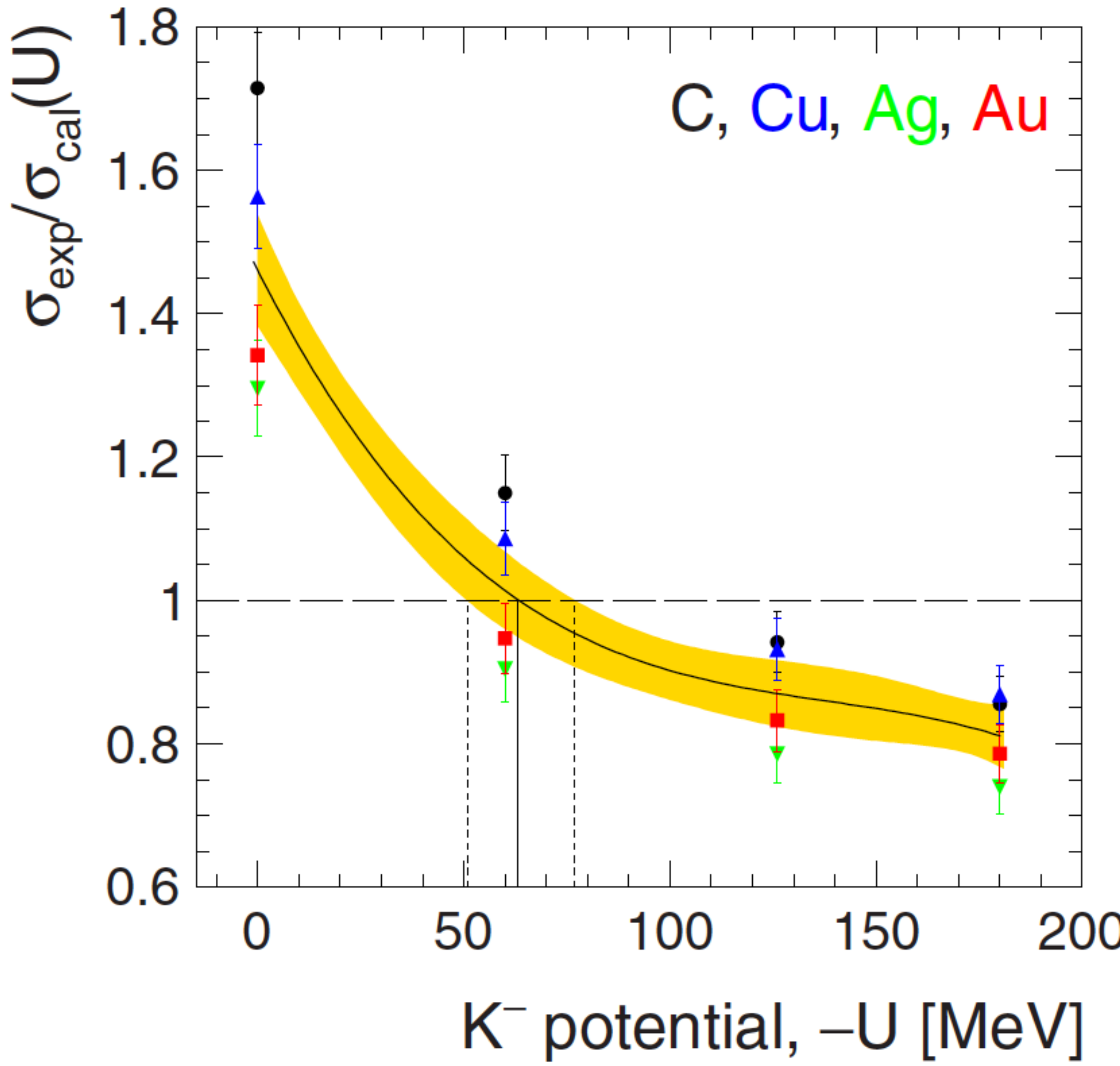

K⁻-momentum spectra in coincidence with K⁺ (200 ≤ p_{K+} ≤ 600 MeV/c) compared to collision model calculations: E. Paryev et al., J. Phys. G 42 (2015) 075107

$V_{K^-}(\rho=\rho_0) = -63^{+50}_{-30}$ MeV accounting for systematic uncertainties

Search for η' - nucleus bound states in $^{12}C(p,d)\eta'X$

Y.K. Tanaka et al., PRL 117 (2016) 202501
Y.K. Tanka et al., PRC 97 (2018) 015202

$^{12}C(p,d)$ near η' - threshold